Effects of silver nanoparticles on bacteria and earthworms

A thesis

submitted in partial fulfilment

of the requirements for the Degree of

Master of Science

at

Lincoln University

by

Yan Zhan

Lincoln University

2012

Abstract of a thesis submitted in partial fulfilment of the

requirements for the Degree of Master of Science

Effects of silver nanoparticles on bacteria and earthworms

by

Yan Zhan

A foreseeably huge increase in the use of nanoparticles (NPs) could potentially result in increasing exposure of humans to environmental NPs. In order to mitigate, eliminate or avoid risks of exposure to these NPs in the environment, it is essential to develop an understanding of their mobility, reactivity, ecotoxicity and persistency. Due to the expected increased usage of silver nanoparticles (AgNP), the models predict an exponential increase in exposure, which would no doubt exacerbate concerns about ecological risks. In this research, the effects of AgNP were evaluated at two trophic levels: *Escherichia coli* (*E. coli*) bacteria, which is the most common bacteria used in commercial toxicity assays, and the earthworm *Aporrectodea caliginosa* (*A. caliginosa*), which is the most abundant species in New Zealand pastures. In order to compare the toxicity of AgNP with an inorganic and a better studied silver compound, silver nitrate ($AgNO_3$) was used as an aqueous counterpart.

In this research, the *E. coli* bacteria toxicity study was accomplished by application of the SciTox^{TM} mediated Direct Toxicity Assessment (DTA) Assay, developed by Lincoln Ventures Limited. The DTA Assay is a rapid and sensitive catalytic microbial method. In addition to the conventional standard DTA assay protocol (Method I), a modified protocol (Method II) with an additional centrifuge step to Method I was developed to eliminate the influence of AgNP on the electrodes used in the assay. Two toxicants – commercial-standard 2,4-dichlorophenol (2,4-DCP) and $AgNO_3$ – were applied to *E. coli* in the DTA assay. Clear and accurate dose-response curves were obtained with both $AgNO_3$ and 2,4-DCP using Methods I and II. However, no dose-dependent response in the DTA assay was observed with either Method I or II on exposure of *E. coli* to AgNP. Hence a growth inhibition assay was conducted by exposing *E. coli* to different concentrations of AgNP. A linear inhibition in bacterial growth was observed after 16 h incubation of bacteria to AgNP.

A genotoxicity study was carried out with *A. caliginosa* earthworms. Three separate acute toxicity studies were conducted to determine the LD_{50} values of AgNP and $AgNO_3$. LD_{50} values were established for $AgNO_3$ in a classical Petri-dish filter-paper study (571 ppm) and a soil-exposure study (418), but AgNP did not appear to be toxic to *A. caliginosa* earthworms even at 2000 ppm. Hence an exposure study was conducted using aqueous AgNP and $AgNO_3$. Based on the results from that study, *A. caliginosa* were exposed to 0, LD_5, LD_{10}, LD_{15}, LD_{20}, and LD_{25} concentrations of aqueous solutions of AgNP and $AgNO_3$. Two classical earthworm genotoxicity tests (the Micronucleus Test and Comet Assay) were performed. In the Micronucleus Test, the frequencies of coelomocyte micronuclei (MN) and binucleate (BN) cells were used to assess chromosomal aberrations and inhibition of cytokinesis, respectively. The frequency of MN at most concentrations was higher than for BN on exposure to both AgNP and $AgNO_3$. The frequencies (i.e. the sum) of BN and MN in coelomocytes were significantly higher ($P < 0.05$) with both AgNP and $AgNO_3$ at concentrations of LD_{15} upwards comparedwith the controls. Thus it appears that both AgNP and $AgNO_3$ are capable of causing chromosomal aberrations and cytokinesis failure at higher exposure concentrations. In this study, no significant changes were observed in the frequency of the three major types of coelomocytes, i.e. eleocytes, acidophils, and basophils, in the earthworms exposed to AgNP and and $AgNO_3$. In the Comet Assay, the comets formed due to DNA single-strand breaks in earthworm coelomocytes were scored for the comet parameters, Tail DNA (TD), DNA Tail Length (TL), and DNA Tail Moment (TM). Results of TD, TL and TM on exposure to both AgNP and $AgNO_3$ were not significant indicating that neither of these two chemicals at the exposure concentrations tested induces DNA damage.

A functional ecotoxicogenomics study was performed using polymerase chain reaction (PCR) and reverse transcriptase quantitative PCR (RT-qPCR). In standard PCR, the superoxide dismutase (*SOD*) gene was for the first time detected in *A. caliginosa* earthworms. Primers were designed from conserved areas identified by multiple alignment of the *SOD* gene from *Lumbricus rubellus*, *Eisenia fetida* and the blue mussel (*Mytilis edulis*). A partial sequence homologous to the *SOD* gene was obtained using the standard PCR protocol. This gene sequence showed 90% similarity to the *SOD* gene in both *L. rubellus* and *L. terrestris* and 88% similarity to that in *E. fetida* . Following *SOD* gene detection and sequencing, a study of *SOD* gene expression in *A. caliginosa* earthworms exposed to AgNP was performed using RT-qPCR. A higher gene expression was observed in *A. caliginosa* exposed to $AgNO_3$ compared with AgNP.

In conclusion, it is apparent that AgNP used in this study was not as toxic as $AgNO_3$ to either *E. coli* bacteria or *A. caliginosa* earthworms. This may be because of the poor solubility of AgNP.

Keywords: *A. caliginosa*, $AgNO_3$, AgNP, Comet Assay, DNA damage, *E. coli*, KFCIII, MN test, SciTox™ DTA Assay, PCR, ROS, RT-qPCR, *SOD* gene.

Acknowledgements

I thank my supervisors, Associate Professor Ravi Gooneratne, Dr Neil Pasco, Dr Hayley Ridgway, and Dr Richard Weld, for all their help and support with both the science during my research experiments and English language for thesis writing. I thank them for their understanding of my personal choice to move up to Auckland after the earthquake during the process of drafting and finalizing chapters.

I thank Dr P.Muangphra, Biology Department, Faculty of Science, Silpakorn University, Thailand, for her help with the Comet Assay by analysing the images of comets from my coelomocyte samples using a digital camera (Nikon DXM 1200C) and the software program LUCIA (Laboratory Universal Computer Image Analyzer). Special thanks also to Wenfeng Song for giving me so many valuable comments and suggestions during my research. As a PhD student of my supervisor Ravi Gooneratne, he provided me guidance, support, technical knowledge, and personal advice.

Many thanks to Nick Glithero, Simon Lee, Giuliana Bernardi, and Martin Wellby for their technical support and help during experimental stages of this research. Giuliana and Martin also helped me to collect and maintain my earthworm colony.

I thank Lincoln Ventures Ltd for offering me laboratory space to conduct the bacterial assay studies.

Finally, thanks to family and friends for their support and understanding.

Table of Contents

Abstract ..... **ii**

Acknowledgements ..... **v**

List of Tables ..... **x**

List of Figures ..... **xi**

Chapter 1 Introduction **1**

1.1 Nanoparticles 1

1.2 Silver 1

1.3 Bacteria and earthworms 2

1.4 Research aims and objectives 3

1.4.1 Aims 3

1.4.2 Objectives 3

1.4.3 Hypotheses 3

Chapter 2 Literature Review **5**

2.1 Nanoparticles 5

2.1.1 Physical and chemical properties of NPs 5

2.1.2 Toxicity of NPs 6

2.1.2.1 Effects of AgNP on the environment 6

2.1.2.2 Effects on animal cells and tissues 7

2.1.2.3 Health issues 9

2.1.2.4 Toxicity to plants and soil 9

2.1.2.5 Effects on aquatic organisms 10

2.1.2.6 Anti-bacterial effects 11

2.1.3 Bioavailability of AgNP 11

2.2 Organisms and applied methods 12

2.2.1 Bacteria 12

2.2.1.1 SciTox^{TM} rapid Direct Toxicity Assay (DTA) 12

2.2.1.1.1 Bacterial growth *13*

2.2.1.1.2 Electron transport chain (ETC) *13*

2.2.1.1.3 Mediator-based biosensors *14*

2.2.1.1.4 Electrochemical analysis *15*

2.2.2 *Aporrectodea caliginosa* earthworm 15
2.2.2.1 Dose–response relationship 16
2.2.2.2 Comet Assay and Micronucleus Test 17
2.2.2.2.1 Coelomocytes in earthworms 17
2.2.2.2.2 Comet Assay 18
2.2.2.2.3 Micronucleus Test 19
2.2.2.3 Polymerase chain reaction (PCR) 19
2.2.2.3.1 Primer design 19
2.2.2.3.2 Reverse transcriptase qualitative PCR (RT-qPCR) 20
2.3 Summary 21
Chapter 3 SciTox™ Rapid DTA Assay 22
3.1 Introduction 22
3.2 Materials and methods 23
3.2.1 Buffer preparation 23
3.2.2 Standard toxicants 24
3.2.3 Culture media for bacteria studies 24
3.2.4 *E. coli* cultures 24
3.2.4.1 Agar plate culture 25
3.2.4.2 Liquid pre-culture 25
3.2.4.3 Main culture 25
3.2.4.4 Cell harvest 25
3.2.5 Optical density measurement 25
3.2.6 SciTox™ DTA Assay 26
3.2.6.1 Method I 27
3.2.6.2 Method II 27
3.2.6.3 Reactants used in both methods (I & II) 28
3.2.7 *E. coli* growth inhibition assay with AgNP 31
3.2.8 Electrochemical analysis 32
3.2.9 Data analysis 33
3.3 Results 34
3.3.1 SciTox™ rapid Direct Toxicity Assay 34
3.3.1.1 Method I 35

3.3.1.2 Method II 37
3.3.2 Growth inhibition assay 38
3.4 Discussion 39
Chapter 4 Earthworm Genotoxicity Study 41
4.1 Introduction 41
4.2 Methods 42
4.2.1 Buffers 42
4.2.2 Agarose solution 43
4.2.3 Acute toxicity study 43
4.2.3.1 Earthworm culture and maintenance 43
4.2.3.2 Petri-dish filter paper acute toxicity studies 44
4.2.3.3 Soil-exposure toxicity assay 45
4.2.3.4 Aqueous-solution-based toxicity assay 46
4.2.4 Comet Assay and Micronucleus Test 47
4.2.4.1 Doses of AgNP and $AgNO_3$ used 47
4.2.4.2 Coelomocyte collection 48
4.2.5 Micronucleus (MN) Test 48
4.2.6 Comet Assay 49
4.2.7 Statistical analysis 50
4.3 Results 51
4.3.1 Acute toxicity study 51
4.3.1.1 Petri-dish filter paper study 51
4.3.1.2 Soil study 52
4.3.1.3 Aqueous solution study 52
4.3.2 Micronucleus (MN) Test 53
4.3.3 Comet Assay 58
4.3.3.1 AgNP 58
4.3.3.2 $AgNO_3$ 60
4.4 Discussion 62
Chapter 5 Functional Ecotoxicogenomics 65
5.1 Introduction 65
5.2 Methods 66

5.2.1 Earthworm collection 66
5.2.2 Primer design 66
5.2.3 DNA extraction 67
5.2.4 PCR and gene sequencing 68
5.2.5 Gene cloning 68
5.3 Reverse transcriptase quantitative PCR (RT-qPCR) 69
5.3.1 RNA stabilization 69
5.3.2 RNA extraction 70
5.3.3 DNase digestion 70
5.3.4 Qiagen OneStep RT-qPCR 71
5.3.5 RT-qPCR data analysis 72
5.4 Results 72
5.4.1 Detection of a *SOD* gene in *A. caliginosa* 72
5.4.2 *SOD* gene expression analysis 74
5.5 Discussion 75
Chapter 6 General Discussion and Future Research 80
6.1 General discussion 80
6.2 Future research 84
References 86
Appendix A Statistical Analysis of Micronucleus Test Results 99
A.1 Regression analysis 111
A.2 Summary of analysis 111
A.3 Estimates of parameters 111
Appendix B Sequencing and Alignment 112
B.1 PCR product forward sequence 112
B.2 PCR product reverse sequence 112
B.3 PCR product concensus sequence (*SOD* gene) 113
Appendix C SOD Protein Alignment 114
C.1 *A. caliginosa* SOD protein alignment with *Lumbricus* 114
C.2 *A. caliginosa* SOD protein alignment with *E. fetida* 115

List of Tables

Table 3.1 DTA Assay with 2,4-DCP 29

Table 3.2 DTA Assay with $AgNO_3$ 30

Table 3.3 DTA Assay with AgNP 31

Table 3.4 Reactants used in growth inhibition toxicity assay 32

Table 3.5 Different combinations of incubation times to standard toxicant 2,4-DCP 34

Table 3.6 EC_{50} (±SD) of *E. coli* derived from the SciTox™ toxicity assay Method I 36

Table 3.7 EC_{50} (±SD) of *E. coli* derived from the SciTox™ toxicity assay Method II 38

Table 4.1 Concentrations (ppm) of the toxicants $AgNO_3$ and AgNP used in the Petri-dish filter paper study 45

Table 4.2 Concentrations (ppm) of the toxicants $AgNO_3$ and AgNP used in the soil-exposure study 46

Table 4.3 Concentrations (ppm) of $AgNO_3$ and AgNP used in the aqueous solution study 47

Table 4.4 Aqueous AgNP and $AgNO_3$ exposure concentrations 48

Table 4.5 Differential coelomocyte count 55

Table 4.6 Mean micronuclei (MN) and binuclei (BN) counts in 1000 coelomocytes per earthworm 56

List of Figures

Figure 2.1: Predicted environmental concentrations (PEC) shown as mode (most frequent) value and risk quotients for Europe and the United States (U.S) for different environmental compartments. For air, surface water and sewage treatment plant effluents the results illustrate 2008 engineered nanomaterial (ENM) concentrations. For soil, sludge-treated soil and sediments, the data are shown as annual increases of ENM concentrations. (Figure sourced from Gottschalk *et al.*, 2009). 7

Figure 2.2: Dose–response relationship curve: on the *x*-axis is the concentration of the chemical exposed to and on *y*-axis is the response. 16

Figure 2.3: Dose–response relationship curve applied to respiratory activity. At higher concentrations, respiration is inhibited. 17

Figure 3.1 Steps in SciTox^{TM} Rapid DTA assay Methods I and II. 27

Figure 3.2 Equipment used for electrochemical analysis in this research. 33

Figure 3.3 Current readings of *E. coli* culture exposed to standard toxicant 2,4-DCP for four incubation periods: current reading results from (A) Method I and (B)Method II. $*P < 0.05$, $**P < 0.01$ compared to control. 35

Figure 3.4 Method I: Dose-response of *E. coli* and fitted model on exposure to the toxicants in Method I: (A) 2,4-DCP ; (B) $AgNO_3$; (C) AgNP. 36

Figure 3.5 Dose-response of *E. coli* and fitted model on exposure to toxicants in Method II: (A) 2,4-DCP; (B) $AgNO_3$; (C) AgNP. 37

Figure 3.6 Means with SD of *E. coli* inhibition growth rate when exposed to fixed AgNP concentrations (0–10 mg L^{-1}) and fitted linear regression $R^2 = 0.98$. 38

Figure 4.1 Mean mortality of *A.caliginosa* earthworms after 48h exposure to $AgNO_3$ in Petri-dish, and fitted model. 51

Figure 4.2 Mean mortality of *A.caliginosa* earthworms after 48h exposure to $AgNO_3$ in soil and fitted model. 52

Figure 4.3 Mean mortality of *A.caliginosa* earthworms after 48h exposure to aqueous solution of AgNP and fitted model. 53

Figure 4.4 Mean mortality of *A.caliginosa* earthworms after 48h exposure to aqueous solution of $AgNO_3$ and fitted model. 53

Figure 4.5 Eleocyte with a prominent micronucleus. 54

Figure 4.6 Acidophil. 54

Figure 4.7 Basophil. 55

Figure 4.8 Total micronulclei (MN) and binuclei (BN) in coelomocytes exposed to different exposure concentrations of AgNP and $AgNO_3$ (n = 3), error bars are standard deviations. Asterisks indicate significant differences from AgNP. *P < 0.05; **P < 0.01; ***P < 0.005; ****P < 0.001. 57

Figure 4.9 A comet (from an earthworm exposed to LD_{10} AgNP concentration). 58

Figure 4.10 Mean coelomocyte tail DNA percentage in earthworms (n = 3) exposed to different concentrations of AgNP; error bars are standard deviations. *significantly different from the control (P < 0.05). 59

Figure 4.11 Mean coelomocyte DNA tail length in earthworms (n = 3) exposed to AgNP; error bars are standard deviations. 59

Figure 4.12 Mean coelomocyte DNA tail moment in earthworms (n = 3) exposed to different concentrations of AgNP; error bars are standard deviations. 60

Figure 4.13 Mean coelomocyte tail DNA percentage in earthworms (n = 3) exposed to different concentrations of $AgNO_3$; error bars are standard deviations. 61

Figure 4.14 Mean coelomocyte tail length of earthworms (n = 3) exposed to different concentrations of $AgNO_3$; error bars are standard deviations. 61

Figure 4.15 Mean coelomocyte tail moment of earthworms (n = 3) exposed to different concentrations of $AgNO_3$; error bars are standard deviations. 62

Figure 5.1 PCR products of *Lumbricus, Eisenia fetida* and *Aporrectodea caliginosa* earthworms with primer sets A&C and B&C. The marker is $1kb^+$ DNA ladder. . 73

Figure 5.2 Similarity tree with sequence similarity (%) of *SOD* mRNA from seven species (*Aporrectodea caliginosa, Lumbricus rubellus, L. terrestrus, Eisenia fetida, Mytilus edulis, Mytilus galloprovincialis,* and *Caenorhabditis elegans*). 74

Figure 5.3 Similarity tree with amino acid (protein) sequence similarity (%) of *SOD* genes from five species (*Aporrectodea caliginosa*, *Lumbricus rubellus*, *L. terrestrus*, *Eisenia fetida*, and *Mytilus galloprovincialis*)..... 74

Figure 5.4 RT-qPCR analysis of *A. caliginosa* earthworms exposure to $AgNO_3$ and AgNP. (A) RT-qPCR analysis result of tissue of whole earthworm with different exposure times (24 h and 48 h); (B) RT-qPCR analysis result with tissues taken from the head and tail regions of *A. caliginosa* earthworms at 48 h. * indicates significant differences; *$P < 0.05$; **$P < 0.01$. 75

Figure 6.1 Alignment result: *SOD* gene (PCR product) forward sequence with sequence identity percentage to *E. fetida SOD* mRNA..... 112

Figure 6.2 Alignment result of *SOD* gene (PCR product) reverse sequence with sequence identity percentage to *L. terrestrus* and *L. rubellus SOD* mRNA. 113

Figure 6.3 Alignment result for the *SOD* gene (PCR product) concensus sequence (confirmed as *A. caliginosa SOD* gene) with sequence identity percentage to *L. terrestrus, L. rubellus* and *E. fetida SOD* mRNA..... 113

Chapter 1
Introduction

1.1 Nanoparticles

Nanoparticles (NPs) are novel chemical substances, both man-made and natural, that appear in the manufacture of a wide range of products, including sporting equipment, pharmaceuticals, disinfectants, and solar devices (Robichaud *et al.*, 2007). The applications for NPs are closely related to our daily life in that they have been considered to improve living standards, and also contribute to stronger and lighter appliances. For example, NPs are already used in the manufacture of scratchproof spectacles, crack-resistant paints, anti-graffiti coatings for walls, transparent sunscreens, stain-repellent fabrics, self-cleaning windows and the ceramic coating for solar cells (SCENIHR, 2006). Moreover, NPs are used in biology and medicine in a wide variety of ways, including direct application to patients (Salata, 2004).

At the end of their product life, NPs are likely to end up in the environment, particularly in soil and water bodies, and thereby affect organisms in those media. NPs have great diffusivity and therefore may cause more frequent contacts with the surfaces of porous media compared to larger sized particles (Wiesner *et al.*, 2006). Some metal NPs bear novel and unique biological properties that allow them to interact specifically with selected proteins and inhibit their activities (Bhattacharya and Mukherjee, 2008). NPs can also penetrate many types of cells and tissues, and move through the body system causing tissue damage.

1.2 Silver

Silver (Ag), a noble metal, has been used over many years as pure silver (Ag), silver nitrate ($AgNO_3$), and silver sulfadiazine (AgSD) for the treatment of burns, wounds, and several bacterial infections. But due to the emergence of more effective antibiotics, the use of these Ag compounds has declined markedly. Recently, nanotechnology has gained tremendous impetus due to its ability to produce metals at nanodimensions, which drastically changes the chemical, physical, and optical properties of metals (Bhattacharya and Mukherjee, 2008) and the current usage of such products is increasing. Therefore, studies on the ecotoxicology of Ag NPs – one of the most used NPs – have become more important.

1.3 Bacteria and earthworms

In order to detect the ecotoxicity of environmental chemicals, many studies have used bacteria or earthworms (Gooneratne *et al.,* 2011; Pasco *et al.,* 2011). Direct toxicity assessment (DTA), using the effect of chemicals on bacterial respiration, has been used as a whole-cell microbial biosensor and offers a powerful approach to environmental monitoring (Tizzard *et al.,* 2004). Bacteria offer many advantages, including low cost, stability, broad-spectrum activity, long shelf life, and adaptability (Rogers, 2006), while earthworms are key organisms in terrestrial ecosystems. *Aporrectodea caliginosa* is the most common worm species found in agricultural ecosystems (Perez-Losada *et al.,* 2009); therefore this species is an interesting candidate for use as an animal model to monitor soil pollution. Generally, juveniles are considered to be more sensitive to toxicants than the adults (Lagadic and Caquet, 1998). Several heavy metals induce genetic damage to coelomocytes, the immunological cells in the earthworms. The Comet Assay of coelomocytes has been used as a sensitive tool to measure DNA damage (Singh *et al.,* 1988; Cotelle and Ferard, 1999; Reinecke and Reinecke, 2004), while the Micronucleus Test, a cytogenetic technique, has been used to detect chromosomal aberrations and nuclear abnormalities such as micronuclei (MN) and binuclei (BN) and these are well-established indicators of cytotoxicity and genetic toxicology, respectively (Sanchez-Galan *et al.,* 2001; Cavas *et al.,* 2005). AgNP have been shown to induce reactive oxygen species (ROS) (Limbach *et al.,* 2007). One of the antioxidant enzymes that give protection against ROS is superoxide dismutase (SOD). Thus to explore the ecotoxicity of AgNP in this study, the DTA Assay in bacteria and selected toxicological changes and genetic damage to coelomocytes, and gene expression of SOD in earthworms, were examined for their potential as biomarkers. It was thought that this would allow screening of exposure of earthworms to AgNP in the environment and so provide an earlier warning of environmental pollution of AgNP.

1.4 Research aims and objectives

1.4.1 Aims

The aim of this study was to evaluate the effects of AgNP on bacteria (*Escherichia coli*) and earthworms (*A. caliginosa*) and compare these with effects of exposure to a conventional aqueous counterpart of Ag, $AgNO_3$.

1.4.2 Objectives

- To measure respiratory inhibition in *E. coli* bacteria using the DTA Assay to establish dose-dependent response curves for AgNP and $AgNO_3$.
- To measure growth inhibition in *E. coli* bacteria exposed to Ag NPs and $AgNO_3$.
- To determine the classical toxicology parameter of acute exposure, the lethal dose 50% (LD_{50}) value in *A. caliginosa* earthworms exposed to AgNP and $AgNO_3$.
- To measure the effect of different concentrations of AgNP and $AgNO_3$ on DNA damage (using the Comet Assay and Micronucleus Test) in *A. caliginosa* earthworms.
- To identify the *SOD* gene in *A. caliginosa* by amplification of a partial sequence with degenerate PCR primers designed from the conserved areas of published *SOD* sequences in other worm species.
- To quantify the expression of the *SOD* gene in *A. caliginosa* earthworms exposed to AgNP and $AgNO_3$ using reverse transcriptase quantitative polymerase chain reaction (RT-qPCR).

1.4.3 Hypotheses

- AgNP is toxic to both bacteria and earthworms at low concentrations. Because of its increased surface-to-volume ratio, AgNP will show a more steep dose-dependent response in both bacteria and *A. caliginosa* compared with its conventional aqueous counterpart, $AgNO_3$.
- In aqueous media, *E. coli* bacteria will display a typical dose-dependent respiration inhibition in the presence of AgNP in a DTA Assay.

- In aqueous media, AgNP will inhibit the growth of *E. coli* bacteria in a dose-dependent manner.
- In aqueous media, AgNP will induce dose-dependent DNA damage in *A. caliginosa* coelomocytes and the effect will be greater than in those exposed to $AgNO_3$.
- The *SOD* gene is present in *A. caliginosa* earthworms.
- In an aqueous medium, gene expression of SOD will be higher in *A. caliginosa* exposed to AgNP than to $AgNO_3$, by RT-qPCR.

Chapter 2
Literature Review

2.1 Nanoparticles

The development of nanotechnology and the manufacture of novel organic and inorganic nano-sized materials may result in the release of substantial amounts of these materials into the environment. Thus, a foreseeably huge increase in the manufacture and use of NPs is likely to increase exposure of humans to environmental NPs. Assessing the risks of these NPs in the environment requires an understanding of their mobility, reactivity, ecotoxicity and persistency (Bhattacharya and Mukherjee, 2008). The current worldwide production of AgNP is estimated at about 500 tonnes a year. But with the growing use of NPs, this is bound to increase in the future. Environmental contamination by AgNP occurs in several ways: during synthesis, manufacture, in the incorporation of NPs into goods, use of these goods, and during recycling or disposal of such goods. According to modelled and experimental data, the concentration of AgNP in surface waters is about one nanogram per litre. Due to the expected increase usage of AgNP, the models predict an exponential increase, which would no doubt exacerbate concerns about ecological risks (Mueller and Nowack, 2008; Geranio *et al.*, 2009). However, considering the lack of experimental results validating such predictions, the estimated concentrations are only a guideline. One of the major issues related to determining the environmental concentration of AgNP is the lack of specific analytical techniques and equipment (Fabrega *et al.*, 2010).

This literature review will focus on three main areas: the physical, chemical, and biological properties of NPs; the toxicity of NPs; and the analytical methods used for evaluating the ecotoxicity of AgNP.

2.1.1 Physical and chemical properties of NPs

NPs are materials that are measured at the nanoscale level, i.e. between 1 and 100 nm in size. NPs can be categorized into two major groups, man-made and natural. These could be further categorized into several sub-groups, including carbon-based (e.g. fullerenes, carbon nanotubes [CNTs]) and inorganic NPs (e.g. metal oxides, metals, and quantum dots [Q-dots]) (Ju-Nam and Lead, 2008). The physical and chemical properties of NPs are highly varied and mainly

depend on the particular NP used, type of surface-coating of the NP, and their manufacture. In contrast to other environmental chemicals (e.g. dicholorophenols, antibiotics, heavy metals), the ecotoxicity of NPs is more unpredictable due to the contribution of its intrinsic physical and chemical properties. Their high mobility plays an important role in the ecotoxicity of NPs and contributes to the great diffusivity that may cause frequent contacts with the surface of porous media (Wiesner *et al.,* 2006). Soil has a complex porous system that is a major natural reservoir of NPs. Most NPs are basically insoluble in water and their catalytic activities vary according to their radius (Hyung *et al.,* 2007). NPs have a large surface area to volume ratio, which is considered to be an important factor in NP-catalysed chemical reactions (Hyung *et al.,* 2007). NPs are a sort of highly reactive chemicals, and some of them (e.g. carbon NPs) are difficult to break down even when treated with strong acids at high temperature (Cataldo, 2002; Robichaud *et al.,* 2007). The large surface area of NPs contributes to absorption of a wide variety of contaminants in the environment. NPs have a high affinity to and interact with organic matter (OM) in the natural environment, and this can result in OM coating the NP surfaces (Hyung *et al.,* 2007).

Some metal NPs, including gold (Au), Ag, and platinum (Pt), can interact specifically with certain proteins and thereby inhibit their activities (Bhattacharya and Mukherjee, 2008). Since many diseases, such as cancer, arthritis, and macular degeneration, are dependent on angiogenesis (the growth of new capillary blood vessels), treatment with NPs opens new possibilities to inactivate the function of 'disease inducing' protein through surface modification. Therefore, the effects on protein structure and surface changes the metal NPs would create in the body during such interactions are also important in toxicity evaluation (Bhattacharya and Mukherjee, 2008).

2.1.2 Toxicity of NPs

Based on the physical, chemical and biological properties of NPs, toxicity of NPs to different organisms, such as bacteria, plants, aquatic organisms and humans, have been studied. These studies provide important scientific knowledge for further ecotoxicology evaluation of NPs.

2.1.2.1 Effects of AgNP on the environment

Because of its wider application, small size, and high diffusivity, AgNP will end up in the environment. Gottschalk *et al.* (2009), using probabilistic methods, estimated the predicted

environmental concentrations (PEC) (Figure 2.1) in Europe and the United States and the risk quotient of AgNP pollution for the year 2008. In European surface waters, the risk quotient (PEC/PNEC [predicted no effect concentration]) is 1.1 and in European sewage treatment plant (STP) effluent it is 61.1. The risk quotient is a risk indicator. When the ratio is greater than 1, it means that the environmental concentration is higher than the no-effect concentration. So according to the values published by Gottschalk *et al.* (2009), AgNP pollution could probably generate adverse effects in the European environment. Using estimates of the worldwide market evolution for products containing engineered nanomaterials (ENM) for the period 2001–2012, Gottschalk *et al.* (2009) also determined the annual increase of ENM concentrations in soil, sludge-treated soil and sediments (Figure 2.1).

	Europe		U.S	
	Concentration (mode value)	Risk quotient (RQ)	Concentration (mode value)	Risk quotient (RQ)
Soil (variation in ng/kg/year)	22.7		8.3	
Sludge treated soil (variation in ng/kg/year)	1581		662	
Surface water (ng/L)	0.7	1.1	0.1	0.2
STP effluent (ng/L)	42.5	61.1	21.0	30.1
STP sludge (mg/kg)	1.7		1.6	
Sediment (variation in ng/kg/year)	952		195	
Air (ng/m3)	0.008	< 0.0005	0.002	< 0.0005

Figure 2.1: Predicted environmental concentrations (PEC) shown as mode (most frequent) value and risk quotients for Europe and the United States (U.S) for different environmental compartments. For air, surface water and sewage treatment plant effluents the results illustrate 2008 engineered nanomaterial (ENM) concentrations. For soil, sludge-treated soil and sediments, the data are shown as annual increases of ENM concentrations. (Figure sourced from Gottschalk *et al.*, 2009).

2.1.2.2 Effects on animal cells and tissues

NPs can enter host cells through caveolae-mediated endocytosis in which NPs either bind to the host cell surface receptors or directly enter the cell via the fluid phase. After migration into the host cells, they enter the lysosomal degradative compartment (Handy *et al.*, 2008). The plasma membrane of cells is made up of a combination of glycosphingolipids and protein receptors organized in glycolipoprotein microdomains termed lipid rafts. NPs can also enter

the host cells by lipid rafts, and therefore are transferred to either Golgi apparatus or endoplasmic reticulum, or they may go through the cell via transcytosis (Moore, 2006). Once inside cells, they may produce toxic effects in the target organ(s). Animal studies have shown that some NPs can penetrate many types of cells and tissues and move through the body systems, including the brain, causing marked biochemical damage. Within the cells, NPs are stored in organelles, such as mitochondria, lysosomes and vesicles. The small particle size, large surface area, and ability to generate ROS are responsible for the toxicity of NPs. Inflammation, necrosis, and fibrosis are effects observed at the tissue level, whereas oxidative stress, antioxidant activity, and cytotoxicity are observed effects at the cellular level (Nowack and Bucheli, 2007).

NPs released as diesel exhaust particles (DEP) and titanium dioxide (TiO_2) can impair mouse spermatogenesis (Ema *et al.,* 2010). However, the mechanisms underlying NP-induced male reproductive dysfunction remain to be elucidated (Yoshida *et al.,* 2006). In a recent study, Komatsu *et al.* (2008) examined the effect of DEP and TiO_2, and carbon black (CB) on mouse Leydig TM3 cells, the testosterone-producing cells of the testis. The uptake of these three NPs into Leydig cells was detected using transmission electron microscopy (TEM) or field emission type scanning electron microscopy (SEM)/energy-dispersive X-ray spectroscopy (FE-SEM/EDS). Komatsu and colleagues examined the cytotoxicity of NPs and their effect on gene expression. TiO_2 was more cytotoxic to Leydig cells than other NPs. The proliferation of Leydig cells was suppressed transiently by treatment with TiO_2 or DEP. The expression of heme oxygenase-1 (HO-1), a sensitive marker for oxidative stress, was markedly induced by treatment with DEP. Furthermore, CB and DEP slightly increased gene expression of the steroidogenic acute regulatory (StAR) protein, which controls mitochondrial cholesterol transfer. In this study, they found that DEPs, TiO_2 and CB were taken up by Leydig cells, and these affected viability, proliferation and gene expression but the type of damage was unique for each NP (Komatsu *et al.,* 2008).

Different *in vitro* studies have shown that AgNP also has the potential to induce cellular toxicity in a variety of organs in mammalian cells. A well-known adverse effect caused by AgNP is the ability to generate free radicals. The ROS produced within cells contains the unpaired electrons and these are capable of producing the free oxygen radicals via normal biochemical reactions (Sayes *et al.,* 2004). The free radicals cause cell damage and ageing and can lead to many diseases such as tumours and heart disease. Sayes *et al.* (2004) showed that the fullerenes can also produce oxidative damage in cultured mammalian cells (Sayes *et al.,* 2004).

2.1.2.3 Health issues

The field of nanotechnology holds the promise of significant improvements in the health and well-being of patients in the future. Studies have shown that the unique size-controlled properties of NPs and their disposition in the body after inhalation are major factors that influence the fate of inhaled NPs (Yang *et al.*, 2008). Prolonged exposure to AgNP in air preferentially affects the lungs and liver tissues. On inhalation, AgNP will reach the lungs, and also the brain through the nasopharyngeal system. In liver cells, AgNP cytotoxicity occurs via oxidative stress (Ahamed *et al.,* 2010). The physiology of the lung makes it an ideal target organ for non-invasive local and systemic drug delivery, especially for protein and poorly water-soluble drugs that have low oral bioavailability. The potential applications of pulmonary drug delivery of NPs to the lungs have been reviewed, specifically in the context of published results reported on NPs in environmental epidemiology and toxicology (Gelperina *et al.,* 2005). The integration of nanotechnology and pulmonary delivery of drug aerosols represents a new and exciting frontier for pharmaceutical dosage forms designed to increase bioavailability and patient compliance, as supported by the results of studies using NPs as either diagnostic or therapeutic agents for lung and systemic diseases (Yang *et al.,* 2008). The potential risk to public health imposed by natural and engineered NPs has been of concern but the knowledge of this impact on public health has so far been limited. Even at non-cytotoxic doses, AgNP is thought to be unsafe probably because its toxic effects are not yet known. It has been shown that AgNP causes toxicity to human mesenchymal stem cells and induces the expression of genes associated with apoptosis in human hepatoma cells. Ahamed (2010) has shown that AgNP provokes cytotoxicity and dopamine depletion in neuroendocrine cells. The effects of AgNP exposure on blood vessels have been investigated. It appears that at low concentrations, AgNP acts as an anti-proliferative and vasoconstrictive factor, whereas at high concentrations, it acts as a proliferative and vasorelaxive factor.

2.1.2.4 Toxicity to plants and soil

The fate and transport of NPs, once they are released into the environment, have not yet been fully addressed, nor have studies detailed the impacts of NPs on plants and soil communities (Dionysiou, 2004; Leacoanet *et al.,* 2004). To date, research on interactions of NPs with plants is minimal, almost non-existent. One hydroponic study reported the effect of aluminium (Al) oxide NP on root elongation (Yang and Watts, 2005). Nano-Al is being used in increasing quantities as an energetic material and it has become one of the most studied NPs for environmental research (Doshi *et al.,* 2008). Research on AlNPs (Doshi *et al.*, 2008)

has addressed the transport of two types of nano-sized Al particles through sand columns along with the associated environmental impact on soil systems. Al-amended soils showed an effect on light output at a lower concentration than the control soil, which suggested a toxic effect on bacteria in Al-amended soil. Moreover, the results suggested that the presence of AlNPs does not have an effect on soil respiration. There were no statistical differences between the time and sizes of peaks in CO_2 production between the AlNP-exposed and control soil samples (Doshi *et al.,* 2008).

2.1.2.5 Effects on aquatic organisms

NPs are toxic to aquatic organisms such as protozoa and fish, and also to bacteria. Protozoa, for example *Stylonychia mytilus*, respond to CNTs in a dose-dependent manner (Zhu *et al.,* 2006) and are a respiratory toxicant to rainbow trout (Smith *et al.,* 2007). Purified CNT did not show any effects on copepods whereas unpurified CNT increased mortality (Templeton *et al.,* 2006). CNT coated with lipids are readily taken up by *Daphnia magna* and the solubility of the CNT is modified through digestion of the lipid, resulting in acute toxicity but only at high concentrations (Roberts *et al.,* 2007).

To more fully assess the toxicity of water-soluble fullerene (nC60), acute toxicity assays have been conducted on several environmentally relevant species including freshwater crustaceans *D. magna* and *Hyalella azteca*, a marine harpacticoid copepod and two fish species, fathead minnow *Pimephales promelas* and Japanese medaka *Oryzias latipes* (Oberdörster *et al.,* 2006). The latter two species have been used to assess the sublethal effects of fullerene exposure by assessing mRNA and protein expression in the liver (Zhu *et al.,* 2005). Previous studies have shown that both sonication and using tetrahydrofuran to solubilize fullerene increased the toxicity of nC60 (Fortner *et al.,* 2005). For the invertebrate studies, nC60 could not be prepared at a high enough concentration to cause 50% mortality (LC_{50}) at 48 or 96 h. The maximum concentrations tested were 35 mg L^{-1} for freshwater and 22.5 mg L^{-1} for full-strength (35 µg L^{-1}) seawater, since at higher concentrations the nC60 precipitated out of the solution. A 21-day exposure study showed a significant delay in mortality in *D. magna* but significantly affected cocoon production at 2.5 and 5 mg L-1 nC60, with a major impact on the population. In fish, neither the mRNA nor protein-expression of cytochrome P450 isozymes CYP1A, CYP2K1 and CYP2M1 appear to be affected. The peroxisomal lipid transport protein PMP70 was significantly reduced in fathead minnow, but not in medaka, indicating potential changes in acyl-CoA pathways (Oberdörster *et al.,* 2006).

2.1.2.6 Anti-bacterial effects

Ag, $AgNO_3$, and AgSD have been applied for the treatment of burns, wounds and several bacterial infections (Percival *et al.,* 2005). The ability to modulate metals into their nanosize can drastically change their chemical, physical and optical properties. Metallic silver in the form of AgNP has made a comeback as a potential antimicrobial agent. The use of AgNP would be beneficial because several pathogenic bacteria have developed resistance to a variety of antibiotics (Rai *et al.,* 2009). Silver in solution ($AgNO_3$) is tolerated by the bacterial strains resistant to Ag^+. The antibacterial activities of AgNP are related to particle size, with smaller sized particles exhibiting higher activity on the basis of equivalent Ag mass content (Morones *et al.,* 2005; Lok *et al.,* 2007). However, the anti-bacterial activity of AgNP may be reduced if particles aggregate in media due to their high electrolyte content. Furthermore, the antibacterial activities of AgNP are dependent on chemisorbed Ag^+, which is readily formed on oxidized surfaces owing to the extreme sensitivity to oxygen (Lok *et al.,* 2007).

2.1.3 Bioavailability of AgNP

The impact of AgNP depends on its bioavailability. Bioavailability is the capacity of a chemical substance to be available for absorption and assimilation by living organisms. In aquatic and terrestrial ecosystems, there are physical, chemical and biological mechanisms which transform contaminants so that they are made more or less accessible for living organisms. According to one study (Lapied *et al.* 2010), the bioavailability of AgNP is lower in soil than in water. Bioavailability and the bioaccumulation of AgNP by organisms are linked to size, shape, chemical composition, charge, surface structure and area, solubility and aggregation state. In many commercial products, AgNP is coated with organic compounds (such as citrate or cysteine) to improve its bioavailability. However, the characteristics that influence AgNP bioavailability require further investigation (Fabrega *et al.,* 2010). Moreover, not only its characteristics have an effect on AgNP bioavailability, but also the environmental conditions play a role too. Indeed, pH, ionic strength and composition, temperature, and NP concentration all interact to affect the aggregation or stabilization of AgNP. The solubility of AgNP determines the proportion of Ag^0, Ag^+ and Ag complexes in a medium. Low solubility makes AgNP less bioavailable. Aggregation of AgNP also creates a lower bioavailability by moving AgNP from the water column to the sediment. However, AgNP aggregation at times could increase its bioavailability for some species (e.g. in filter-feeding bivalves). So, aggregation might reduce the bioavailability of AgNP to some organisms but increase

exposure for others that feed on sediments, algal mats, or biofilms (Fabrega *et al.*, 2010). Only a few studies have investigated the behaviour of AgNP in terrestrial or aquatic environments. In order to evaluate the potential risk induced by AgNP, more studies are necessary. The changes that would be observed in the parameters selected in the two model systems (earthworms and bacteria) would also indirectly measure the bioavailability of AgNP.

2.2 Organisms and applied methods

2.2.1 Bacteria

Bacteria are single-celled organisms that are widespread in the environment (Berg *et al.*, 2002). Bacterial cells are extracellularly surrounded by a cell wall, which maintains the cell's shape and protects it from bursting as a result of osmosis. Most bacterial cells have an additional structure, a capsule or slim-layer, which secrets the cell wall (Van Heijenoort, 2001). Bacterial cells are enclosed by a cell membrane, also known as cytoplasmic membrane, which mainly consists of phospholipids and proteins. The bacterial cell membrane acts as a semi-permeable barrier to regulate the flow of substances such as water and nutrients into and out of the cell and as a surface where some important cellular reactions occur (Koch, 2003).

2.2.1.1 SciTox™ rapid Direct Toxicity Assay (DTA)

It is estimated that there are now over 100,000 chemical substances on the market with about 200 more being added each year. There is the attendant possibility that many of these chemical substances could be released into the environment. One way of testing organisms in the environment to see if they are affected by NPs is to use the SciTox™ method, developed by Lincoln Ventures Ltd. The SciTox™ Assay is a rapid catalytic microbial-based method in which the natural respiratory co-substrate of living cells, oxygen (O_2), is substituted by a synthetic mediator (Tizzard *et al.*, 2004). The electron transport chain (ETC) plays a major role in the respiratory activity of all living cells. In eukaryote cells, the most common electron donor is NADH, and the natural terminal electron acceptor is O_2. In the SciTox™ Assay, O_2 is replaced by a water-soluble redox mediator, ferricyanide (KFCIII). The electrons generated from ETC are captured by KFCIII, which is then reduced to ferrocyanide (KFCII). The rate of microbial oxidation is substantially accelerated because KFCIII is highly soluble relative to

O_2. In the SciTox™ Assay, the redox mediator (KFCIII) functions both as the final electron acceptor in the microbial ETC and a way to quantify the amount of bioconversion through the accumulation of the reduced mediator. This redox process can be illustrated as shown below in Equation 1:

$$e^- + [Fe(CN)_6]^{3-} \text{ (KFCIII)} \rightarrow [Fe(CN)_6]^{4-} \text{ (KFCII)} + H_2O \; . \qquad \text{(Equation 1)}$$

When bacteria are exposed to toxins, respiratory activity is inhibited, resulting in a reduced yield of KFCII. When the electrochemical analysis combined with a toxicity assay, bioconversion occurs through the accumulation of reduced mediator to a current, which can be recorded. The basic principle of SciTox™ is to compare the current produced by healthy cells with the current produced by cells that have been subjected to toxin concentrations.

2.2.1.1.1 Bacterial growth

Most bacterial cells divide by binary fission (Thiel, 1999). In binary fission, one cell divides into two identical single cells, known as clones. The number of cell divisions could be measured as 2^n (where n is an integral number). Growth of the bacterial cell can be divided into four distinct phases. In the lag phase, there is no increase in cell number because cells need time to adjust their metabolism to the new conditions. In the growth phase, cell numbers increase exponentially. However, cells cannot maintain growth exponentially in a closed system, in which growth is affected by a decline in nutrients and a build-up of growth-inhibiting substances. In the stationary phase, cells stop their rapid growth and slow their metabolism. In the decline phase, cells lose their ability to divide and the cells start dying. To maintain optimal cell viability, it is best to grow bacterial cultures to an early stationary phase (Thiel, 1999).

2.2.1.1.2 Electron transport chain (ETC)

The components of ETC are located in the inner membrane of mitochondria in eukaryote cells or cytoplasmic membrane in bacteria. The high energy molecule adenosine triphosphate (ATP) is synthesized from adenosine diphosphate (ADP) in the catalysis by ATPase, driven by the energy generated from electrons transferred through membranes (Fenchel *et al.*, 2006). The NADH (nicotinamide adenine dinucleotide, reduced form) and FADH (flavin adenine

dinucleotide, reduced form) act as electron carriers, and molecular O_2 is the final electron acceptor (Voet *et al.*, 2006). Thus in the ETC, energy from the oxidation of carbon compounds such as glucose is used to pump protons across the membrane, and the electrons passing through the ETC are, in many cases, ultimately transferred out of the ETC to reduce O_2 to carbon dioxide (CO_2) and water (H_2O). In contrast to eukaryotes, the bacterial ETC is more complex. For example, *E. coli* contain 15 different dehydrogenases and several oxidases (Calhoun and Gebbis, 1993).

2.2.1.1.3 Mediator-based biosensors

A biosensor is a device that detects, records, and transmits information regarding a physiological change on exposure to various chemicals or biological materials in the environment. More technically, a biosensor is a probe that integrates a biological component, such as a whole bacterium, or a biological product, such as an enzyme or antibody, with an electronic component to yield a measurable signal. In general, biosensor technology does not offer superior performance relative to traditional laboratory-based assays, particularly in terms of sensitivity, selectivity and reproducibility. However, biosensors do offer advantages for environmental monitoring because of their specificity, fast response times, low cost, ease of use, and continuous real-time signals. The enormous diversity of microbial species available makes whole cells potentially valuable biocatalysts for biosensors in environmental applications (Pasco *et al.*, 2005). A biosensor normally has two components: a biological component and a transducer. A receptor is responsible for the selectivity of the sensor. Examples include enzymes, antibodies, nucleic acid, lipid layers, and whole tissues of higher organisms or, in the case of microbial biosensors, whole microorganisms, which are usually immobilized onto an electrode surface. The transducer translates the physical or chemical change by recognizing the analyte and relaying it through an electrical signal.

In a biosensor, the biological component converts the substrate to a product. This reaction is determined by the transducer, which converts it to an electrical signal. The output from the transducer is amplified, processed and displayed. The principal transducers used in biosensor technologies are electrochemical, photometric, acoustic optical, piezoelectric or thermal devices (D' Sousa, 2001).

2.2.1.1.4 Electrochemical analysis

There are several transducers applied for whole-cell biosensors, including electrochemical, optical, photometric, calorimetric, acoustic and electronic. The most often used transducer, and the one used in my research, is an electrochemical transducer which measures indirectly both the generation and consumption of electrons during a biochemical reaction (Chaubey and Malhotra, 2002). In electrochemical analysis, the reduced form of the mediator (KFCII) is converted back to the oxidized form (KFCIII) at the electrode external to the cell. Therefore, the quantity of charge required for re-oxidation of the mediator is a direct measure of the substrate oxidation, as shown in Equation 2:

$$[Fe(CN)_6]^{4-} \rightarrow [Fe(CN)_6]^{3-} + e^- . \qquad \text{(Equation 2)}$$

There are three electrodes involved in the MICREDOX® Assay; an auxiliary electrode, a working electrode, and a reference electrode. The working electrode is poised at a fixed potential relative to the reference electrode. The current flow between the working electrode and auxiliary electrode is equal to the rate of charge transfer. The change in concentration of the electrochemical mediator is measured based on the electrochemical oxidation or reduction at the applied potential that is detected at the working electrode. By comparing the ratio of the measurable response obtained in the presence and absence of a toxin, it is possible to obtain an index of respiratory inhibition. The toxic effects are reported as an inhibition index of the measurable cellular activity.

2.2.2 *Aporrectodea caliginosa* earthworm

Aporrectodea caliginosa is the most abundant earthworm species in grasslands and agricultural ecosystems (Pérez-Losada *et al.,* 2009). It is also the most common introduced earthworm in New Zealand. *A. caliginosa* live in the top 20–30 cm of soil. An adult *A. caliginosa* has a clearly visible clitellum close to the head whereas a juvenile does not. They produce mounds of digested soil and plant matter which help to improve soil structure and contain nutrients in a form easily taken up by plants. These earthworms rarely come to the surface voluntarily. Sometimes they go as deep as 3 m into the ground and literally plough up the top metre of the ground. For that reason, earthworms are of great value for garden and agriculture cultivation. Because of their abundance in New Zealand farms, including on the Lincoln University Dairy Farm, *A. caliginosa* was used in all experiments for ecotoxicity evaluations of NPs compared with the effects caused by $AgNO_3$.

2.2.2.1 Dose–response relationship

Toxicology is based on the principle of a relationship between the dose (amount of the chemical exposed to) and the reaction to it, which is the response (Figure 2.2). In general, the greater the range of chemical concentrations exposed to, the more accurate the dose–response relationship..

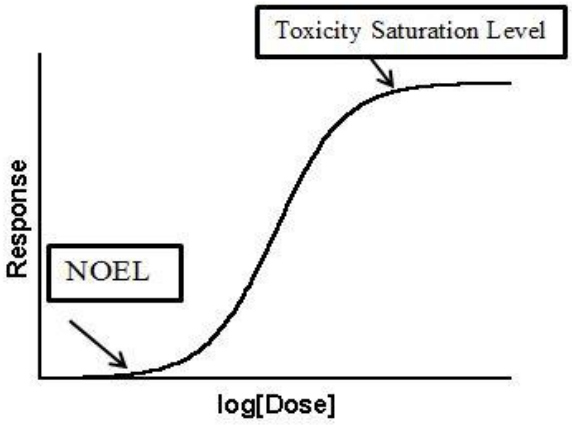

Figure 2.2: Dose–response relationship curve: on the *x*-axis is the concentration of the chemical exposed to and on *y*-axis is the response.

Generally, the dose-response is quite variable in individual organisms even when they belong to the same species. The dose–response relationship can be experimentally derived and is a measure of the toxicity of all individuals from the same group when they are exposed to a toxic chemical.

When applied to the effect of chemicals on bacterial respiration (Figure 2.3), the entire dose-dependent profile could be classified as: at low toxicant concentrations (sub-inhibitory level), there are no observed effect levels (NOEL); at concentrations above the toxicant threshold, the respiratory activity of living bacteria declines as the concentration of toxic compounds increases; and at high toxicant concentrations, bacteria are killed due to the inhibition of key metabolic pathways (toxicity saturation level).

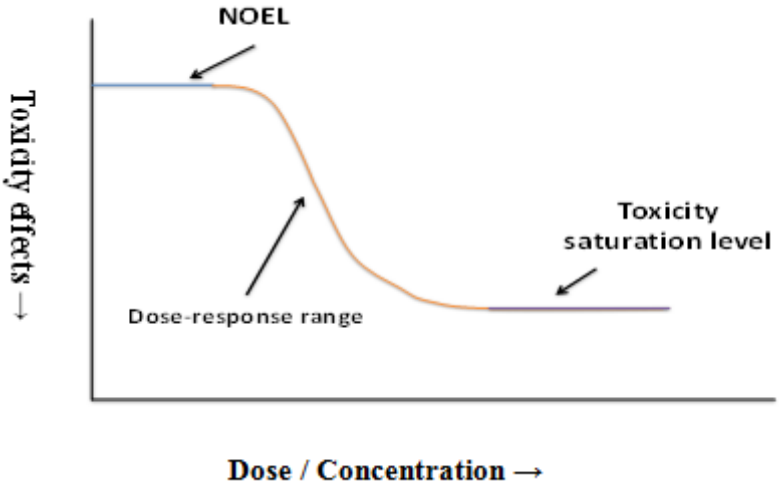

Figure 2.3: Dose–response relationship curve applied to respiratory activity. At higher concentrations, respiration is inhibited.

2.2.2.2 Comet Assay and Micronucleus Test

Both the Micronucleus Test and Comet Assay have been proposed as biomarkers of DNA damage. The Comet Assay has been used as a sensitive tool for measuring DNA damage in a variety of organisms including earthworms. It has been used for genotoxicity assessment to detect even low level DNA damage in single cells (Tice *et al.*, 2000; Muangphra and Gooneratne, 2011a, b; Muangphra *et al.*, 2012). The Micronucleus Test is a well-established assay in genotoxicity testing and human biomonitoring for detecting several nuclear anomalies. The frequencies of coelomocyte MN and BN have been used to assess chromosomal aberrations and inhibition of cytokinesis, respectively (Muangphra and Gooneratne, 2011a, b; Muangphra *et al.*, 2012).

2.2.2.2.1 Coelomocytes in earthworms

In earthworms, coelomocytes are the circulating leukocytes present in the coelomic cavity and play an important role in immune defence. They have been used to study the effect of heavy metal genotoxicants such as nickel (Ni) and cadmium (Cd) (Reinecke and Reinecke, 2004). Coelomocytes respond to environmental and experimental challenge by the activation of stress markers, such as heat shock protein hsp70 (Homa *et al.*, 2005). Coelomocytes are of different shapes in different species. For example, coelomocytes in *Caenorhabditis elegans* are ovoid in shape, while they can occur as stellate shaped in some other species. Each

coelomocyte is about 10–15 µm in diameter and its cytoplasm contains a distended rough endoplasmic reticulum (RER) and many membrane-bound vesicles of various sizes (Fares and Greenwald, 2001).

Coelomocytes, of several distinct types, circulate in fluid-suspension in the earthworm coelomic cavity. Earthworm coelomocytes have been classified largely on the basis of differential staining, ultrastructural morphology, the chemical nature of their inclusion granules, as well as functional traits (Hamed *et al.*, 2002). Two main populations of coelomocytes are the eleocytes: hyaline amoebocytes also known as acidophils, and granular amoebocytes also known as basophils (Cooper and Stein, 1981). They are present in various proportions in different species.

2.2.2.2.2 Comet Assay

The Comet Assay, also called single-cell gel electrophoresis, is a sensitive and a rapid method to detect DNA damage in cells. This method has been used in biomedical research, environmental bio-monitoring studies and genotoxicity testing. Since DNA damage may result in severe consequences for individuals, species and ecosystems, this technique is regarded as an important indicator in the assessment of earthworm health (Casabé *et al.*, 2007).

The Comet Assay is an extremely sensitive assay of DNA damage. It can be used to detect DNA damage caused by double-strand breaks, single-strand breaks, alkali labile sites, oxidative base damage, and DNA cross-linking with DNA or protein. The concept of the Comet Assay is that undamaged DNA retains a highly organized association with matrix proteins in the nucleus. When damaged on exposure to toxins, this organization is disrupted. The individual strands of DNA lose their compact structure, relax, and are released. When an electrical field is applied, the DNA is drawn towards the anode, which is positively charged. Undamaged DNA strands are too large and travel slowly, whereas the smaller damaged fragments are free to move farther in the same period of time. Therefore, the amount of DNA fragments that travel farthest is a measure of cellular DNA damage. The image analysis of the Comet Assay measures the overall intensity of the fluorescence for the whole nucleoid and the fluorescence of the migrated DNA, and compares the two signals. That is, the greater the signal from the faster migrating DNA fragments, the larger the amount of DNA damage. The overall DNA structure resembles a ‘comet’, with a circular head corresponding to the

undamaged DNA and a tail of damaged DNA. According to the fluorescence image, the brighter and longer the faster travelling tail is, the greater the extent of DNA damage.

2.2.2.2.3 Micronucleus Test

The Micronucleus Test is used in toxicological screening to identify potential genotoxic compounds. The aim of the test is to detect MN, which is small membrane-bound DNA fragments formed during the metaphase/anaphase transition of mitosis in cell division. Chromosomal damage, which is caused by toxin exposure, leads to the formation of MN in bi- or multinucleated interphase cells. Harvested and stained interphase cells can then be examined microscopically for the presence of MN or BN and quantified. MN test detects the activity of clastogenic and aneugenic chemical / physical stress.Scoring of MN and BN can be performed in mononucleated cells that did not divide and binucleated cells that completed nuclear division but this was not followed by cytoplasmic division. In such conditions, the frequency of MN and BN in cells provides an indication of the background level of chromosome/genome mutations that can occur *in vivo* on exposure to genotoxic compounds.

2.2.2.3 Polymerase chain reaction (PCR)

PCR was developed by Kary Mullis in the 1980s (Shampo and Kyle, 2002) and it has facilitated DNA research in many scientific fields. PCR is a fast and efficient technology that can amplify even a small amount of tissue of interest into a large amount of DNA sequences (2^n, where n is the cycle number). PCR is an enzyme-mediated, temperature-based reaction. A typical PCR cycle involves denaturing of the DNA double-strand for 2–3 min at 95°C, primer annealing for 30–60 s at *c*. 60°C, and primer extension at 72°C (Judelson, 2002). The extension period is based on the size of PCR products (normally 1 min for 1kb). There are many factors that could influence the specificity [yield of interest PCR product(s)] and fidelity (accuracy) of PCR, including heat-stable DNA polymerase, pH, GC content of primers and DNA targets (Grunenwald, 2003).

2.2.2.3.1 Primer design

A successful PCR starts with good primer design. Poorly designed primers give either non-specific PCR results or even no PCR results. Because of the interactions between the primer

itself or primers and the template, a few rules should be followed in the design of proper primers (Hyndman and Mitsuhasi, 2003):

- Melting temperature between 55°C and 65°C (usually corresponds to 45 –55% G+C).
- Around 20–26 base length.
- Prevent formation of primer dimers.
- Absence of significant hairpin formation (usually > 3 bp).
- Low specific binding at the 3’ end to avoid mispriming.
- Lack of secondary priming sites in the template.

2.2.2.3.2 Reverse transcriptase qualitative PCR (RT-qPCR)

Quantifying gene expression has become a popular assay in many molecular biological laboratories. By measuring the amount of cellular RNA, it is possible to determine to what extent that particular gene is being expressed. For many genes, the expression levels change significantly from gene to gene, cell to cell, and on exposure to xenobiotics. Some examples of quantitative gene expression include validation of the extent of transcription of a gene, to study the difference in expression of a gene in a diseased state compared to the normal state, change in gene expression during cell differentiation or development, change in expression in cells that are exposed to a chemical substance, quantification of non-coding RNA gene expression to validate the effectiveness of small interfering RNA or anti-sense oligonucleotides, and as a diagnostic tool (Schmittgen and Livak, 2008). Development of PCR technology is based on reverse transcription and fluorophores that permit measurement of DNA amplification during PCR in real time, i.e., the amplified product is measured at each PCR cycle. Hence, it is also called real-time PCR (RT-qPCR). Real-time PCR can also be applied to detect and quantify DNA in samples to determine the presence and abundance of a particular DNA sequence in the samples (Ponchel *et al.*, 2003).

There are several real-time PCR detection methods. SYBR Green-based detection is the least expensive and one of the easier methods available for real-time PCR. Most real-time systems detect and accommodate SYBR Green, making it also the most flexible method. SYBR Green specifically binds to double-stranded DNA by intercalating between base pairs, and fluoresces only when bound to DNA. Detection of the fluorescent signal occurs during the PCR cycle at the end of either the annealing or the extension step when the greatest amount of double-stranded (ds) DNA product is present. However, SYBR Green can also detect any dsDNA non-specifically. Therefore, the reaction must contain a combination of primers and a master

mix that generates only a single gene-specific amplicon without producing any non-specific secondary products.

2.3 Summary

With the increasing number of applications of NPs in different industries, assessing the risks posed by NPs has become a research area that more and more scientists are interested in. In this study, evaluation of the ecotoxicity of AgNP will be performed on both *E. coli* bacteria and *A. caliginosa* earthworms.

The SciTox^{TM} rapid DTA Assay has been widely used as a whole-cell biosensor. The principle of the DTA Assay is based on comparing the electric current produced by healthy bacterial cells relative to that produced by cells exposed to toxicant concentrations. The dose–response relationship and EC_{50} will be determined in *E. coli* cultures exposed to known AgNP, $AgNO_3$ and standard toxicant 2, 4-DCP concentrations. A growth inhibition assay will also be performed in *E. coli* cultures exposed to known AgNP and $AgNO_3$ concentrations.

Earthworms are primary decomposers of soil organic matter and earthworm population effects are used as bioindicators of soil pollution. In addition, physiological and biochemical reactions that occur in earthworms are used as biomarkers of exposure to soil pollutants. Assessment of earthworm DNA damage is also an important aspect of ecotoxicity studies. In this research, the doses selected for all *A. caliginosa* experiments were based on a fraction of the LD_{50} values determined from an acute toxicity study. Comet Assay and Micronucleus Tests were performed to measure DNA damage in earthworms following exposure to AgNP, again to a fraction of the LD_{50} values determined from an acute toxicity study. PCR is an indispensable technique in biochemistry. It effectively amplifies a particular DNA sequence. The purpose of using PCR in this research was to sequence the *SOD* gene for the first time in the *A. caliginosa* earthworm and then to determine the gene expression of the *SOD* gene using RT-qPCR.

Chapter 3
SciTox™ Rapid DTA Assay

3.1 Introduction

AgNP is well known for its anti-microbial activity (Ahmad *et al.,* 2007; Lok *et al.,* 2007; Su *et al.,* 2007) and it is used to control bacterial growth in a variety of applications including painting and burn woods (Dibrov *et al.,* 2002). The toxicity of AgNP has been recognized by the contribution of two main factors, released free Ag^+ ions (Lok *et al.,* 2007; Su *et al.,* 2007) and the size of particles (Ahmad *et al.,* 2007). Ag^+ is an anti-bacterial agent that inhibits bacterial cell growth by reacting with electron donor groups (especially sulfhydryl groups) (Slawson *et al.,* 1992) thereby inhibiting the activity of several enzymes (containing mainly thiol groups) (Jung *et al.,* 2008; Park *et al.,* 2009). At low Ag^+ concentration, the Na^+ translocating NADH: ubiquinone oxidoreductase (NQR) is one of the primary targets for Ag^+ ions. Ag^+ ions have been shown to inhibit energy-dependent Na^+ transport in membrane vesicles of *Bacillus* sp. strains (Semykina and Skulachev, 1990) and also inhibit purified NQR of *Vibrio alginolyticus* (Hayashi *et al.,* 1992). Additionally, it has been reported that smaller sized particles of AgNP have a greater toxic effect on bacteria than larger sized particles (Lok *et al.,* 2007).

Whole-cell biosensors technology has been widely employed to assay the toxicity of environmental compounds by directly linking the catabolic activity of living bacterial whole cells to their analytes (Kaiser and Palabrica, 1991; Farré *et al.,* 2001; dos Santos *et al.,* 2002). This offers many advantages including fast response, low cost and the ease with which to grow bacterial cells (Hansen and Sørensen, 2001). The SciTox™ rapid DTA is a whole-cell microbial assay that measures toxicity through the inhibition of bacterial respiration (Tizzard *et al.,* 2004). It is currently used commercially to measure the impact of toxic chemicals on biological materials resident in the environment (Pasco *et al.,* 2004, 2005). It is a rapid catalytic microbial-based method in which the natural co-substrate, O_2, is substituted by a synthetic mediator, KFCIII. Oxidation of the substrate drives electrons into the ETC and ultimately to the mediator, KFCIII. The subsequent transfer of electrons from the reduced mediator to an electrode can generate a measurable current. This measurement can be used to quantify the magnitude of respiration inhibition and thus, the toxicity (Tizzard *et al.,* 2004).

The dose–response relationship is one of the key parameters used to indicate the toxicity of traditional chemicals, and is also the first step in toxicity assessment. It has been used previously to detect environmental chemicals (Pasco *et al.,* 2008) and monitor waste waters (Tizzard *et al.,* 2004). In this study, the dose–response relationship of bacterial cells to AgNP will be determined in a SciTox^{TM} DTA Assay. Clearly, it is advantageous to study bacterial cells initially before using higher organisms such as earthworms. By using the SciTox^{TM} DTA Assay, the respiratory activity of bacterial cells could be assessed in relation to the toxicity of AgNP and compared with the effect on $AgNO_3$. The extent of toxicity can then be determined by using the index EC_{50} (50% inhibition of respiration).

To do this, *E. coli* bacteria were used as the sensor strain because *E. coli* has been employed previously in toxicity assays (Kaiser and Palabrica 1991; dos Santos *et al.,* 2002). To better understand the toxic effects of AgNP, simultaneous toxicity measurements were made with a traditional Ag toxicant, $AgNO_3$, and with the standard toxicant 2,4-DCP.

3.2 Materials and methods

3.2.1 Buffer preparation

- *Washing Buffer:* 10.62 mg L^{-1} of KH_2PO_4 and 21.25 mg L^{-1} of K_2HPO_4 made up to 1 L with double-distilled water, autoclaved, and stored at room temperature.
- *Re-suspension Buffer:* 10.62 mg L^{-1} of KH_2PO_4, 21.25 mg L^{-1} of K_2HPO_4 and 7.46 mg L^{-1} of KCl made up to 1 L with double-distilled water, autoclaved, and stored at room temperature.
- *PEG (Polyethyleneglycol) solution:* 0.25 g of PEG was mixed with 100 ml of distilled water, boiled and then cooled to room temperature; prepared fresh for use.
- *GTE (Glucose-Tris-EDTA) solution:* 50 mM glucose, 25 mM Tris-Cl (pH adjusted to 8.0) and 10 mM EDTA (ethylenediaminetetraacetic acid; pH is 8.0), autoclaved and stored at 4°C.
- *NaOH/SDS alkaline lysis solution:* 0.2 M of NaOH and 1% of SDS (sodium dodecyl sulfate) were mixed, autoclaved and stored at 4°C.
- *STESDS solution:* 10 mM Tris, 1 mM EDTA, 100 mM NaCl and 1% SDS were mixed, autoclaved and stored at 4°C.

- *10 × TBE stock:* 108 g Tris base, 55 g boric acid and 40 ml of 0.5 M EDTA (pH 8.0) were made up to 1 L with dH_2O, autoclaved and stored at room temperature.
- *Herbert salt:* 10.1 g MgO, 2 g $CaCO_3$, 53 ml of concentrated HCl, 5.6 g $FeSO_4$, 1.4 g $ZnSO_4 \cdot 7H_2O$, 0.25 g $MnSO_4 \cdot 4H_2O$, 0.25 g $CuSO_4 \cdot 5H_2O$; 0.28 g $CoSO_4 \cdot 7H_2O$ and 0.06 g H_3BO_4 were mixed, made up to 1 L with dH_2O, autoclaved and stored at 4°C.

3.2.2 Standard toxicants

- $AgNO_3$ and AgNP (100 nm) were purchased from Sigma Aldrich Chemical Co. (St Louis, USA). In experiments, $AgNO_3$ and AgNP were diluted in distilled water to achieve the desired concentrations. The AgNP powder purchased from Sigma was relatively insoluble at higher concentrations and therefore existed as a suspension.
- 2,4-Dichlorophenol (2,4-DCP): weighed 140 mg and made up to 100 ml with dH_2O in a 100-ml flask. The final concentration was 1,400 mg L^{-1}.

3.2.3 Culture media for bacteria studies

- *PC agar:* 1.7 g of m-plate count broth with 15 g agar, made up to 1 L with distilled water, autoclaved and stored at 4°C.
- *Nutrient Broth (NB):* weighed 8 g of nutrient broth, made up to 1 L with distilled water, autoclaved and stored at 4°C.
- *Davis Minimal Media (DMM):* mixed K_2HPO_4 (7 g), KH_2PO_4 (2 g), $(NH_4)_2SO_4$ (1 g), glucose (1 g), sodium (tri-) citrate (0.5 g), $MgSO_4 \cdot 7H_2O$ (0.1 g), and made up to 1 L with distilled water, autoclaved and stored at 4°C.

3.2.4 *E. coli* cultures

In this research, three-step cell culture was used in sterile conditions. Firstly, the bacterial cells were transferred from the stock to micro-plate, then to a liquid-pre-culture, and finally to the main culture.

3.2.4.1 Agar plate culture

All the *E. coli* (strain BW25113) bacterial cultures were stored at -80°C. The bacterial cells were then streaked into PC agar (to keep the sample pure). After that, agar plates were wrapped with parafilm and placed in an incubator to allow amplification. For *E. coli*, the optimal growth conditions were 16 h at 37°C. Finally, they were stored in the refrigerator at 4°C until required. I continued culturing every 2 weeks to maintain fresh cultures.

3.2.4.2 Liquid pre-culture

A single colony was selected from an appropriate m-plate, and transferred into pre-culture media (NB) in a 100-ml conical flask. The volume of pre-culture media was 20 ml. Each pre-culture was grown at the optimal temperature of 37°C, in a shaking incubator (Ratek OM11) at 200 rpm (ideal conditions for bacterial cell amplification in an oxygen/nutrient-rich environment), for 16 h. After growth, cells were stored at 4°C until required.

3.2.4.3 Main culture

Cultured microorganisms in media were inoculated with 1% of the pre-cultures and grown until late exponential stage. DMM was used for the main culture, and the optimal condition was at 37°C, 200 rpm for 16 h.

3.2.4.4 Cell harvest

After main-culture, the *E. coli* bacterial cells were ready for harvest. The bacteria-containing cultured solutions were transferred into several plastic tubes, and then centrifuged at 11,000 rpm for 5 min at 20°C. After centrifugation, bacterial cells formed pellets at the bottom of tubes. The clear liquid was poured out and washing buffer added to thoroughly wash the cells before centrifuging again. Cell washing was repeated three times. Then phosphate-buffered saline solution was added to re-suspend the bacteria.

3.2.5 Optical density measurement

Optical density (OD), also known as the index of light transmission, is also referred to as the absorbance. It is a measure of the light intensity at a specified wavelength that passes through

a sample relative to the intensity of the incident light. The higher the OD of a material, the slower the movement of the wave through the material. Generally, OD is used as the measure of the concentration of a target solution. It is widely used in biochemistry, and can be calculated by using the following formula (Voet *et al.*, 2006):

$$A = - \log_{10} (I / I_0), \qquad \text{(Equation 3)}$$

where A indicates the absorbance, OD; I is the intensity of the transmitted light and I_0 is the intensity of the incident light.

In the SciTox™ toxicity assay, the *E. coli* cells were adjusted to optical density of 25 at 600 nm (OD_{600}), using a UNICAM 8625 UV/VIS spectrophotometer. An OD of 25 (1:40) at 600 nm represents the final concentration of the bacterial resuspension solution used for toxicity assay, which is about 4×10^9 bacterial cells per millilitre. In the SciTox™ rapid mediated DTA Assay, the lowest concentration of bacterial cells at OD_{600} should be at least 25 to obtain good results (Pasco *et al.*, 2008). In the first step, 25 µl of concentrated bacteria-solution was diluted 40-fold with 975 µl of buffer, mixed (25 µl bacteria; 975 µl buffer solution) and the absorbance of the 1-ml solution at 40-fold dilution read, as 'A'. Assume the absorbance reading is 1.429. For subsequent estimations the following calculation was used: (A × N) ÷ 0.625, where N was always equal to 1 ml in this case. For example, 1.429 × 1 ml ÷ 0.625 = 2.286 ml (this means we actually required 2.286 ml of buffer solution). The buffer solution added was calculated as: 2.268 ml - 1 ml = 1.286. After mixing with 1.286 ml of buffer solution, step 2 was repeated until the final reading was as close to 0.625 as possible. Then the final solution was ready for use in toxicity tests.

3.2.6 SciTox™ DTA Assay

Due to the physical properties of AgNP, a modified experimental method (Method II) based on the original method (Method I) had to be employed. The main difference between the two methods was that there was a centrifuge step in Method II prior to addition of the mediator (Figure 3.1). The extra centrifuge step was implemented so that *E. coli* cells could be separated from the toxicant and re-suspended in buffer before addition of the KFCIII redox mediator.

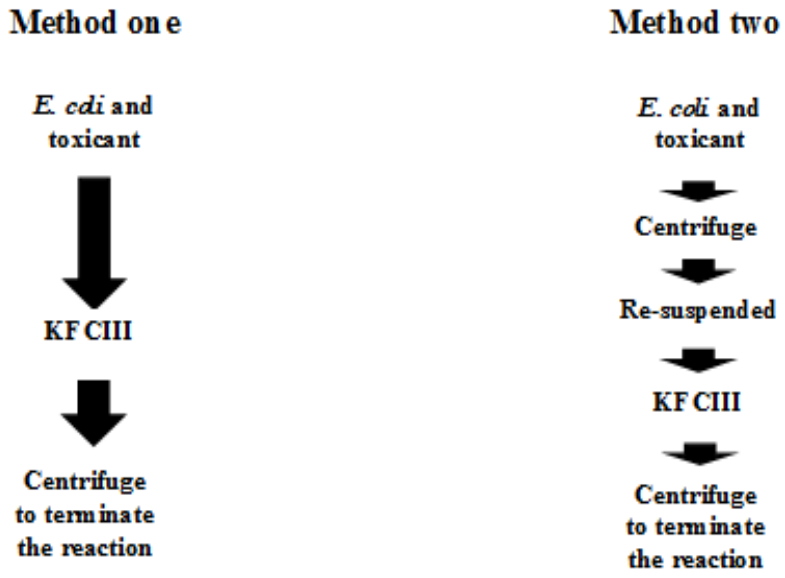

Figure 3.1 Steps in SciTox™ Rapid DTA assay Methods I and II.

3.2.6.1 Method I

Method I as shown in Figure 3.1 was employed with all three toxicants. Assays were set up in 96-well microtitre plates. Freshly cultured cells were harvested and concentrated to OD_{600} of 25. All the assay solutions (as shown in Tables 3.1 – 3.3) were added using a 12-channel pipette and the bacterial cells were added last. The 96-well plate was covered with foil, and placed in a shaking incubator at 37°C at 200 rpm for a 1-h single-incubation. Reactant solutions were transferred from each well to clean Eppendorf tubes. The reaction was terminated by centrifuging samples at 11,000 rpm for 5 min. Pellets were removed, supernatants were transferred to clean Eppendorf tubes, and stored at 4°C, until required for electrochemical analysis.

The effects of 2,4-DCP, $AgNO_3$ and AgNP on fresh *E. coli* cell respiration was monitored using the SciTox™ toxicity assay. Cell respiration activity was calculated as shown in Equation 4. The EC_{50} value was subsequently derived using the computer program SigmaPlot.

3.2.6.2 Method II

Method II, with all three toxicants, followed the same procedure as in Method I except for an additional centrifuge/resuspension of the *E. coli* cells before adding KFCIII. The inclusion of this step prevents any interaction between KFCIII and the toxicant AgNP. Initially, assays

were set up in 96-well microtitre plates. The standard toxicant 2,4-DCP at different dilutions and bacterial cells was added using a 12-channel pipette. The 96-well plate was covered with foil, and incubated in a shaking incubator at 37°C, 200 rpm, for different incubation times: 15 min and 30 min. Next it was centrifuged at 4000 rcf for 5 min. Supernatants were carefully removed and the pellets re-suspended in 200 µl buffer; 70 µl of the KFCIII mediator (molecular weight 329.25 g mol^{-1}; 4.12 g of KFCIII was added to 50 ml of distilled water and made up to a final concentration of 250 mM, covered with foil to avoid light, and stored in a refrigerator at 4°C) was added to the resuspended solutions and incubated in an orbital shaker at 37°C, 200 rpm, for three different incubation times: 30 min, 45 min and 60 min. Reactant solutions from each well were then transferred into clean Eppendorf tubes. The reaction was terminated by centrifuging samples at 11,000 rpm for 5 min. Pellets were removed, supernatants were transferred to clean Eppendorf tubes, and stored at 4°C until required for electrochemical analysis. The EC_{50} value was then calculated.

3.2.6.3 Reactants used in both methods (I & II)

The reactants (sensor cells and toxicants) used in the two methods are shown in the following tables (Tables 3.1 – 3.3).

Table 3.1 DTA Assay with 2,4-DCP

2,4-DCP concentration (mg L^{-1})	**Volume of 2,4-DCP (µl)**	**Volume of dH_2O for dilution (µl)**	**Volume of bacterial cells (µl)**	**Volume of KFC III 60 mM (µl)**	**Total volume Reaction mix (µl)**
0 (control)	0	500	200	70	770
0.3	0.15	499.85	200	70	770
1	0.5	499.5	200	70	770
3	1.5	498.5	200	70	770
10	5	495	200	70	770
30	15	485	200	70	770
100	50	450	200	70	770
300	150	350	200	70	770
500	250	250	200	70	770
700	350	150	200	70	770

Table 3.2 DTA Assay with $AgNO_3$

$AgNO_3$ concentration (mg L^{-1})	**Volume of $AgNO_3$(µl)**	**Volume of dH_2O for dilution (µl)**	**Volume of bacterial cells (µl)**	**Volume of KFC III 60 mM (µl)**	**Total volume reaction mix (µl)**
0 (control)	0	500	200	70	770
0.04	0.04	499.96	200	70	770
0.4	0.4	499.6	200	70	770
1	1	499	200	70	770
2	2	498	200	70	770
4	4	486	200	70	770
10	10	490	200	70	770
40	40	460	200	70	770
100	100	400	200	70	770
400	400	100	200	70	770

Table 3.3 DTA Assay with AgNP

AgNP concentration (mg L^{-1})	Volume of AgNP toxicant (µl)	Volume of dH_2O for dilution (µl)	Volume of bacterial cells (µl)	Volume of KFC III 60 mM (µl)	Total volume reaction mix (µl)
0 (control)	0	500	200	70	770
0.01	0.01	499.99	200	70	770
0.1	0.1	499.9	200	70	770
1	1	499	200	70	770
5	5	495	200	70	770
10	10	490	200	70	770
50	50	450	200	70	770
100	100	400	200	70	770
200	200	300	200	70	770
500	500	0	200	70	770

3.2.7 *E. coli* growth inhibition assay with AgNP

Since there were no effects of AgNP on the respiratory activity of *E. coli* with either Method I or II, a growth inhibition assay was conducted. Assays were set up the in 24-well microtitre plates. AgNP at different dilutions was added to the pre-culture media (Table 3.4). To every 10 ml of stock AgNP solution (700 mg L^{-1}) 4 ml of distilled water was added to give an AgNP solution of 500 mg L^{-1} and this was used in this assay at the volumes shown in Table 3.4. A single colony from an appropriate m-plate was transferred into each well containing a mixture of substance and media. The plate incubation was carried out in an orbital shaker at 37°C, 200 rpm, for 16 h. After incubation, optical density measurements were carried out to determine the growth of *E. coli* bacteria inhibited by AgNP.

Table 3.4 Reactants used in growth inhibition toxicity assay

AgNP concentration (mg L^{-1})	Volume of AgNP (µl)	Volume of dH_2O for dilution (µl)	Volume of NB media (µl)	Total volume (µl)
0 (control)	0	20	200	1000
0.1	0.2	19.8	200	1000
0.3	0.6	19.4	200	1000
0.5	1	19	200	1000
1	2	18	200	1000
1.5	3	17	200	1000
2	4	16	200	1000
3	6	14	200	1000
5	10	10	200	1000
10	20	0	200	1000

3.2.8 Electrochemical analysis

The analytical signal in whole-cell-mediated bioassays is generally derived from the biological generation of reduced mediator that occurs during incubation. Limiting-current microelectrode amperometry is an electrochemical method available for measuring the quantity of the reduced electron acceptor, KFCII. The equipment used for electrochemical analysis in this research is shown below (Figure 3.2).

To begin with, the working electrode was polished for 20 s using a flocked twill polishing pad containing slurry of 0.05 µm of an alumina powder. The electrode was rinsed with distilled water and any residual water removed without contact with the Pt disc. The working electrode was placed directly into the electrolyte solution containing the test sample along with the Ag/AgCl reference electrode and Pt auxiliary electrode. The working electrode was poised at +450 mV relative to the Ag/AgCl reference electrode. The anodic current, obtained 10 s after imposing the applied potential was read as the limiting-current value. After each analysis, the

working-electrode was re-polished and the BAS MF-2031 2 ml minicell rinsed in distilled water, using a lint-free tissue to dry it (Pasco *et al.*, 2008).

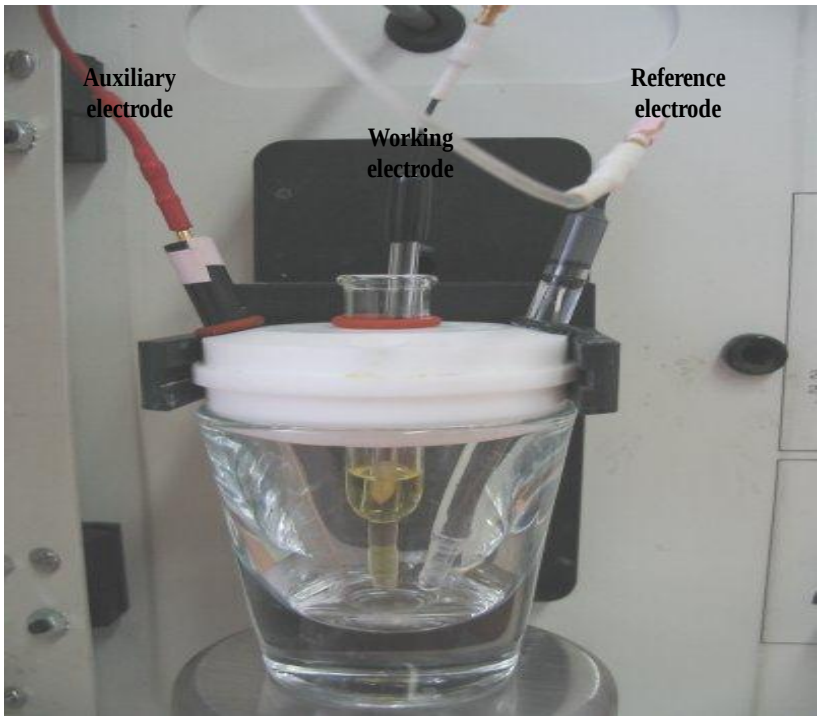

Figure 3.2 Equipment used for electrochemical analysis in this research.

3.2.9 Data analysis

After electrochemical analysis, the data were collected and cell activity calculated using Equation 4. Activity here represents the normal activity of bacterial cells as affected by target toxicants, which is proportional to the toxic effects.

$$\text{Activity} = [i_{lim}\ (\text{sample}) / i_{lim}\ (\text{control})] \times 100\% , \qquad \text{(Equation 4)}$$

where i_{lim} (control) is the limiting current measured in the control, and i_{lim} (sample) is the limiting current of samples measured in electrochemical analysis.

The computer programme SigmaPlot was used to plot the dose–response relationship. The toxicant concentrations and activity calculated relative to each fixed concentration were transferred to SigmaPlot directly. Both the standard error and EC_{50} were calculated.

Analysis of variance was used to determine any significant differences between the current readings of *E. coli* culture exposed to the standard toxicant 2,4-DCP at four different incubation times to determine the optimal incubation period in the two SciTox^{TM} DTA Assay methods (the classical method [Method I] and the modified method [Method II]

3.3 Results

3.3.1 SciTox™ rapid Direct Toxicity Assay

A standard toxicant 2,4-DCP was used in the SciTox™ rapid DTA Assay. Stock concentrations of the standard toxicant were prepared as 1,400 mg L^{-1} and the total volume of the reaction mix was 770 µl. The reaction was carried out for different incubation times after addition of the toxicant and the mediator (KFCIII) was applied to determine optimal assay conditions (Table 3.5).

Table 3.5 Different combinations of incubation times to standard toxicant 2,4-DCP

Incubation points	**Time combination 1**	**Time combination 2**	**Time combination 3**	**Time combination 4**
After addition of 2,4-DCP	15 min	30 min	15 min	30 min
After addition of KFCIII	30 min	30 min	45 min	60 min

Current readings (nA) were measured at the four different time combinations and the results were graphed (Figure 3.3).

According to Figure 3.3, the most significant response was observed with the incubation time of 15 + 45 min in both Method I and II. Therefore, this combination was used for the SciTox™ rapid DTA Assay.

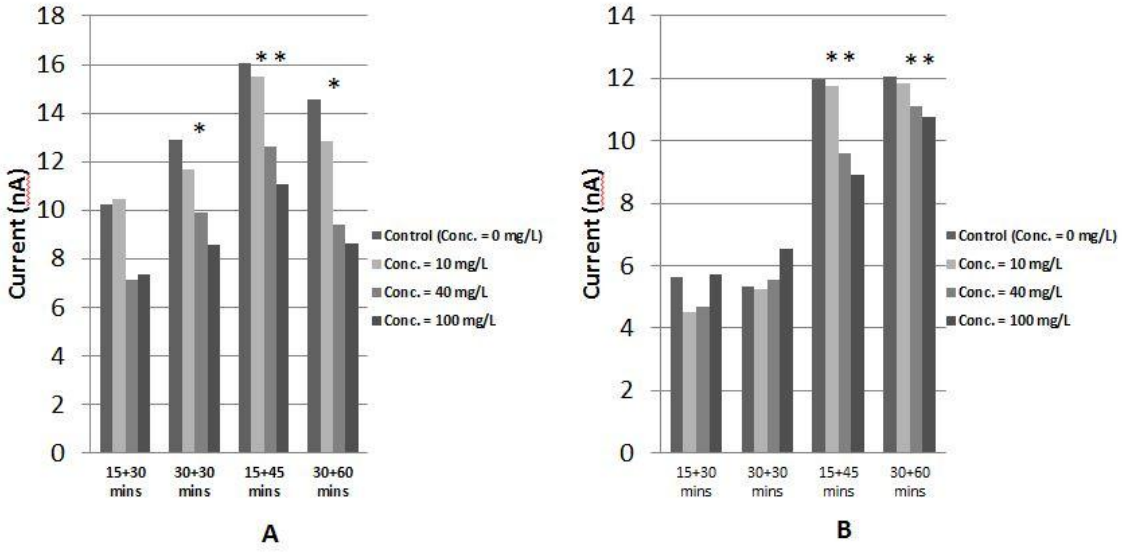

Figure 3.3 Current readings of *E. coli* culture exposed to standard toxicant 2,4-DCP for four incubation periods: current reading results from (A) Method I and (B)Method II. **P* < 0.05, ***P* < 0.01 compared to control.

3.3.1.1 Method I

The toxicants 2,4-DCP, $AgNO_3$ and AgNP were used in the SciTox™ rapid DTA Assay. Stock concentrations of the toxicants were prepared at 14,000 mg L^{-1} for 2,4-DCP and 7,000 mg L^{-1} for both $AgNO_3$ and AgNP. A total volume of 770 µL was applied. The dose–response relationship of fresh cells to variable toxicant concentrations was determined using the SciTox™ rapid DTA Assay (Figure 3.4).

The dose-response of *E. coli* was measured on exposure to the three toxicants, and the EC_{50} value (Table 3.6) determined using SigmaPlot from the dose–response curve. The dose–response curve reported for $AgNO_3$ was much steeper than for 2,4-DCP. Moreover, it seems that there was no dose-response observed in *E. coli* cells exposed to AgNP.

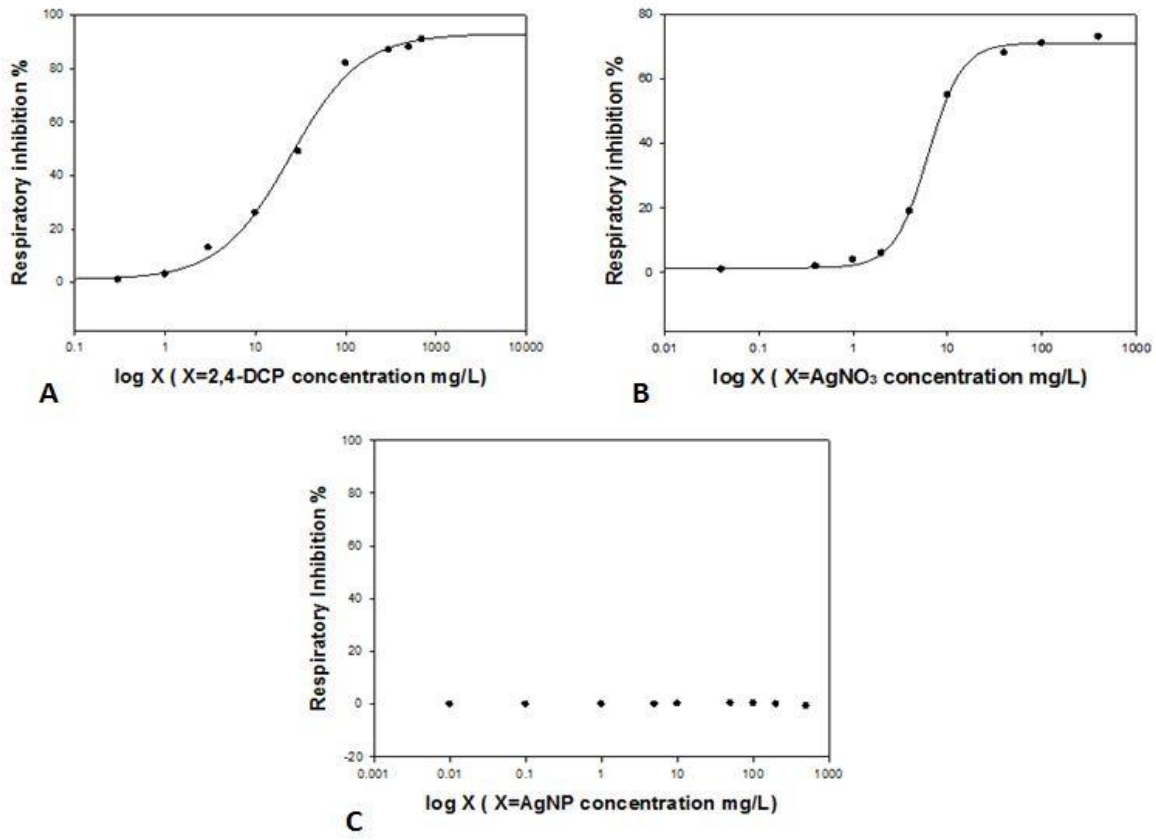

Figure 3.4 Method I: Dose-response of *E. coli* and fitted model on exposure to the toxicants in Method I: (A) 2,4-DCP ; (B) $AgNO_3$; (C) AgNP.

Table 3.6 EC_{50} (±SD) of *E. coli* derived from the SciTox™ toxicity assay Method I

Toxicant	**EC_{50} (mg L^{-1})**
2,4-DCP	24.3 ± 1.0
$AgNO_3$	6.1 ± 0.3
AgNP	Not observed

$AgNO_3$ is more toxic to *E. coli* than 2,4-DCP based on its lower EC_{50} value. EC_{50} was not able to be determined for AgNP in Method I. Therefore Method I was modified to include an additional centrifuge step after the first incubation step in order to develop a better dose–response relationship for AgNP.

3.3.1.2 Method II

Method II was performed (Method I with an additional centrifuge step following re-suspension of *E. coli* cells before adding the mediator KFCIII). The dose–response relationship was determined using the SciTox™ rapid DTA Assay (Figure 3.5).

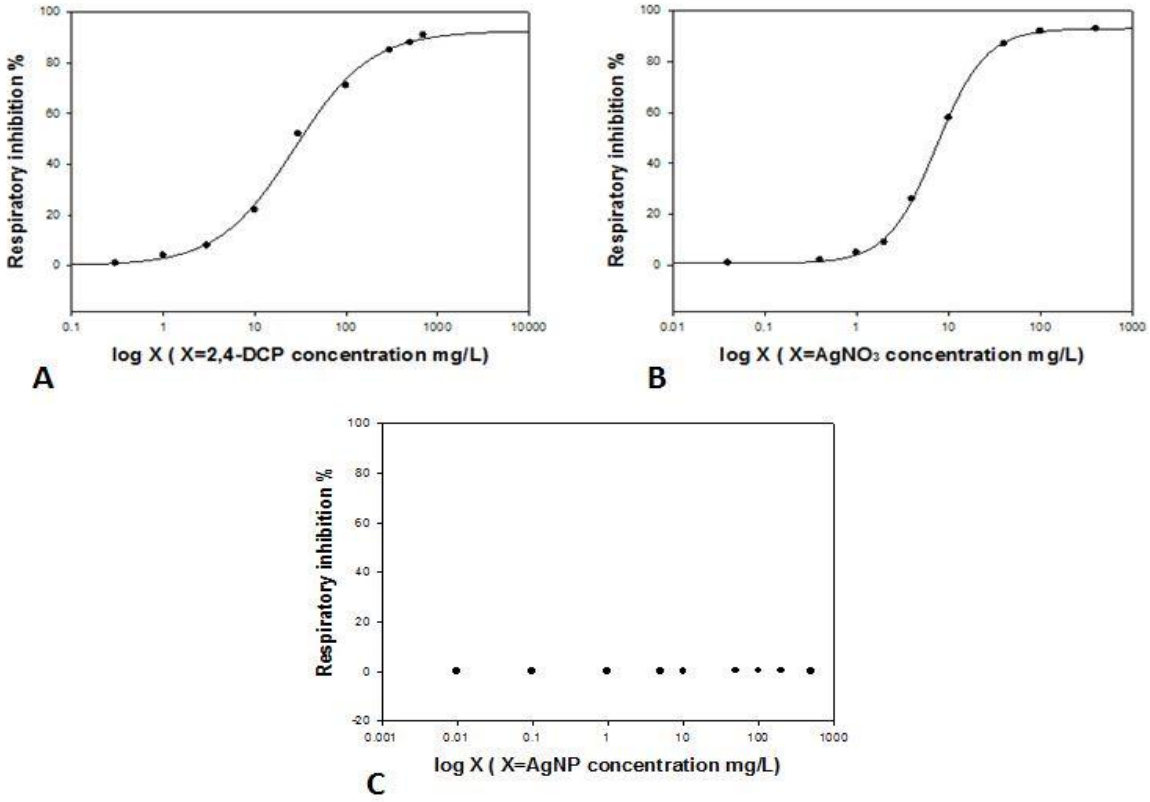

Figure 3.5 Dose-response of *E. coli* and fitted model on exposure to toxicants in Method II: (A) 2,4-DCP; (B) $AgNO_3$; (C) AgNP.

EC_{50} values (Table 3.7) were determined using SigmaPlot based on the dose–response curves. The dose–response curve reported for $AgNO_3$ was much steeper than for 2,4-DCP. Again, there was no dose-response observed in *E. coli* cells exposed to AgNP.

$AgNO_3$ is more toxic to *E. coli* than 2,4-DCP on the basis of its lower EC_{50} value. It was not possible to determine the EC_{50} value for AgNP in Method II.

Table 3.7 EC_{50} (±SD) of *E. coli* derived from the SciTox™ toxicity assay Method II

Toxicant	EC_{50} (mg L^{-1})
2,4-DCP	27.2 ± 0.8
$AgNO_3$	7.3 ± 0.6
AgNP	Not observed

3.3.2 Growth inhibition assay

Freshly cultured *E. coli* were exposed to fixed AgNP concentrations. Cell growth inhibition (expressed as a percentage of the growth of the control cell) to different AgNP concentrations was determined (Figure 3.6). In this study, even exposure to smaller concentrations (0–10 mg L^{-1}) of AgNP caused growth inhibition in *E. coli* with the response observed as a linear relationship (R^2 = 0.98).

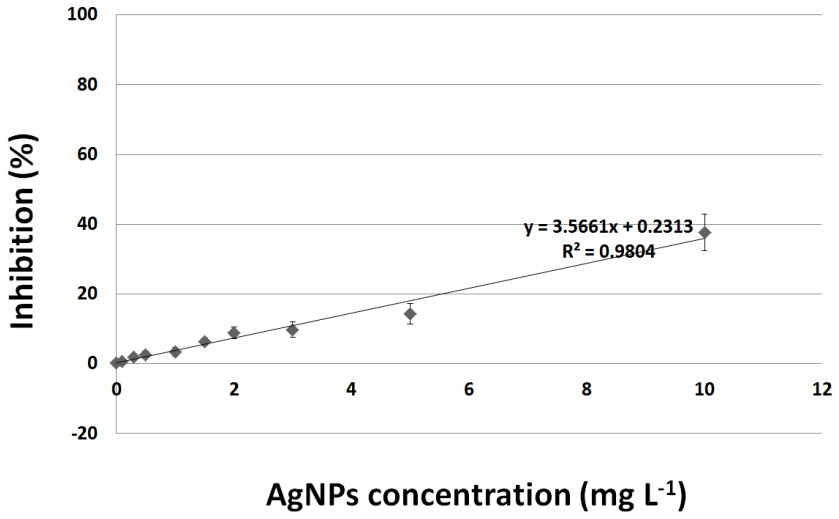

Figure 3.6 Means with SD of *E. coli* inhibition growth rate when exposed to fixed AgNP concentrations (0–10 mg L^{-1}) and fitted linear regression R^2 = 0.98.

3.4 Discussion

The basic principle of the SciTox™ rapid DTA Assay is to compare the current produced by healthy bacterial cells with the current produced by bacterial cells that have been exposed to a fixed toxin concentration. It is possible to gauge the index of respiratory inhibition, and this is proportional to the toxin concentration. In this chapter, the toxicity of AgNP was evaluated using *E. coli* as a bio-component in a whole-cell-based toxicology bio-assay SciTox™, and compared with the response using $AgNO_3$. Since respiratory activity was not affected by AgNP in Method I, in order to avoid the possibility of a direct interaction between the mediator, KFCIII, and the toxicant, AgNP, a variation to Method I was devised so that these two reagents were never in the same solution during the course of the assay. In the standard method (Method I), a single incubation was performed and it was possible that an interaction between KFCIII and the toxicant AgNP may have affected the outcome of the measurement.

As can be calculated from Figure 3.4, with the traditional toxicants, 2,4-DCP and $AgNO_3$, a dose-dependent response was detected using Method I with EC_{50} values of 24.3 mg L^{-1} and 6.1 mg L^{-1}, respectively, but with no respiratory inhibition evident when the bacteria were exposed to AgNP. The reason for conducting Method II with an additional centrifuge step was to remove AgNP after the reaction and thereby eliminate the influence of AgNP to the KFCIII in the SciTox™ rapid assay. The results seen in Figure 3.5, using Method II, demonstrated little change to the observations in Method I. With the normal toxicants 2,4-DCP and $AgNO_3$, Method 2 reported EC_{50} values of 27.2 mg L^{-1} and 7.3 mg L^{-1}, respectively, similar to the values of 24.3 mg L^{-1} and 6.1 mg L^{-1} observed in Method I and again no respiratory inhibition was evident with the toxicant AgNP. EC_{50} values of 2,4-DCP from both methods were relatively similar, which meant that the modified Method II was as accurate as the original SciTox™ rapid assay to the standard toxicant 2,4-DCP. Moreover, the EC_{50} value derived for $AgNO_3$ was also credible since values derived from both Method I and II were fairly close to each other.

The above results obtained with Methods I and II when using the standard toxicant, 2,4-DCP, demonstrate that both methods are accurate in reporting toxicities. Likewise the results obtained with $AgNO_3$ as the toxicant; at the concentrations examined, the convergence of Methods I and II demonstrates that there is no interaction between Ag^+ ions and the redox mediator, KFCIII. Comparing the EC_{50} values from both Methods I and II to the standard toxin 2,4-DCP, the values observed in this study were lower than 393 mg L^{-1}, a value reported by Pasco *et al.* (2005) with the CellSense® method, but very close to the value 33.83

mg L^{-1} reported by Shaw *et al.* (1999) with the Lux method. According to my results, $AgNO_3$ is much more toxic than 2,4-DCP to *E. coli* cells on the basis of its relatively lower EC_{50} value.

Unfortunately, when AgNP was used as the toxicant in both Methods I and II (reported in Figures 3.4 and 3.5 respectively), no respiratory inhibition was evident. Given the reliable results with the standard toxicant, 2,4-DCP, and the consistency of the results obtained with $AgNO_3$, the results obtained for the toxicity of AgNP goes against our expectation that AgNP would show increased toxicity compared with $AgNO_3$.

The bacterial growth inhibition assay was performed as a last resort to derive a toxicity value for AgNP. The inhibition in this assay was 38% at an AgNP concentration of 10 mg L^{-1}, which is lower than the 86% reported by Choi and Hu (2008) at an AgNP concentration of 1 mg L^{-1} although these authors used a different method, the extant respirometric assay. The growth inhibition assay described in my study involved 16-h incubation at 37°C at different AgNP concentrations. However, in the extant respirometric assay, the stock Ag^+ concentration used to make up the AgNP suspensions was 27 mg L^{-1}, whereas at the completion of the reaction, the residual Ag^+ concentration was 0.6 ± 0.1 mg L^{-1}, and the Ag^+ concentration remained largely unchanged at the end of 1 day at room temperature (Choi and Hu, 2008). So, it appears that AgNP may have deteriorated during the assay. Overall, a value for the toxicity of AgNP to *E. coli* was obtained, not with the standard SciTox™ assay but through inhibition of bacterial growth. It is possible that the bioavailability of the AgNP used in this study may have been low and hence there was relatively minimal toxicity.

Chapter 4
Earthworm Genotoxicity Study

4.1 Introduction

As discussed in chapter 2, the dose–response relationship plays an essential role in toxicology. An acute toxicity experiment was designed to determine the LD_{50} values by exposing *A.caliginosa* earthworms to AgNP and $AgNO_3$ in a Petri-dish filter paper study (skin exposure), a study exposing the earthworms to the two toxicants in soil (oral and skin exposure), and also by exposing the earthworms to aqueous solutions of AgNP and $AgNO_3$ in Petri dishes.

NPs damage DNA by generation of ROS to the point where they overwhelm the antioxidant defence system (Risom *et al.*, 2005). A more recent study demonstrated that DNA damage by NPs is considered to mimic the same pathways as in ionizing radiation (Mroz *et al.*, 2008). Ag^+ has been reported to interact with DNA and RNA and induce toxic effects (Hossain and Huq, 2002). The toxicity of AgNP is more unpredictable and might be affected by many factors, including chemistry, size, shape, agglomeration state, and electromagnetic properties (Buzea *et al.*, 2007).

Recently, many studies have focused on assaying the genotoxicity of NPs in human and mouse cells (Rai *et al.*, 2009; Trouiller *et al.*, 2009; Bourdon *et al.*, 2012), while less work has been done on the toxicity of AgNP in earthworms. Therefore, in this research, the genotoxic effects of AgNP on *A. caliginosa* earthworm coelomocytes were studied, and compared with those caused by $AgNO_3$. Two genotoxicity assays, the Micronucleus Test and Comet Assay, were performed because they have been commonly used to assay the genotoxicity of NPs in recent research (Benedicte *et al.*, 2009; Rai *et al.*, 2009). Therefore, the Micronucleus Test and Comet Assay have been proposed as a biomarker of DNA damage. DNA damage induced in animals by chemical and physical agents can lead to the appearance of micronuclei (Schlegel and MacGregor, 1982; Udroin, 2006). Micronuclei are cytoplasmic chromatin masses resembling minute nuclei, formed when a whole chromosome or acentric chromosomal fragments lag during anaphase and fail to become incorporated into daughter-cell nuclei during cell division (Farah *et al.*, 2006). The Micronucleus Test can also provide information on other nuclear anomalies such as binucleated, blebbed, notched and lobed

nuclei. Binucleate cell formation can occur in abnormal cytokinesis and during cell proliferation (Toyoshima *et al.,* 1999).

The Comet Assay has been used for genotoxicity assessment of DNA single-strand breaks to detect even low level DNA damage in single cells (Tice *et al.,* 2000). It is based on the further migration of damaged DNA during electrophoresis, with the DNA then resembling a 'comet' with a brightly fluorescent head and a long tail region that increases with the severity of DNA damage. It has been used to assess DNA damage in earthworms, e.g., *Eisenia fetida* exposed to nickel (Ni) (Reinecke and Reinecke, 2004); *Amynthas diffringens*, *A. caliginosa*, *Dendrodrilus rubidus*, and *Microchaetus benhami* exposed to cadmium (Cd) (Fourie *et al.*, 2007); coelomocytes of *Pheretima peguana* exposed to lead (Pb) and Cd (Muangphra and Gooneratne, 2011a) and neem extract (Muangphra and Gooneratne, 2011b).

Coelomocytes are the immune cells in the earthworm and can be categorized in many ways. The classification of earthworm coelomocytes is largely based on differential staining, ultrastructure and granule composition, as well as behavioural traits such as adherence and chemotaxis (Hamad *et al.,* 2002). The main populations of coelomocytes are amoebocytes (hyaline amoebocytes [mid-sized with small filopodia] also known as acidophils), and granular amoebocytes (smaller cells with small granules inside, also known as basophils) and the larger eleocytes (derived from detachment of chloragogen cells covering the intestinal tract and the mesenchymal lining of the coelom) (Cooper and Stein, 1981). In this study, coelomocytes were isolated from earthworms exposed to AgNP and $AgNO_3$, characterized, and the Micronucleus Test and Comet Assay performed to evaluate genotoxicity.

4.2 Methods

4.2.1 Buffers

- *Phosphate buffer saline (PBS):* 8 g NaCl, 0.2 g KCl, 0.3 g KH_2PO_4, 1.25 g Na_2HPO_4, 0.1 g $MgCl_2 \cdot 6H_2O$ and 0.1 g $CaCl_2 \cdot 2H_2O$ were made up to 1 L with distilled water.
- *Extrusion buffer (EB):* 4.161 g NaCl, 1.091 g EGTA and 9.09 g Guaiacol glycerol ether were made up to 950 ml with distilled water and 50 ml absolute ethanol added to make it to 1 L, and pH adjusted to 7.5 with 1.0 M NaOH.

- *Lumbricus balance salt solution (LBSS):* 4.178 g NaCl, 0.358 g KCl, 0.099 g $MgSO_4$, 0.054 g K_2HPO_4, 0.036 g $Na_2H_2PO_4$ and 0.353 g $NaHCO_3$ were made up to 1 L with distilled water and pH adjusted to 7.3 with 1.0 M NaOH.
- *High salt Lysis buffer:* 146 g NaCl, 4.2 g EDTA and 1.2 g Trizma base were made up to 1 L with distilled water and stored in a refrigerator at 4°C. 89% (v/v) of the above solution was mixed with 1% (v/v) Triton X-100 and 10% (v/v) DMSO. For each run, a fresh Lysis solution was used.
- *Electrophoresis buffer:* 40 g NaOH wase made up to 100 ml in a flask with distilled water to prepare the NaOH stock solution; 14.89 g Na_2EDTA was made up to 300 ml with distilled to prepare the Na_2EDTA stock solution. Then 30 ml of the NaOH stock solution and 5 ml of the Na_2EDTA stock solution were made up to 1 L with distilled water and pH adjusted to ≥13.
- *Neutralization buffer:* 48.5 g Tris base was made up to 1 L with distilled water and pH adjusted to 7.5.

4.2.2 Agarose solution

- *Normal melting point (NMP) agarose:* 0.5% NMP was prepared with 0.5 g NMP made up to 100 ml with PBS and thoroughly mixed and heated in a microwave oven for 3 min.
- *Low melting point (LMP) agarose:* 2% LMP was prepared with 2 g LMP agarose made up to 100 ml with PBS, and thoroughly mixed at 40°C.
- *LMP agarose 5%:* 5% LMP was prepared with 0.5 g LMP agarose made up to 100 ml with PBS, thoroughly mixed and heated before use.

4.2.3 Acute toxicity study

4.2.3.1 Earthworm culture and maintenance

Adult *A. caliginosa* earthworms (Savigny, 1826) were sourced from the colony based at the Johnstone Memorial Laboratory (JML), Lincoln University. Species identification was based on the taxonomic features described in http://www2.uclan.ac.uk. The worms were maintained in JML using a stock soil (50% loamy topsoil, 30% composted dry grass and 20% cow

manure) in the dark at 20°C. Water was added once a week to keep the soil moist. Adult individuals (weighing between 400 and 600 mg and measuring approximately 60–100 mm in length) with a well-developed clitellum were used in all experiments.

The concentration of $AgNO_3$ and AgNP used for the three sets of experiments depended on the exposure method (Petri dish filter paper, soil, or aqueous solution) (Tables 4.1 – 4.3). At the higher concentrations, AgNP was relatively insoluble and existed as a suspension. In each of the three experiments, a similar number of earthworms as used in the test groups were exposed to water instead of the chemical and acted as the negative control.

4.2.3.2 Petri-dish filter paper acute toxicity studies

The Petri-dish filter paper study of AgNP and $AgNO_3$ acute toxicity to earthworms was conducted using seven different concentrations of each chemical, AgNP and $AgNO_3$ (n = 10 earthworms per concentration per chemical). The doses were selected on the basis of a preliminary study. Whatman No. 1 filter paper was used in the Petri-dish study. In the range-finding preliminary study, two adult *A. caliginosa* earthworms in each Petri-dish were exposed to a range of toxin concentrations ranging from 10 to 1000 µg ml^{-1} (ppm) for $AgNO_3$ and 10 to 2000 ppm for AgNP, with 2 ml of each solution added to filter paper. Based on this, the final Ag^+ concentrations in $AgNO_3$ used in the filter paper exposure experiment to determine 48-h LD_{50} were 450–750 ppm; the concentrations of AgNP selected for use were 10–2000 ppm (Table 4.1). All experiments were carried out in the dark at 20°C for 48 h. The percentage mortality was determined at 48 h. Worms were considered dead when they did not respond to touch of the anterior region. Tests were carried out according to OECD guideline (1984). Results of the treatment group were analyzed using SigmaPlot to calculate the 48-h LD_{50} for AgNP and $AgNO_3$.

Table 4.1 Concentrations (ppm) of the toxicants $AgNO_3$ and AgNP used in the Petri-dish filter paper study

$AgNO_3$	**AgNP**
450	10
500	50
550	100
600	200
650	500
700	1000
750	2000

4.2.3.3 Soil-exposure toxicity assay

Soil from the Lincoln University organic farm in Canterbury, New Zealand, was collected and dried at 30°C for 24 h to kill any macroinvertebrates. The soil was then rehydrated to produce a moisture content of 37% by mass with concentrations of 150–700 ppm for $AgNO_3$, and 10–2000 ppm for AgNP (Table 4.2) in small glass bottles containing 25 g of soil. The pH of the reconstituted soil was approximately 6.9. Two adult *A. caliginosa* earthworms were maintained in each container, with 10 adult earthworms per concentration per chemical, and kept in the dark at 20°C for 48 h. The percentage mortality was determined at 48 h. The results were analyzed using SigmaPlot to determine the 48-h soil LD_{50} for AgNP and $AgNO_3$.

Table 4.2 Concentrations (ppm) of the toxicants $AgNO_3$ and AgNP used in the soil-exposure study

$AgNO_3$	**AgNP**
150	10
200	50
300	100
400	200
500	500
600	1000
700	2000

4.2.3.4 Aqueous-solution-based toxicity assay

Since the *A. caliginosa* earthworms were relatively resistant to AgNP, an acute toxicity study of AgNP and $AgNO_3$ aqueous solution to earthworms was assessed in Petri dishes using seven concentrations of each chemical (n = 10 earthworms per concentration per chemical) on the basis of a preliminary range-finding study. Two adult earthworms were transferred to each of the five Petri dishes containing 20 ml of either $AgNO_3$ or AgNP solution. The final AgNP concentrations used in the aqueous solution exposure experiment were 125–2000 ppm; the final concentrations used in the $AgNO_3$ solution exposure experiment were 0.5 to 7ppm (Table 4.3). All experiments were carried out in the dark at 20°C for 48 h. Results were analyzed using SigmaPlot to determine the 48-h LD_{50}.

Table 4.3 Concentrations (ppm) of $AgNO_3$ and AgNP used in the aqueous solution study

Toxicant	$AgNO_3$	AgNP
Concentrations	0.5	125
	0.625	250
	0.833	300
	1	400
	1.5	500
	2	600
	4	1000
	7	2000

4.2.4 Comet Assay and Micronucleus Test

4.2.4.1 Doses of AgNP and $AgNO_3$ used

Since the earthworms were relatively resistant to AgNP in the Petri-dish filter paper test and the soil study, the earthworm exposure doses were based on data from the aqueous solution study. This was because the maximum concentration that could be prepared with the AgNP purchased from Sigma Chemical Co. (St Louis, USA) was 2000 ppm and no deaths occurred with either the Petri-dish filter paper test or the soil-exposure study even at this concentration.

From the aqueous solution study LD_5, LD_{10}, LD_{15}, LD_{20}, LD_{25} values for AgNP and $AgNO_3$ were derived using SigmaPlot (Table 4.4). In this study, adult *A. caliginosa* earthworms (n = 5 earthworms per dose per chemical) were exposed to the different concentrations ranging from LD_5 to LD_{25} aqueous solutions of $AgNO_3$ and AgNP for 48 h.

Table 4.4 Aqueous AgNP and $AgNO_3$ exposure concentrations

LD values	AgNP concentration (ppm)	$AgNO_3$ concentration (ppm)
LD_5	360	0.64
LD_{10}	390	0.75
LD_{15}	410	0.85
LD_{20}	428	1
LD_{25}	433	1.1

4.2.4.2 Coelomocyte collection

Coelomic fluid containing coelomocytes was obtained from the coelomic cavity using the extrusion method of Eyambe *et al.* (1991). Three earthworms per dose per chemical were required but I used five earthworms per dose for the study to account for any deaths that may have occurred during the experiment, especially at the LD_{25} concentration, and also because of time constraints. Briefly, the earthworms were allowed to depurate for 24 h and each earthworm was transferred to a Petri dish of 0.5 ml of EB. Forceps were used to massage earthworms to collect coelomocytes and the cell suspension of coelomocytes was collected into a 1-ml centrifuge tube. Extruded cells were transferred to LBSS solution as described by Brousseau *et al.* (1997).

Coelomocyte morphology was examined microscopically. Coelomocytes were counted in a haemocytometer and the cell concentration adjusted to 10^5 cells ml^{-1}. Cell viability was determined using the trypan blue exclusion test, after mixing equal volumes of the coelomocyte suspension and a 0.5% (w/v) trypan blue (Sigma, St Louis, USA) solution. Cell viability always exceeded 95%. Then the Micronucleus Test and Comet Assay were carried out on coelomocytes collected from the earthworms.

4.2.5 Micronucleus (MN) Test

An aliquot of 20 µl of coelomic fluid cell suspension from section *4.2.4.2* was smeared on a clean microscope slide using one slide each from three earthworms (a total of three slides per concentration per chemical). After the microscope slides were air-dried, the coelomocytes

were fixed in absolute ethanol for 15 min and stained with Wright's rapid stain for 30 s for differential staining of cellular components. Slides were permanently fixed by mounting with DPX solution. A total of 3,000 coelomocytes from three earthworms per concentration (including the negative control) were scored using a compound microscope at 400× magnification to characterize the coelomocytes into the three major types, namely eleocytes, acidophils (hyaline amoebocytes), and basophils (granular amoebocytes), and the frequencies of coelomocyte micronuclei and binucleate cells were used to assess chromosomal aberrations and inhibition of cytokinesis, respectively. The remaining coelomic fluid was used for the Comet Assay.

4.2.6 Comet Assay

Coelomocytes from the coelomic fluid collected from three earthworms as described in section *4.2.4.2* were used in this study. To detect coelomocyte DNA damage, alkaline lysis followed by alkaline single-cell gel electrophoresis was conducted. Four microgel slides were prepared for each chemical (AgNP, $AgNO_3$) concentration from each earthworm according to the protocol of Singh *et al.* (1988) as modified by Reinecke and Reinecke (2004). All steps were conducted in dim light at 4°C to prevent additional DNA damage. Initially, the microscope slides were cleaned with 70% methanol. The slides were then coated with three layers of 0.5% NMP agarose. Then 20 µl coelomocyte cell suspension was mixed with 75 µl of LMP agarose at 40°C in a 1-ml centrifuge tube as described by Brousseau *et al.* (1997). Next, 40 µl of 2% LMP agarose at 40^{o}C was added to the centrifuge tube and mixed. Duplicates of the 40-µl mixed cell suspension were overlaid on the microscope slide pre-coated with normal LMP agarose, and covered immediately with a cover glass. Agarose was allowed to solidify by keeping slides on ice packs for 3 min. Cover slips were then removed gently from the slide and 40 µl of 0.5% LMP agarose was layered on the slide and covered with a cover glass. Slides were then transferred onto ice packs for another 3 min. After solidification of the gel, slides were immersed in freshly made high-salt lysis solution for 24 h at 4ºC to remove cellular proteins and liberate damaged DNA.

On the following day, slides were transferred to a horizontal electrophoresis tank containing fresh cold alkaline electrophoresis buffer for 15 min at 4ºC to unwind the DNA and to express DNA single-strand and double-strand breaks and alkali labile sites. Next electrophoresis was carried out using the same buffer at 12 V and 300 mA for 40 min at 4^{o}C. After electrophoresis, slides were neutralized by washing 3 times with 0.4 M neutralization buffer

to remove excess alkaline for 5 min each. Finally, slides were washed / fixed with absolute ethanol for 15 min. Slides were stored in a moisture box fully covered with foil at 4ºC until analysis.

Two slides from each earthworm were then analysed at the Faculty of Science, Silpakorn University, Thailand, by Dr Muangphra, a collaborator of my supervisor Dr Ravi Gooneratne. Slides were examined under a Nikon eclipse 801 fluorescent microscope with fritter black UV-A (excitation filter 510–560 mm, decroic mirror 575 nm, emission 590 nm). Slides were stained with 20 µg ml^{-1} ethidium bromide for 5–10 min and washed with deionized water to remove excess stain for visualization of DNA damage. Two slides from each earthworm of each dose of each chemical were examined. At least 100 non-overlapping comets per slide were captured randomly at 400× magnification and scored for the comet parameters described below using a digital camera (Nikon DXM 1200C) and analysed with the software programme LUCIA (Laboratory Universal Computer Image Analyser). The comets were then scored for the comet parameters, namely Tail DNA (TD) % (expressed as percentage of fluorescent intensity in tail), DNA Tail Length (TL) (the distance from the nuclear centre to the end of comet tail), and DNA tail moment (TM: a measure of both the smallest detectable size of migrating DNA [incorporating a measure of the smallest detectable size of migrating DNA reflected in the comet tail length] and the number of relaxed/broken pieces [represented by the intensity of DNA in the tail]).

4.2.7 Statistical analysis

Results were expressed as the mean $\pm$ standard deviation. Results were analysed by analysis of variance (ANOVA). For analysis of MN and BN, an augmented factorial model (GenStat version 14) was used after logarithmic transformation [$\log_{10}(x+1)$] (Appendix A). Significant differences between the results of the different treatment groups were determined using one-way ANOVA (to detect effects) and Tukey's multiple comparisons (to detect difference between treatments).

4.3 Results

4.3.1 Acute toxicity study

No mortality was observed in controls at 48-h. Results of earthworms exposed to $AgNO_3$ and AgNP were expressed by plotting percentages of dead earthworms exposed to different concentrations of these two toxicants. The 48-h LD_{50} of $AgNO_3$ and AgNP (exposure) of *A. caliginosa* earthworm in a Petri dish, soil, and aqueous solution were determined by SigmaPlot. By comparing the LD_{50} values, it was possible to compare the differential toxicities of $AgNO_3$ and AgNP in the different media.

4.3.1.1 Petri-dish filter paper study

There were no deaths in the Petri-dish filter paper study of *A. caliginosa* earthworms exposed to AgNP (up to 2000 ppm) for 48 h. There were also no deaths of earthworms on exposure to $AgNO_3$ at 24 h. However, deaths occurred between 24 and 48 h in earthworms exposed to $AgNO_3$ (Figure 4.1). Based on the results, the LD_{50} was determined as 571 ppm for $AgNO_3$ (n = 10).

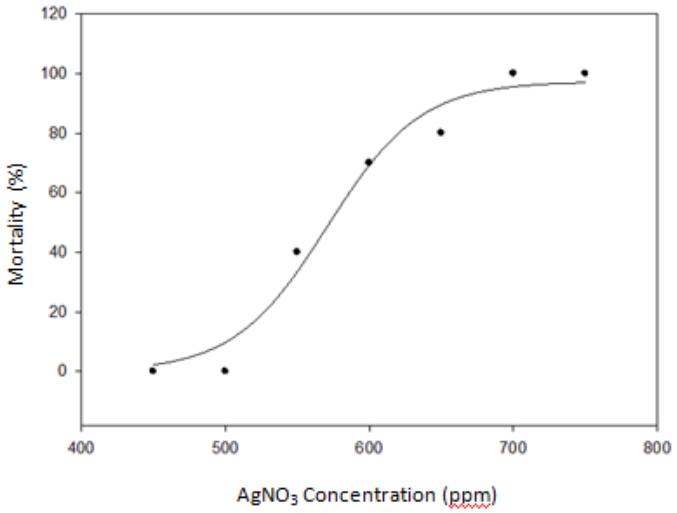

Figure 4.1 Mean mortality of *A.caliginosa* earthworms after 48h exposure to $AgNO_3$ in Petri-dish, and fitted model.

4.3.1.2 Soil study

There were no deaths of *A. caliginosa* earthworms at 48 h in the soil study on exposure to AgNP (up to 2000 ppm). There were also no deaths on exposure of earthworms to $AgNO_3$ at 24 h. However, there were deaths between 24 and 48 h exposed to $AgNO_3$ (Figure 4.2). Based on the results, the 48-h LD_{50} was determined as 418 ppm for $AgNO_3$ in the soil study (n = 10).

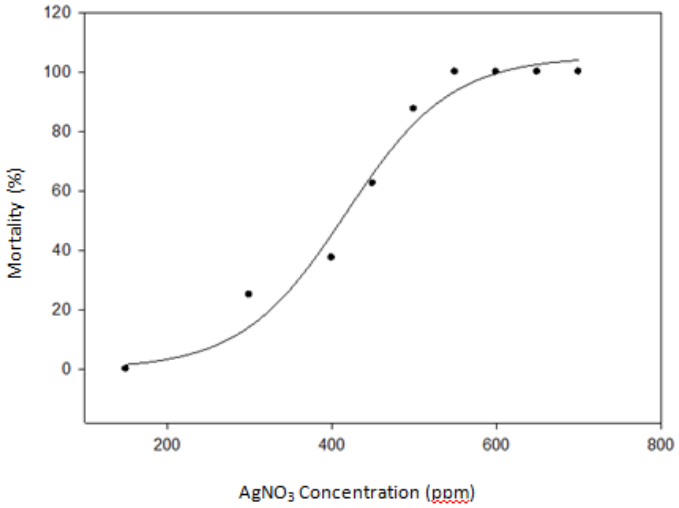

Figure 4.2 Mean mortality of *A.caliginosa* earthworms after 48h exposure to $AgNO_3$ in soil and fitted model.

4.3.1.3 Aqueous solution study

There were no deaths in earthworms exposed to $AgNO_3$ or AgNP aqueous solution at 24 h. However, there were deaths with both $AgNO_3$ or AgNP between 24 and 48 h. With AgNP, the 48-h LD_{50} was determined as 483 ppm (Figure 4.3). With $AgNO_3$, the LD_{50} was determined as 1.64 ppm (n = 10) (Figure 4.4).

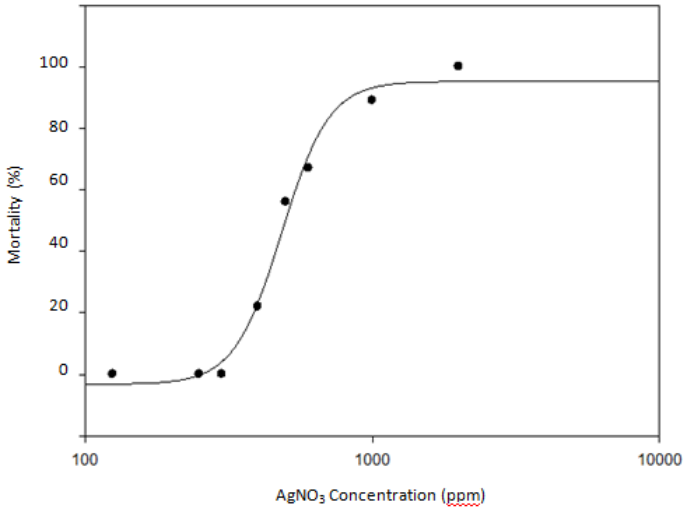

Figure 4.3 Mean mortality of *A.caliginosa* earthworms after 48h exposure to aqueous solution of AgNP and fitted model.

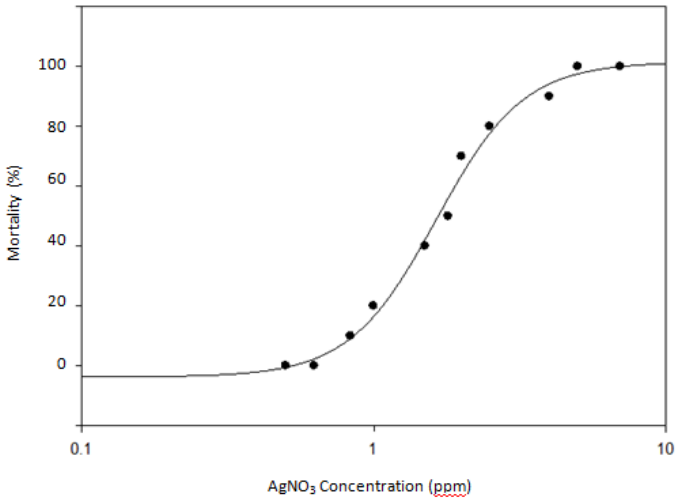

Figure 4.4 Mean mortality of *A.caliginosa* earthworms after 48h exposure to aqueous solution of $AgNO_3$ and fitted model.

4.3.2 Micronucleus (MN) Test

A total of 1000 coelomocyte cells were counted from each earthworm. Samples from three earthworms were used for each dose of each chemical and the control. Coelomocytes were categorized as eleocytes (Figure 4.5), acidophils (hyaline amoebocytes) (Figure 4.6) or basophils (granular amoebocytes) (Figure 4.7) (Table 4.5). There were no significant

differences between treatments or doses and the controls except that the eleocyte count was low (but not statistically different) at the highest dose of both AgNP and $AgNO_3$, LD_{25}.

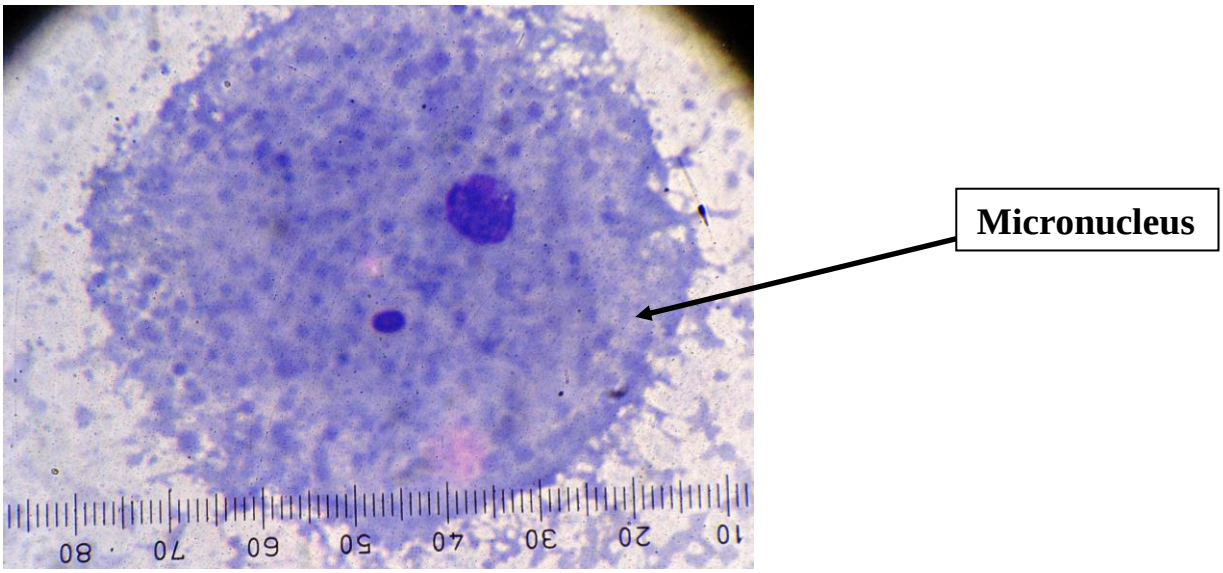

Figure 4.5 Eleocyte with a prominent micronucleus.

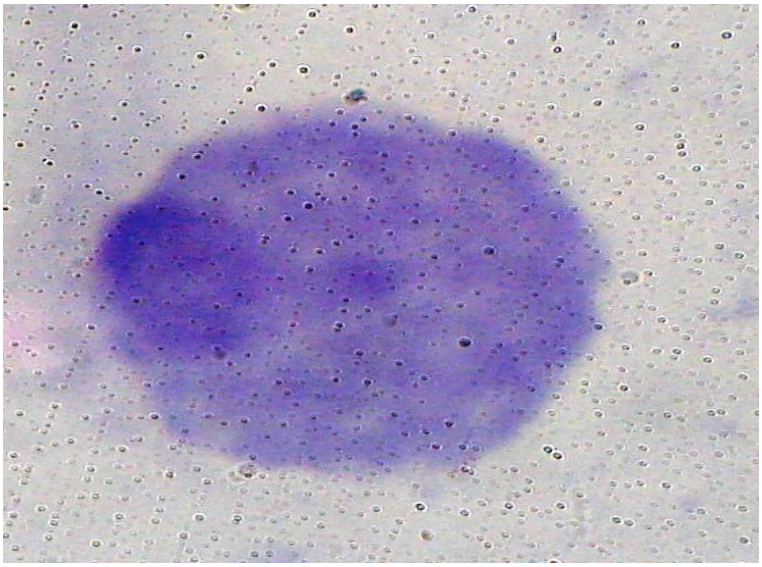

Figure 4.6 Acidophil.

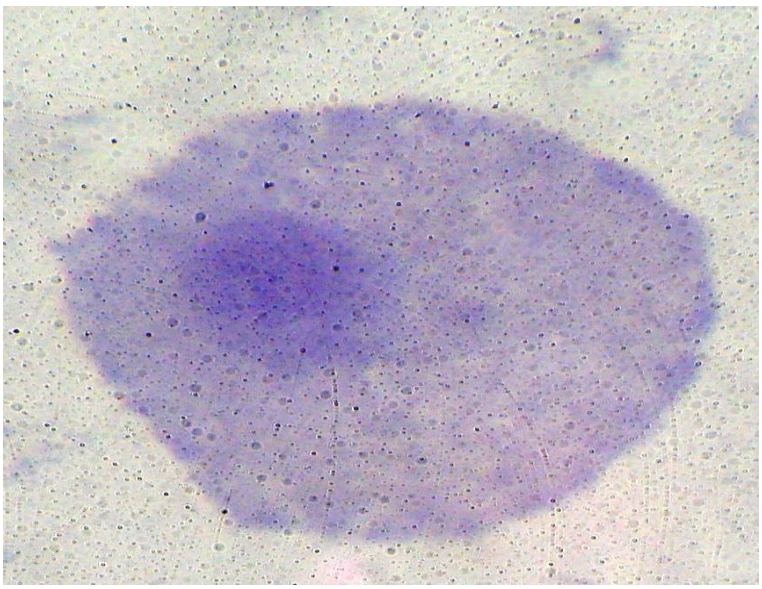

Figure 4.7 Basophil.

Table 4.5 Differential coelomocyte count

Treatment	Dose	Type of coelomocyte (Mean ± SD)		
		Acidophils	**Basophils**	**Eleocytes**
Control	0	898.7 ± 5.5	2.0 ± 0.8	99.0 ± 5.5
$AgNO_3$	LD_5	974.0 ± 2.9	2.3 ± 0.9	21.7 ± 2.7
	LD_{10}	913.3 ± 5.1	2.3 ± 0.9	82.3 ± 5.0
	LD_{15}	870.0 ± 6.1	2.0 ± 0.8	122.7 ± 6.0
	LD_{20}	902.0 ± 5.4	5.7 ± 1.4	85.3 ± 5.1
	LD_{25}	961.0 ± 3.5	3.0 ± 1.0	23.0 ± 2.7
AgNP	LD_5	944.0 ± 4.2	1.0 ± 0.6	53.3 ± 4.1
	LD_{10}	949.0 ± 4.0	6.3 ± 1.4	42.7 ± 3.7
	LD_{15}	912.7 ± 5.2	3.0 ± 1.0	81.7 ± 5.0
	LD_{20}	918.0 ± 5.0	2.0 ± 0.8	74.0 ± 4.8
	LD_{25}	952.7 ± 3.9	0 ± 0.0	38.7 ± 3.5

LD = lethal dose; SD = standard deviation; *n* = 3.

Micronuclei and BN were counted in 1000 coelomocytes from each of the three earthworms in each treatment (AgNP, $AgNO_3$), and also from the three negative controls. There was a clear statistically significant ($P < 0.005$) response of MN > BN with the two treatments compared to the controls (Appendix A). The sums of MN and BN were higher in both test groups and were statistically significant ($P < 0.05$) from LD_{15} onwards when compared with the controls (Table 4.6). Thus both AgNP and $AgNO_3$ appear to cause cytokinesis failure and chromosomal aberrations in the form of binucleates and micronuclei, respectively, from LD_{15} onwards.

The frequency of MN was greater than for binuclei, especially at higher exposure concentrations. The BN in coelomocytes of one of the earthworms exposed to $AgNO_3$ LD_{15} concentration was unusually high and this group also had a greater number of eleocytes.

Table 4.6 Mean micronuclei (MN) and binuclei (BN) counts in 1000 coelomocytes per earthworm

Treatment	Dose	MN	BN	MN + BN
Control	0	0.3 ± 0.3	0 ± 0	0.3 ± 0.3
$AgNO_3$	LD_5	1.0 ± 0.6	1.0 ± 0.6*	2.0 ± 0.8*
	LD_{10}	1.0 ± 0.6	1.0 ± 0.6*	2.0 ± 0.8*
	LD_{15}	1.7 ± 0.7*	36.7 ± 1.1*	5.3 ± 1.3*
	LD_{20}	3.0 ± 1.0*	4.1 ± 1.2*	7.0 ± 1.5*
	LD_{25}	9.3 ± 1.8*	3.7 ± 1.1*	13.0 ± 2.1*
AgNP	LD_5	0.3 ± 0.3	1.3 ± 0.7*	1.7 ± 0.7*
	LD_{10}	1.3 ± 0.7	0.7 ± 0.5*	2.0 ± 0.8*
	LD_{15}	0.7 ± 0.5	2.0 ± 0.8*	2.7 ± 0.9*
	LD_{20}	4.7 ± 1.2*	1.3 ± 0.7*	6.0 ± 1.4*
	LD_{25}	4.3 ± 1.2*	4.3 ± 1.2*	8.7 ± 1.7*

Total numbers of MN and BN in 1000 coelomocytes are shown as Figure 4.8. The frequency of the sum of MN and BN at each concentration was higher in the AgNP and $AgNO_3$ exposed earthworms compared with the controls. The dose response was highly significant ($P < 0.001$) and also linear (Appendix A). The frequency of the sum of BN and MN in coelomocytes was highly significant ($P < 0.001$) at $AgNO_3$ concentrations of LD_{25} compared with AgNP (Figure 4.8).

Comparing the two polynomial trend lines for $AgNO_3$ and AgNP. $AgNO_3$ was more toxic than AgNP ($P < 0.001$).

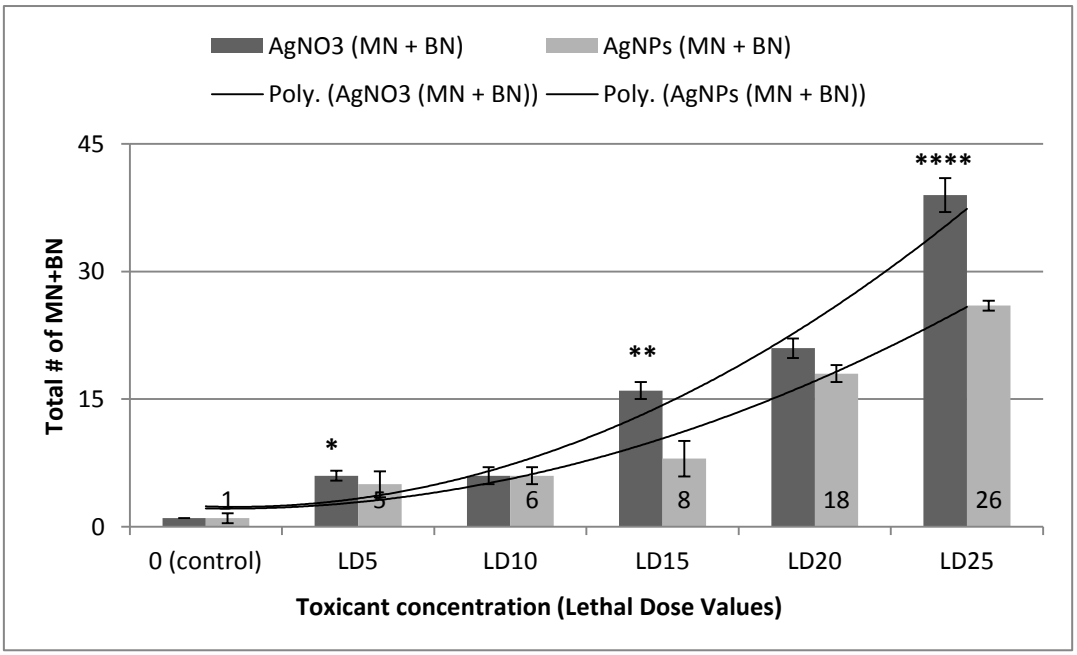

Figure 4.8 Total micronulclei (MN) and binuclei (BN) in coelomocytes exposed to different exposure concentrations of AgNP and $AgNO_3$ ($n = 3$), error bars are standard deviations. Asterisks indicate significant differences from AgNP. *$P < 0.05$; **$P < 0.01$; ***$P < 0.005$; ****$P < 0.001$.

4.3.3 Comet Assay

4.3.3.1 AgNP

For the Comet Assay (Figure 4.9) five earthworms were exposed to 5 different concentrations of AgNP.

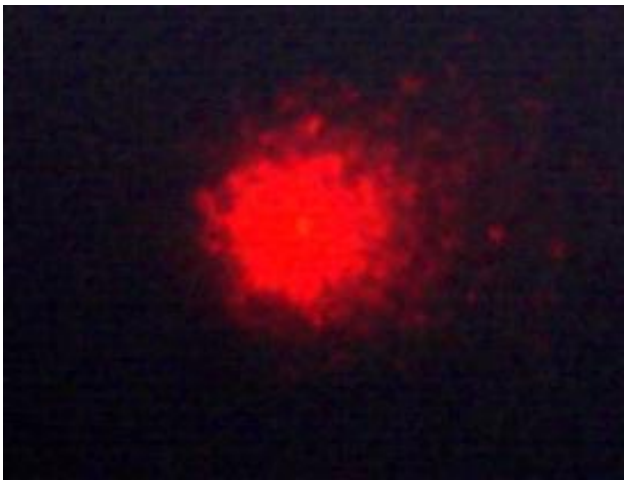

Figure 4.9 A comet (from an earthworm exposed to LD_{10} AgNP concentration).

The mean (±SD) coelomocyte TD increased significantly on exposure to LD_{10} AgNP concentration compared to the controls (Figure 4.10). However, the results were not consistent, there was no particular pattern, and a dose-response effect was not apparent in TD, TL and TM.

The mean (±SD) coelomocyte TL for the three earthworms exposed to different AgNP concentrations is shown in Figure 4.11 and the mean (±SD) coelomocyte TM in Figure 4.12.

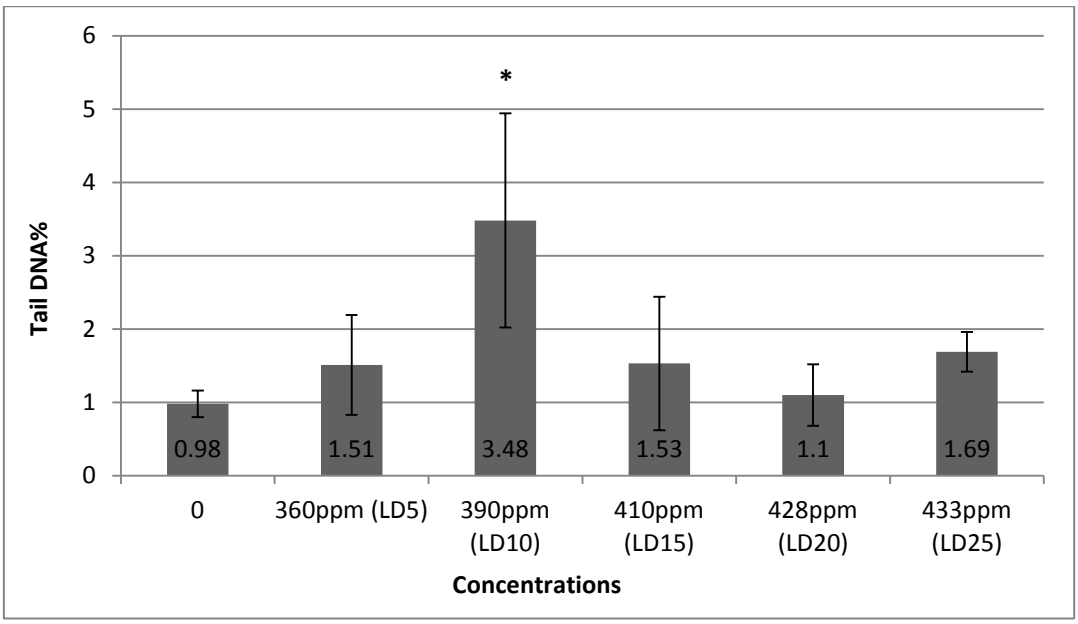

Figure 4.10 Mean coelomocyte tail DNA percentage in earthworms (n = 3) exposed to different concentrations of AgNP; error bars are standard deviations. *significantly different from the control ($P < 0.05$).

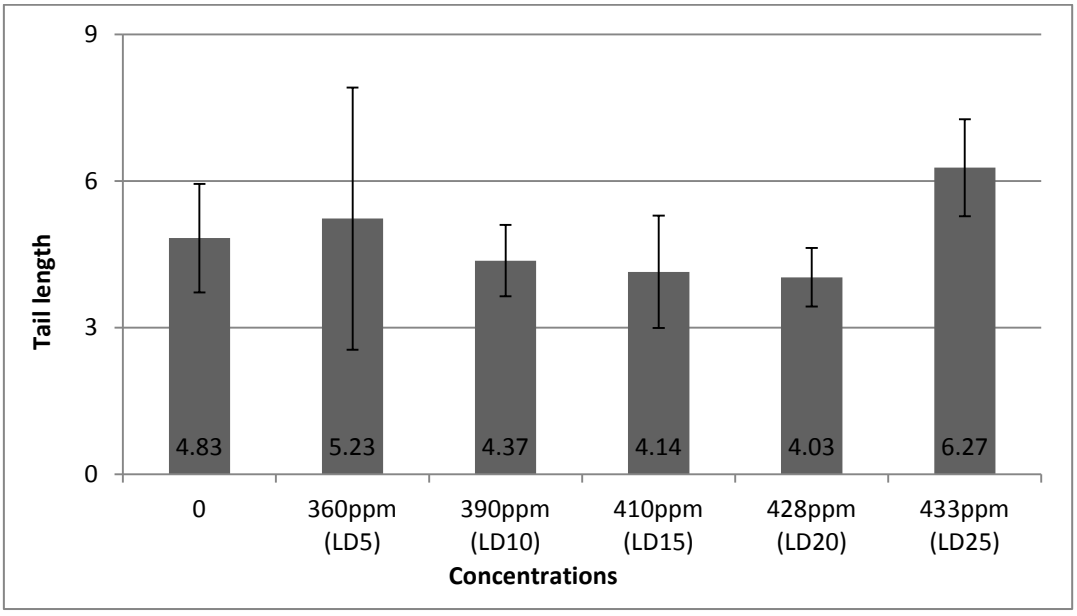

Figure 4.11 Mean coelomocyte DNA tail length in earthworms (n = 3) exposed to AgNP; error bars are standard deviations.

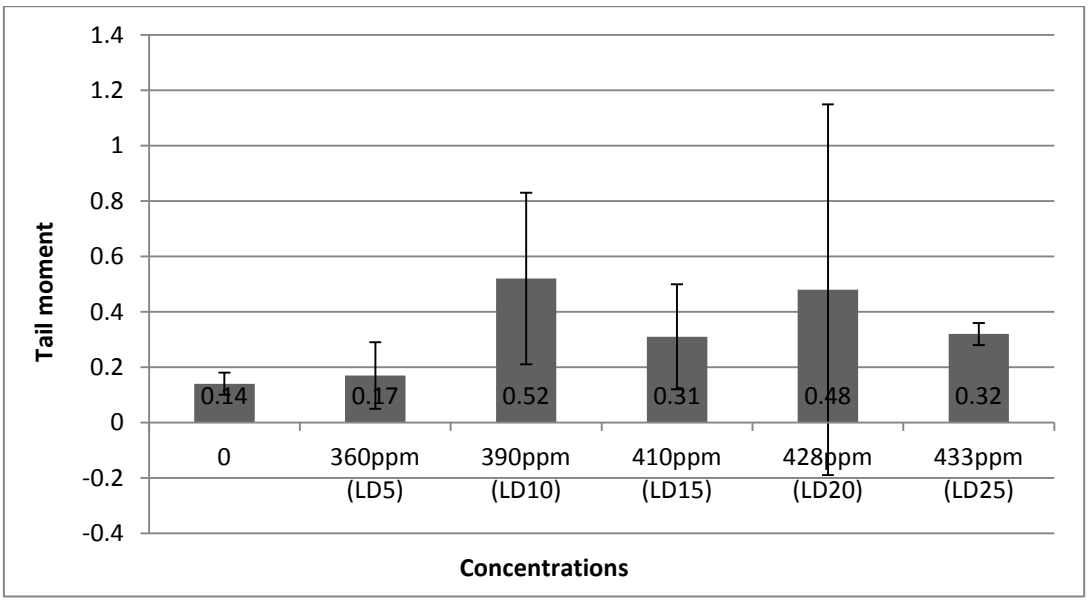

Figure 4.12 Mean coelomocyte DNA tail moment in earthworms (n = 3) exposed to different concentrations of AgNP; error bars are standard deviations.

4.3.3.2 $AgNO_3$

Again, as with AgNP, the TD, TL, and TM results were not consistent and there was no particular pattern and a dose-response effect was not evident. The mean (±SD) coelomocyte TDs of three earthworms exposed to different concentrations of $AgNO_3$ are shown in Figure 4.13.

The mean (±SD) coelomocyte DNA tail lengths of the three earthworms exposed to different $AgNO_3$ concentrations are shown in Figure 4.14, and the mean (±SD) of coelomocyte DNA tail moments in Figure 4.15.

There were no significant differences in TD, TL and TM with either $AgNO_3$ or AgNP except for the observation of an increase in TD in earthworms exposed to an AgNP concentration of LD_{10} (Figure 4.10). The reason for this is not known.

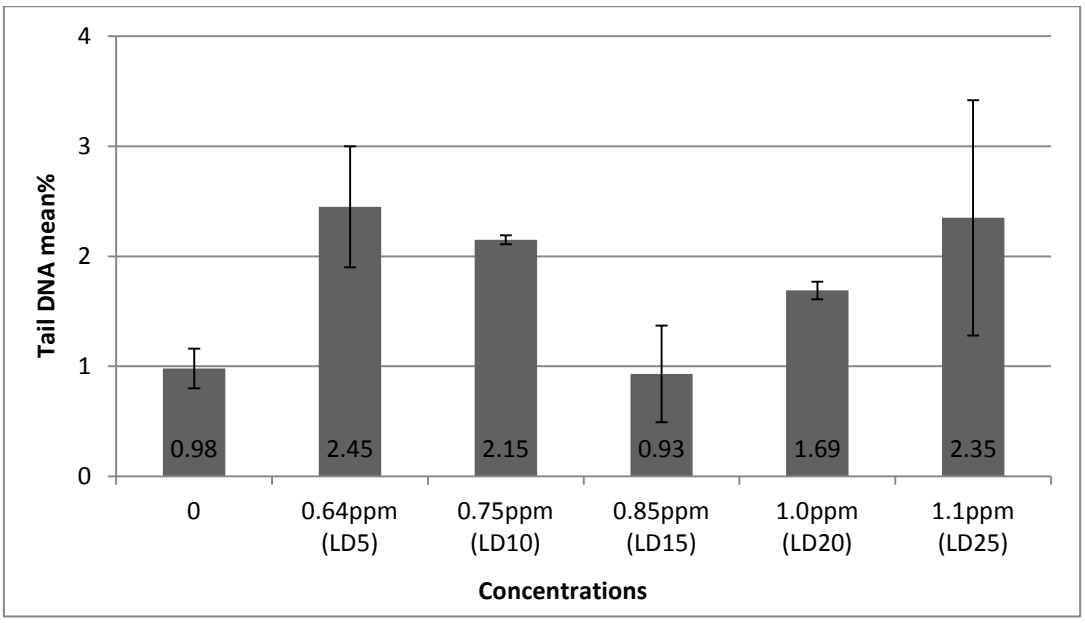

Figure 4.13 Mean coelomocyte tail DNA percentage in earthworms (n = 3) exposed to different concentrations of $AgNO_3$; error bars are standard deviations.

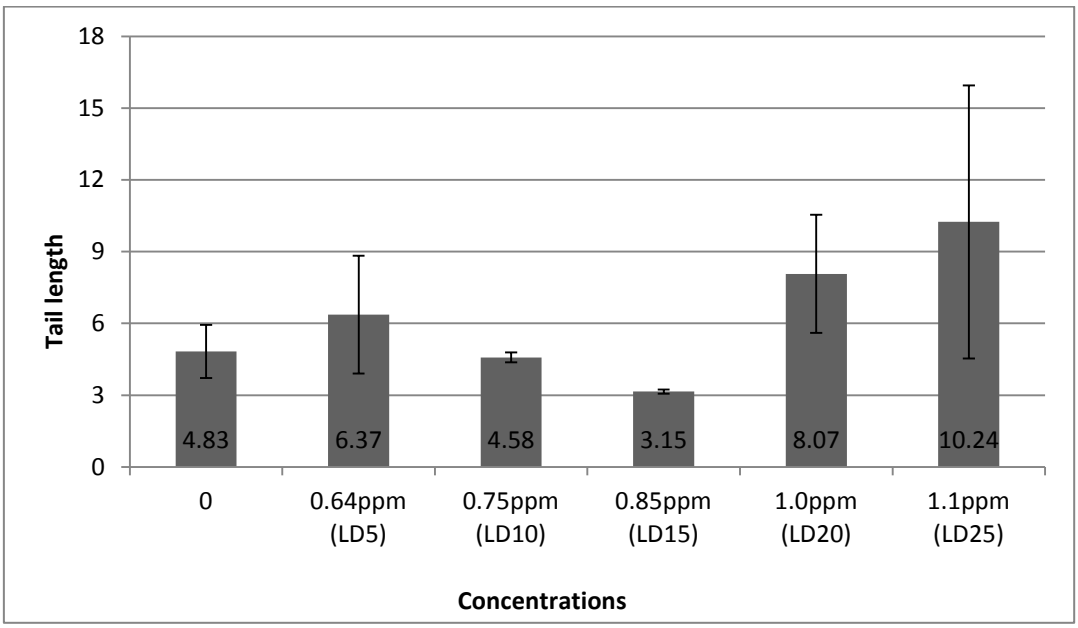

Figure 4.14 Mean coelomocyte tail length of earthworms (n = 3) exposed to different concentrations of $AgNO_3$; error bars are standard deviations.

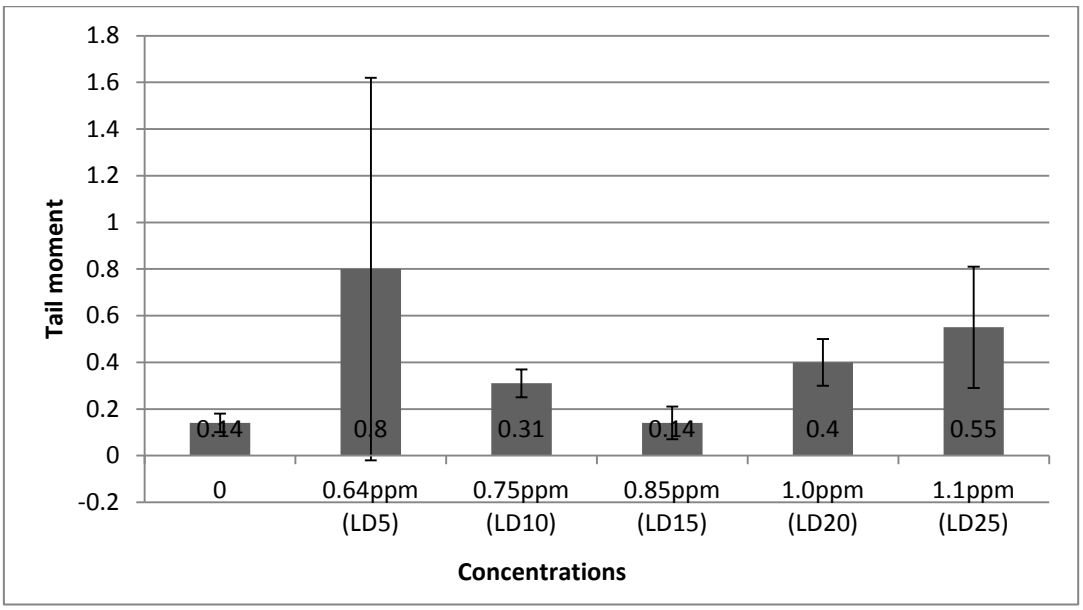

Figure 4.15 Mean coelomocyte tail moment of earthworms (n = 3) exposed to different concentrations of $AgNO_3$; error bars are standard deviations.

4.4 Discussion

Only a few toxicity studies have been carried out on earthworms exposed to $AgNO_3$ or AgNP and this is the first for the *A. caliginosa* earthworm. There is some evidence for avoidance of AgNP by the *E. fetida* earthworm described by Shoults-Wilson *et al.* (2011). Soil avoidance assays, inductively coupled plasma mass spectrometry (ICP-MS) analyses and fatty acid methyl ester (FAME) analyses were performed in that study. It was found that *E. fetida* consistently avoided soils containing AgNP and $AgNO_3$ at similar concentrations of Ag. Moreover, in this study, the avoidance of $AgNO_3$ was immediate whereas the avoidance of AgNP occurred later, after 48 h, indicating the greater toxicity of $AgNO_3$. It appears that earthworms are generally tolerant of AgNP and this study supports those findings since no deaths were observed at 48 h with AgNP even at exposure of earthworms to 2000 ppm in the Petri-dish filter paper and the soil exposure studies. Total 48-h earthworm mortality in the control replicates in all my studies was nil and according to the validity criteria of the OECD test protocols (1984) for earthworms it should be less than 10%, and therefore my studies fully comply with OECD guidelines.

It appears that even inorganic Ag as in $AgNO_3$ is not that toxic, which is different to the reports for heavy metals such as Cd and lead (Pb). Muangphra and Gooneratne (2011a) observed significant toxic effects in *Pheretima peguana* earthworms in Petri-dish filter-paper test and deaths occurred at all tested heavy metal concentrations of Cd (4.70, 5.85, 7.05, 8.23,

9.40 and 10.58 µg cm^{-2}) and Pb (32.90, 37.60, 42.30, 47.00, 51.70 and 56.40 µg cm^{-2}) and were most marked at the highest tested concentrations: 10.58 µg cm^{-2} for Cd and 56.40 µg cm^{-2} for Pb. In that study the 48-h LC_{10} and LC_{50} values for Cd were 1.65 and 6.09 µg cm^{-2} respectively and for Pb, 26.64 and 43.43 µg cm^{-2}. Thus Cd was acutely more toxic than Pb to *P. peguana* with the LC_{10} and LC_{50} values of Cd for earthworms being 15-fold and 7-fold lower, respectively, than those of Pb.

Among the different coelomocyte types, the eleocytes in earthworms exposed to the highest dose of both AgNP and $AgNO_3$ were less in number but not statistically significant ($P > 0.05$) from the controls. It is important to understand that eleocytes are the most active immune cells in the earthworm and derived from detachment of chloragogen cells covering the intestinal tract and the mesenchymal lining of the coelom (Cooper and Stein, 1981); therefore, a decrease in these cells may have an effect on earthworms being not able to cope with stress and being more susceptible to disease-causing agents.

According to the Micronucleus Test results, there was a significant increase in MN and BN in coelomocytes of *A. caliginosa* earthworms exposed to higher concentrations of AgNP and $AgNO_3$ in their aqueous solutions and this was most marked in earthworms exposed to the $AgNO_3$ concentrations. This detection of MN and BN, which are usually formed in the bi- or multinucleated interphase cells, is indicative of chromosomal damage caused by exposure to the two toxicants being greater as the toxicant concentration increased.

In contrast, the results of TD, TL and TM in the Comet Assay did not show a clear trend in earthworms exposed even to the higher toxicant concentrations. It is possible that the 48-h exposure to AgNP and $AgNO_3$ aqueous solutions may not have been adequate to cause DNA damage in *A. caliginosa* earthworm coelomocytes. In other studies with heavy metals, toxicological effects of TiO_2 and ZnO NPs in soil on earthworm *E. fetida* have been observed in the Comet Assay (Hu *et al.*, 2010). Hu and colleagues showed that TiO_2 and ZnO NPs could induce significant damage to earthworms when doses were greater than 1.0 g kg^{-1} in soil and that toxicity of ZnO NPs was higher than with TiO_2.

In conclusion, under the conditions of the experiment, AgNP was more toxic to *A. caliginosa* but the LD_{50} values for both the Petri-dish filter paper test and soil test were relatively high with values 571 and 418 ppm, respectively. The frequency of MN at most concentrations was higher than for BN on exposure to both AgNP and $AgNO_3$ with one exception. The frequencies of the sum of BN and MN in coelomocytes were significantly higher with both AgNP and $AgNO_3$ at concentrations of LD_{15} upwards compared to the controls. Thus it

appears that both AgNP and $AgNO_3$ are capable of causing chromosomal aberrations and cytokinesis failure at higher exposure concentrations. TD, TL and TM were measured by the Comet Assay to assess DNA single-strand breaks but results with both AgNP and $AgNO_3$ were not significant, indicating that neither of these two chemicals induces DNA single- or double-strand breaks.

Chapter 5
Functional Ecotoxicogenomics

5.1 Introduction

Ecotoxicogenomics is the study of gene and protein expression in non-target organisms that are viewed as important or sentinel species in their responses to exposure to environmental toxicants (Snape *et al.,* 2004). Silver nanoparticles are currently one of the most widely used commercially available nanomaterials (Chen and Schluesener, 2008). Therefore, recent investigations of AgNP pollution have concentrated on identifying the potential toxic mechanisms including gene expression (induction/suppression) in the most ecologically relevant soil organism, the earthworm, and downstream long-term risks to the environment (Hoet *et al.,* 2004; Handy *et al.,* 2008). Earthworms account for the majority of animal soil biomass (Bohlen, 2002). Because of their intimate contact with soil, earthworms are exposed to a wide range of contaminants. Therefore, they are one of the most relevant sentinel organisms for assessing the impact of ecotoxicological stresses in the soil (Spurgeon *et al.,* 2002). As an indigenous taxon and the most abundant earthworm in New Zealand farmland, *A. caliginosa* is preferred over *E. fetida* for environmental monitoring (Klobučar *et al.,* 2011).

Oxidative stress as a toxic mechanism of AgNP was reported in microorganisms (Choi and Hu, 2008) and reactive oxygen species (ROS) generated by AgNP or Ag^+ ions were reported to be responsible for the bactericidal activity observed (Kim *et al.,* 2007). Moreover, a recent study of the mechanisms of AgNP toxicity using stress-specific, bioluminescent bacteria demonstrated toxicity of AgNP via oxidative damage (Hwang *et al.,* 2008). Superoxide dismutase belongs to a ubiquitous family of enzymes that efficiently catalyse the dismutation of superoxide anions (Zelko et al., 2002). At present, three distinct isoforms of SODs have been biochemically and molecularly characterized. SOD1, or CuZn-SOD, was the first enzyme to be characterized and is a copper (Cu) and zinc (Zn)-containing homodimer found in the cytoplasm, nuclear compartments, and lysosomes of mammalian cells (Chang *et al.,* 1988; Keller *et al.,* 1991; Crapo *et al.,* 1992). *SOD*2, or Mn-SOD, exists as a tetramer and is localized to mitochondria of aerobic cells (Weisiger and Fridovich, 1973). SOD3 is the most recently discovered and least characterized member of the SOD family. The expression pattern of SOD3 is restricted to specific cell types and tissues where its activity can exceed that of SOD1 and SOD2 (Zelko *et al.,* 2002). Toxicity of AgNP has been studied in *C. elegans* by *SOD*1 and *SOD3* gene expression responding to ROS in comparison to $AgNO_3$

(Roh *et al.,* 2009). The *SOD* gene has not previously been identified or studied in *A. caliginosa* earthworms. Only one complete *SOD* gene from *E. fetida* and two partial *SOD* genes from *Lumbricus* have been sequenced from annelid species. Therefore, it is valuable to identify the *SOD* gene in *A. caliginosa*, even partially, and obtain more information from gene expression after exposed to the toxicants AgNP and $AgNO_3$.

Detecting changes in gene expression profiles following pollutant or toxicant exposure, such as by reverse transcriptase quantitative PCR (RT-qPCR), appears to provide a more accurate and sensitive insight into the mechanism(s) of toxicity than by typical ecotoxicological parameters such as mortality, growth or reproduction (Hamadeh *et al.,* 2001; Menzel *et al.,* 2005). These assays are particularly useful in toxicity screening of chemicals, such as AgNP, with largely unknown modes of action (Roh *et al.,* 2009).The aim of this study was to (1) use degenerate PCR to amplify the *SOD* gene from *A. caliginosa* earthworms and (2) study the expression of the *SOD* gene in earthworms exposed to AgNP and $AgNO_3$.

5.2 Methods

5.2.1 Earthworm collection

Adult *A. caliginosa* with well-defined clitellum weighing between 300 and 500 mg and measuring approximately 60–100 mm in length were collected from maintained earthworms in section *4.2.3.1*.

5.2.2 Primer design

Genomic sequences of *Lumbricus rubellus* and *E. fetida* earthworms and blue mussel (*Mytilus edulis*) were sourced from Wormbase (http://www.wormbase.org/). Primers were based on areas conserved between *L. rubellus, E. fetida* and *M. edulis SOD* genes. The close phylogenetic relationship and conservation of the *SOD* gene allowed the design of primers without degeneracy.

Two pairs of degenerate primers were designed. Both forward primers were designed within the first exon of the *SOD* gene and were called primer A: 5’- GGTTGCACAAGTGCAGG TG - 3’and primer B: 5’- GGTGCTCACTTCAACCCATT - 3’; and one reverse primer was

designed within the third exon and was called primer C: 5'- AGATCRTCCACCAGCTCAT GT- 3'. The expected product sizes were 204 bp and 192 bp from primer combinations A/C and B/C, respectively.

5.2.3 DNA extraction

Genomic DNA was extracted from *L. rubellus*, *E. fetida* and *A. caliginosa* earthworms using the PureGene DNA Extraction kit (PuregeneTM, Gentra Systems, Minneapolis, USA) according to the manufacturer's instructions. A 5-mm (~ 5–10 mg) portion of fresh or frozen head or tail tissue (minced) was placed into a 1.5-ml tube containing 300 µl of cell lysis solution. A 1.5-µl aliquot of proteinase K solution (Fermentas, 900 U ml^{-1}, 20 mg ml^{-1}) was added to the lysate and mixed by inverting 25 times. This solution was incubated at 55°C overnight or until the tissue has dissolved. Following incubation, 1.5 µl RNase A (QIAGEN, Cat # 19101, 100 mg ml^{-1}) was added to the cell lysate, the sample mixed by inverting the tube 25 times and incubated at 37°C for 15–60 min. The sample was then cooled to room temperature (RT) and 100 µl of protein precipitation solution was added to the cell lysate. The mixture was vortexed at high speed for 20 s to mix the protein precipitate solution uniformly with the cell lysate and then centrifuged at 13,000–16,000 *g* for 3 min to pelletize the precipitated proteins. If the protein pellet was not tight, the vortex step was repeated and the mixture incubated on ice for 5 min prior to centrifuging again at the same speed.

The supernatant containing the DNA was poured into a clean 1.5-ml tube containing 300 µl 100% isopropanol (Autopure 100% isopropanol, QIAGEN, Cat # 949016) and mixed by inverting gently 50 times to precipitate the DNA. The DNA was pelletized by centrifugation at 13,000–16,000 *g* for 1 min. The DNA was visible as a small white pellet. The supernatant was discarded and the pellet washed by the addition of 300 µl of 70% ethanol. The washed DNA was collected by centrifugation at 13,000–16,000 *g* for 1 min. The ethanol was carefully discarded, the tube inverted on a clean paper towel and the pellet allowed to air-dry for 10–15 min.

DNA was rehydrated by the addition of between 20 and 50 µl of nuclease-free water (Ultrapure distilled water, Gibco) and incubating the sample for 1 h at 65°C. The DNA was stored temporarily at 4°C or ─80°C for long-term (> 6 weeks) storage. The purity and quantity of the DNA were then measured by spectrophotometry (NanoDrop® Technologies Inc., Delaware, USA).

5.2.4 PCR and gene sequencing

A PCR reaction was run initially for each pair of primers (A & C and B & C). Each 25-µl reaction contained 1 × buffer [50 mM Tris/HCl, 10 mM KCl, 5 mM $(NH_4)_2SO_4$, 2 mM $MgCl_2$, pH 8.3], 200 µM of each dNTP (Fermentas Life Sciences, Cat # R0192), 2 µM forward primer, 2 µM reverse primer, and 1.25 unit (U) FastStart Taq DNA polymerase (5 U μl^{-1} Roche Applied Science, Mannheim, Germany), nuclease-free water, and 40 ng of DNA from either *L. rubellus*, *E. fetida* or *A. caliginosa*. The PCR was done for both the A/C and B/C primer combinations. A negative control to which sterile water had been added instead of DNA was included in every PCR. The thermal cycle was as follows: 94°C for 3 min followed by 40 cycles of 94°C for 30 s, 60°C for 90 s and 72°C for 30 s. A final extension was done for 7 min at 72°C.

Five microlitres of the resultant PCR products were mixed with 3 µl of loading dye (0.25% bromophenol blue, 0.25% xylene cyanol and 40% sucrose in water) and loaded onto a 1.3% agarose gel, and separated by electrophoresis at 10 V cm^{-1} for 1 h in 1 ×TAE buffer (48.4 g Tris, 11.42 ml acetic acid and 7.44 g EDTA dissolved in dH_2O to make up the final volume of 2 L). An aliquot of the 1kb plus DNA ladder™ (Invitrogen) was run alongside the PCR products as a molecular weight standard.

PCR products of the expected size were sequenced in both directions at the Lincoln University DNA Sequencing Facility. Returned sequences were manually trimmed for ambiguities using DNAman (Lynnon Biosoft version 4.0). The putative identity of the returned sequence was investigated using the Basic Local alignment Search Tool (BLAST) on the GenBank database (http://blast.ncbi.nlm.nih.gov/Blast.cgi).

5.2.5 Gene cloning

The ligation reaction was done using TA cloning with the pGEMT Easy™ kit as described by the manufacturer's (Promega, Madison, Wisconsin, USA) instructions. The ligation reaction was done in a total volume of 10 µl and consisted of 1 µl of PCR product together with 5 µl of 1 × rapid ligation buffer, 1 µl of pGEM®-T easy vector, 1 µl of T4 DNA ligase (3 U μl^{-1}) and nuclease-free distilled water to reach 10 µl. A positive control contained 1 µl of control insert DNA instead of PCR product and the negative control used pure water to replace the insert. The reaction was incubated overnight at 4°C.

Transformation was achieved by electroporation of *E. coli* DH5α cells using the PCR product ligated into the pGEMT Easy™ vector. A 40-µl aliquot of cells was gently thawed on ice and then mixed with 1 µl of the ligation reaction. The cells and vector were incubated on ice for 1 min prior to placing the entire contents in an ice-cold 0.2-cm electroporation cuvette (Promega). The cuvette was placed in a pre-cooled gene pulsar slide (Promega). The gene pulsar was set to Bacteria / Ec2, and the contents in the cuvette pulsed once. One millilitre of SOC medium [2.0 g of Bacto®-tryptone, 0.5 g of Bacto®-yeast extract, 1 ml 1 M NaCl and 0.25 ml 1M KCl added to 97 ml distilled water, autoclaved and cooled to room temperature. Next were added 1 ml 2 M Mg^{2+} (2.033 g $MgCl_2 \cdot 6H_2O$ and 2.465 g $MgSO_4 \cdot 7H_2O$ add distilled water to 10 ml) and 1 ml 2 M glucose, each to a final concentration of 20 mM. This was brought to 100 ml with sterile distilled water and the final pH should be 7.0] was added to the cells and the cells were incubated in a shaker at 37°C and 1,400 rpm (Ratek OM11) for 1 h. LB-agar plates [8.25 g of LB Miller (Difco™ Luria-Bertani) mixed with 3 g of agar, made up to 300 ml with distilled water, autoclaved and cooled down to <50 °C, supplemented where appropriate with ampicillin (Amp) 100 ug ml^{-1}, kanamycin (Kan) 50 ug ml^{-1}, and Tet 10 ug ml^{-1}]. Between 40 and 100 µl of transformed cells were spread onto dried LB plates that had been prewarmed to 37˚C, and incubated overnight at 37°C. Transformed colonies (white colonies) were randomly chosen and amplified by colony PCR using primers (10 µM) M13 F (5'- CTGGCCGTCGTTTTAC - 3') and M13 R (5'-CAGGAAACAGCTATGAC - 3') that are complementary to the plasmid region of insertion. PCR products of expected size (PCR product size + 257 bp) were sequenced.

5.3 Reverse transcriptase quantitative PCR (RT-qPCR)

5.3.1 RNA stabilization

Before excizing the tissue sample, the weight of the sample to be stabilized in RNA*later* RNA stabilization reagent (RNA*later*, QIAGEN, Cat # 76104) was estimated. This stabilization reagent prevents RNA degradation and maintains RNA stability for up to 4 weeks at 2–8°C. For extraction of RNA, the tissue was removed from the stabilization reagent. In this experiment, 30–50 mg of tissue (head and tail) was used from each worm. Therefore, 500 µl of RNA*later* RNA stabilization reagent was aliquotted into 1.5-ml tubes. Excised tissue from both the head (anterior) and tail (posterior) of the worms was cut into thin slices less than 0.5

cm thick and immediately submerged in the 500 µl RNA*later* RNA stabilization reagent. Samples were kept at 4°C.

5.3.2 RNA extraction

RNA extraction requires general precautions to minimize contamination by RNAses, including wearing gloves during all steps and changing them often, using RNAse-free glassware treated with diethylpyrocarbonate (DEPC at 0.1% in distilled water), commercially supplied RNase and DNase- free plasticware and water, a set of pipettes specific for RNA use and barrier pipette tips.

The tissue from each aliquor of head and tail region tissue was ground in liquid nitrogen with a mortar and pestle and the frozen powder placed in a clean 1.5-ml tube. RNA was extracted using a Nucleic Acid Isolation kit (E.Z.N.A.® Mollusc RNA isolation Kit, Omega Biotek Inc., Georgia, USA) according to the manufacturer's instructions. To the powder, 500 µl buffer RB/2-mercaptoethanol was added and vortexed vigorously to ensure that all clumps were dispersed. The mixture was centrifuged at 10,000 *g* for 5 min at RT and the supernatant carefully transferred to a clean 1.5-ml tube. Five hundred microlitres of 70% ethanol was added and then the entire mixture applied to a HiBind® RNA column assembled in a 2-ml collection tube. The tube was centrifuged at 13,000 *g* for 45 s and the flow-through discarded. RNA buffer I (500 µl) was added and the tube again centrifuged at 13,000 *g* for 45 s. The flow-through was discarded and the column placed in a clean 2-ml collection tube. Five hundred microlitres of Wash Buffer II was added and centrifuged at 13,000 *g* for 30 s at real-time and the flow-through discarded. This washing step was repeated once before the column was centrifuged at 13,000 *g* for 1 min at full speed to completely dry the HiBind™ matrix. The column was transferred into a clean 1.5-ml tube and the RNA eluted with 50 µl of DEPC-treated water. The isolated RNA was placed on ice at 4°C.

5.3.3 DNase digestion

Prior to DNase digestion, spectrophotometry (NanoDrop® Technologies Inc., Delaware, USA) was applied to determine the RNA concentration for each sample. DNA contamination was removed using a Deoxyribonuclease I Amplification Grade kit (DNase, Amp Grade, Invitrogen). One microgram of RNA sample was incubated in 1 × DNase I Reaction Buffer

[20 Mm Tris-HCl (pH8.4), 2 mM $MgCl_2$, 50 Mm KCl], 1 U of DNase (1 U μl^{-1}) and RNase-free water (diethylpyrocarbonate treated water, UltraPure™) in a total volume of 10 µl. The reaction mixture was incubated at room temperature for 15 min, and then the DNase inactivated by adding 1 µl of 25 mM EDTA (pH 8.0) and heating at 65°C for 10 min. The DNA-free RNA sample was ready to use in RT-qPCR.

5.3.4 Qiagen OneStep RT-qPCR

RT-qPCR was performed on a real-time PCR instrument (ABI PRISM® 7000 Sequence Detection System-Applied BioSystems, CA, USA) using 96-well reaction plates for real-time PCR (Global Sciences, AYPCR96ABC) and optical adhesive covers for the microplates (Raylab EXTSSRQ100). A QIAGEN real-time PCR one-step kit (Cat # 210212) was used following the manufacturer's instructions. The kit, kept at ─80°C, was thawed at room temperature for use. Each 16 µl of reaction solution contained 0.8 U of FastStart Taq polymerase, 1× buffer [50 mM Tris/HCl, 10 mm KCl, 5 mM $(NH_4)_2SO_4$, 2 mM $MgCl_2$, pH 8.3], 2 mM of $MgCl_2$, 200 µM of each dNTPs, 0.4 µM of each primer, 1.25 × ROX reference dye (Invitrogen, Cat # 12223-012), 0.23 µl of pre-diluted SYBR® Green I (1:1000, nucleic acid gel stain, 10,000 × concentration in DMSO, Invitrogen Molecular Probes) and 1.25 ng of template (RNA sample). The reference primers for the β-actin gene were used at a concentration of 0.2 µM. Each template was a subsample from a pool of three RNA samples extracted individually from the same experimental container in order to minimize the inherent differences in gene expression levels between individual organisms. Each pool was run as three replicate samples. A non-template control, to which the RNA template was substituted with distilled water, was applied to ensure all reactions were free of contamination.

The PCR thermal cycler parameters were set to an initial denaturation of 50°C for 30 min followed by 40 cycles of 15 s at 95°C (denaturation), 15 s at 94°C (primer annealing) and 30 s at 60°C (extension).The fluorescence signal was measured at 94°C during the annealing step and results were represented as C_q values. In the RT-qPCR instrument used, the melting point analysis was automatically carried out by a dissociation stage provided in the manufacturer's software (ABI Prism 700 by DLS Inc., version 1.0) following amplification.

5.3.5 RT-qPCR data analysis

The generated Cq values were transferred to Microsoft Excel and the average of the technical replicates calculated. The target Cqs were normalized by subtracting the endogenous reference gene (β-actin) Cq value. Normalization of target gene expression levels was performed to compensate for intra- and inter-kinetic RT-qPCR variations, also known as sample-to-sample and run-to-run variations (Derveaux *et al.,* 2010).

The RT-qPCR data of this research was analysed by the comparative Cq method also referred to as the $2^{-\Delta\Delta Cq}$ method (Livak and Schmittgen, 2001; Schmittgen and Livak, 2008).

Fold change = $2^{-\Delta\Delta Cq}$

(Equation 5)

Equation 5 was used to compare the gene expression in two different samples (samples A and B). In this research, sample A was RNA extract from *A. caliginosa* earthworms exposed to fixed concentration of toxicants and sample B was the untreated earthworms as a control. In this case, Equation 5 can be expanded to its full form:

$2^{-\Delta\Delta Cq}$ = [(Cq gene of interest – Cq internal control) sample A – (Cq gene of interest – Cq internal control) sample B]. (Equation 6)

The 2− ΔΔCq values represented the fold change in mRNA amounts in treated samples relative to the untreated control, arbitrarily set at 1. Results greater than 1 indicated increase in gene expression due to treatment (Schmittgen and Livak, 2008). The analysis of variance (P-value) between treated and untreated earthworms was done using single-factor ANOVA in Microsoft Excel and a P-value < 0.05 was considered statistically significant.

5.4 Results

5.4.1 Detection of a *SOD* gene in *A. caliginosa*

Amplification with primers A and C produced a single product of approximately 200 bp using DNA from *A. caliginosa* and no bands using DNA from either of the other two species (Figure 5.1). Amplification with primers B and C produced a single product of approximately

200 bp using DNA from *A. caliginosa* and one band of approximately 1650 bp using DNA from *Lumbricus*, but no band of *E. fetida* (Figure 5.1).

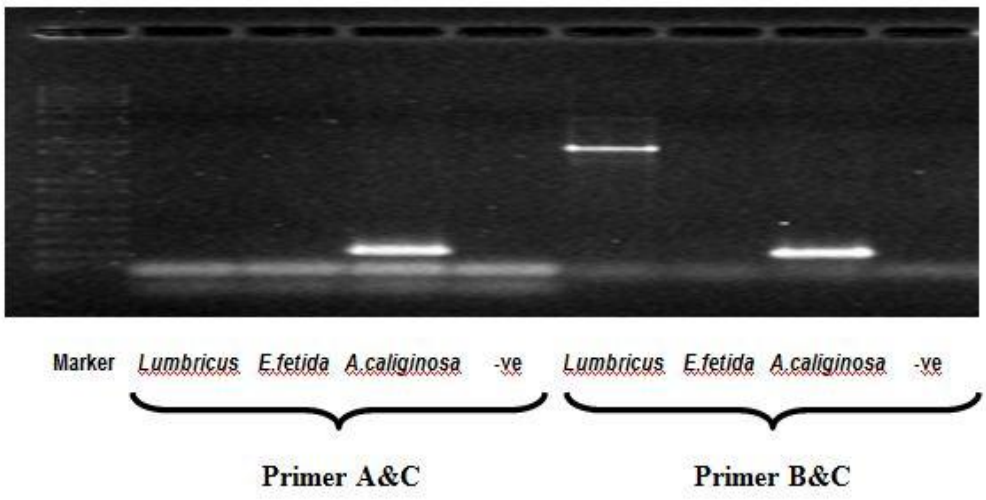

Figure 5.1 PCR products of *Lumbricus*, *Eisenia fetida* and *Aporrectodea caliginosa* earthworms with primer sets A&C and B&C. The marker is 1kb^{+} DNA ladder.

The two products of the expected size for *A. caliginosa* produced sequences that had similarity to *SOD* genes from other species. The bigger size sequence, which is approximately 1650 bp, is an unknown product. The PCR product amplified with primer B&C showed the greater similarity with both reference sequences (See Appendix B).

According to the similarity tree shown in Figure 5.2, all earthworm sequences clustered together with ≥ 88% similarity in *SOD* gene base sequence. The position in the tree reflected taxonomic relationships, with *A. caliginosa* more related to *Lumbricus* species than to *E. fetida*.

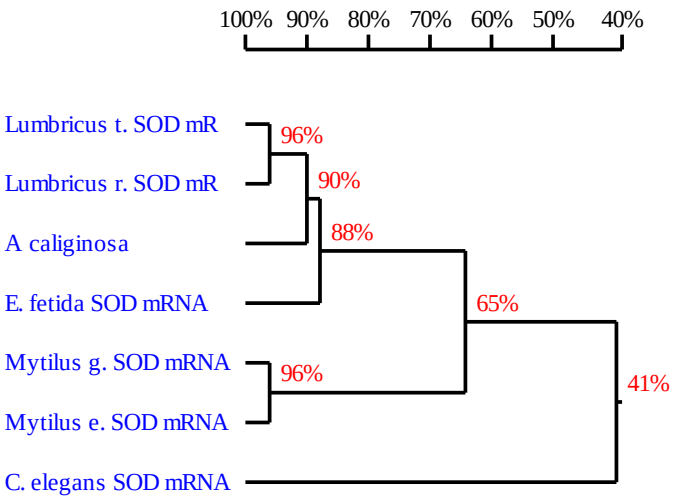

Figure 5.2 Similarity tree with sequence similarity (%) of *SOD* mRNA from seven species (*Aporrectodea caliginosa, Lumbricus rubellus, L. terrestrus, Eisenia fetida, Mytilus edulis, Mytilus galloprovincialis*, and *Caenorhabditis elegans*).

According to the similarity tree shown in Figure 5.3, all earthworm sequences clustered together with ≥93% similarity in *SOD* amino acid sequence. Again *A. caliginosa* is more similar to *Lumbricus* species than to *E. fetida.*

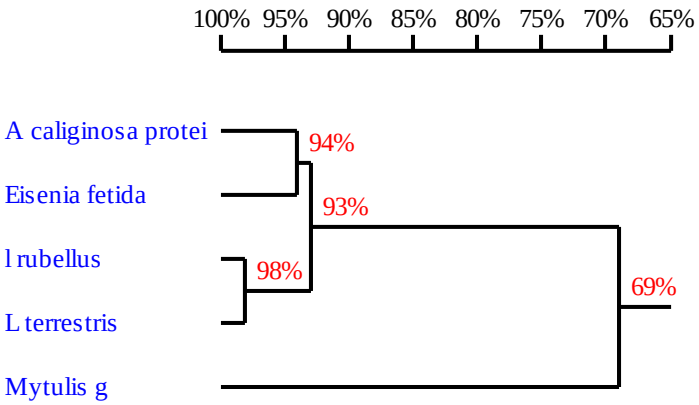

Figure 5.3 Similarity tree with amino acid (protein) sequence similarity (%) of *SOD* genes from five species (*Aporrectodea caliginosa, Lumbricus rubellus, L. terrestrus, Eisenia fetida,* and *Mytilus galloprovincialis*).

5.4.2 *SOD* gene expression analysis

Two parameters, exposure periods and body region of earthworms, that might influence gene expression, were analysed (Figure 5.4).

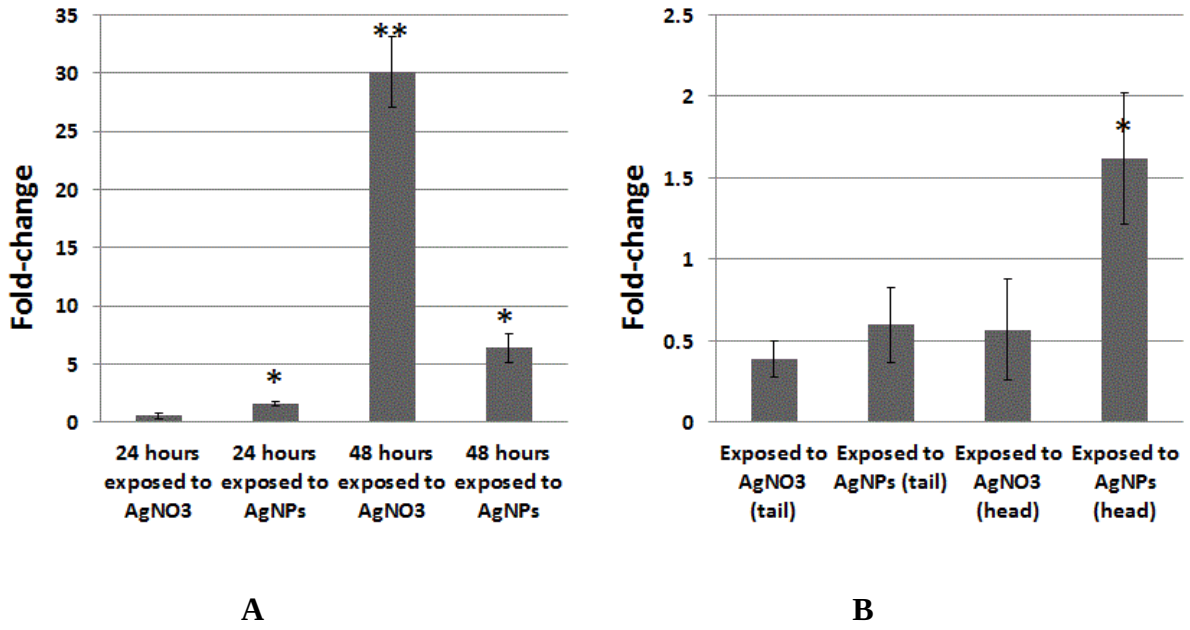

Figure 5.4 RT-qPCR analysis of *A. caliginosa* earthworms exposure to $AgNO_3$ and AgNP. (A) RT-qPCR analysis result of tissue of whole earthworm with different exposure times (24 h and 48 h); (B) RT-qPCR analysis result with tissues taken from the head and tail regions of *A. caliginosa* earthworms at 48 h. * indicates significant differences; *$P < 0.05$; **$P < 0.01$.

For mRNA extracted from the whole worm there was significantly ($P < 0.05$) higher expression of SOD (2.05-fold) in response to AgNP at 24 h compared to $AgNO_3$. In contrast after 48 h there was a 5-fold greater expression of SOD in response to $AgNO_3$ when compared to AgNP. Overall expression of SOD increased over time. When the expression of SOD was compared between the head and tail portions of the worms at 48 h there was no difference for worms exposed to $AgNO_3$. In contrast there was a 1.5-fold greater expression in the head when exposed to AgNP for 48 h.

5.5 Discussion

The subsequent study of *SOD* gene expression in *A. caliginosa* exposed to AgNP by RT-qPCR provided an overview of molecular responses to toxicants in the earthworm. This research describes the discovery of a partial sequence of the *SOD* gene from *A. caliginosa*, which is the most abundant species in grasslands and agricultural ecosystems (Pérez-Losada *et al.*, 2009) in New Zealand, by using a PCR-based strategy. Superoxide Dismutase [Cu-Zn]

(Cu/Zn-SOD) has high amino acid sequence similarity between species. For example, *L. terrestrus* and *L. rubellus* have 96% identity of SOD protein sequence, whereas, *E. fetida* has 88% identity of SOD protein sequence to either of the two Lumbricidae species (Figures 5.2 and 5.3). The translated partial sequence of the *A. caliginosa SOD* gene had high amino acid sequence identity (93%) to the Cu/Zn-SOD of the two *Lumbricus* species and 94% identity to *E. fetida* (Appendix C2). According to Hennessy and Spiers (2007), homologies with amino acid sequence of >40% identities compared to the known sequences from other species predicts the gene family relationship. Therefore, it is the first time that a partial sequence of *SOD* gene has been detected and identified from *A. caliginosa*.

Two pairs of primers were designed from conserved areas identified by multiple alignments of *SOD* mRNA sequences from *L. terrestrus*, *L. rubellus,* and *E. fetida*. Originally, *SOD1* mRNA sequence from *C. elegans* was included, but the distant taxonomic relationship of this species to earthworms was evident and reduced the identity of aligned sequences to <40%. According to Hennessy and Spiers (2007), *C. elegans* is not a species in the same phylum as earthworms. It is likely that other lumbricid *SOD* sequences will be valuable in the design of primers in this study, but they are rarely well known and sequenced. In this study, the main product of the *A. caliginosa SOD* gene was effectively isolated and identified by the insertion of the PCR product into *E. coli* DH5α cells for cloning.

The consensus *SOD* gene sequence obtained from *A. caliginosa* was 198 bp long. Genetic information from http://www.ncbi.nlm.nih.gov/nuccore showed that complete *E. fetida SOD* mRNA is 753 bp, and *SOD* mRNAs from both *Lumbricus* species are only partial sequences of 319 bp and 300 bp, respectively. Therefore, the consensus sequence from this work is only approximately 26% of the putative complete mRNA. This partial sequence of the putative *A. caliginosa SOD* gene should be extended to obtain the full length genomic sequence. The information obtained from a full-length *A. caliginosa SOD* sequence may further confirm the identity of the gene fragment and clearly differentiate it from closely related genes within the SOD subfamily. At present, Cu/Zn-SOD, or SOD1, was the first characterized SOD and it is a Cu and Zn-containing homodimer (Chang *et al.,* 1988). Other *SOD* genes from the same subfamily, such as *SOD*2 and *SOD*3, were also found in the same organism, *C. elegans* (Roh *et al.,* 2009). To date, the *SOD* genes sequenced from *E. fetida* and both *Lumbricus* have only been identified as *SOD* genes, without a subgroup assigned. Since they all have Cu-Zn active binding sites according to their known protein structure, they seem to be more closely related to known Cu/Zn-SOD, which are also called *SOD*1 in other species. However, it is unknown whether there are other *SOD* genes (*SOD2* or/and *SOD3*) in *E. fetida* and *Lumbricus* species.

In addition, a full-length *SOD* sequence would provide more detailed information on the base sequence and structure of this gene in Lumbricidae family members and may facilitate gene discovery in other earthworm species.

The *SOD* gene in *Lumbricus* is a Cu/Zn-*SOD*, which is responsible for the key enzyme in the dismutation of superoxide radicals resulting from cellular oxidative metabolism into hydrogen peroxide (Fridovich, 1978). According to the results (Appendix C), the new *A. caliginosa* sequence was aligned towards the 3'- end of *Lumbricus* and *E fetida SOD* genes. Even though it is a partial sequence, translation showed that it contained many active site residues that are highly conserved in *E. fetida* and both *Lumbricus* species, such as histidine at the Cu binding site, aspartate at the Zn binding site, and isoleucine and glycine at the dimer interface (Appendix C). The presence of these conserved active site residues strongly indicates that the partial *A. caliginosa* sequence is a Cu/Zn-*SOD*.

After detecting the *SOD* gene in *A. caliginosa* an RT-qPCR assay to measure the transcriptional copies of this *SOD* gene was developed. Although RT-qPCR using fluorescent probes is a common method for measuring gene expression, at present there was only one study of *SOD* gene expression in *E. fetida* earthworms using this approach (Chen *et al.*, 2011), presumably due to the lack of genetic information on the *SOD* gene from earthworms. In related work, the β-actin gene was isolated and sequenced from *A. caliginosa* by Giuliana Bernardi (2011). This gene was used as a reference gene in the RT-qPCR assay design.

An important step in RT-qPCR is the selection of proper reference genes (Piana *et al.*, 2008). Always, there are two sources of variation within experiments: one is the technical induced variation, and the other one is the true biological variation. The purpose of using reference genes in RT-qPCR is to remove or minimize the technical variation as much as possible (Piana *et al.*, 2008). The reference gene used in this study is β-actin, which is one of the six different actin isoforms, is a highly conserved protein that is involved in cell motility, structure and integrity. It was considered to be one of the most frequently investigated control genes in RT-qPCR assays (Yperman *et al.*, 2004). Previously, the β-actin gene has been widely used as the most common reference gene or a loading control in gene expression studies in earthworms (Homa *et al.*, 2010; Chen *et al.*, 2011; Wang *et al.*, 2011). However, according to a summarized guideline for successful and reliable real-time PCR experiments, the most appropriate and universally applicable method is to normalize against three or more validated reference genes (Derveaux *et al.*, 2010). In my study, only one reference gene, β-actin, was applied due to the limitation of availability of resources. In this case, there might still be some technical variation remaining in the final RT-qPCR results. Therefore, increased

number of reference genes, in addition to β-actin, could be applied in RT-qPCR of future studies on earthworms. The approach used to find the β-actin gene in *A. caliginosa* could be used to facilitate the discovery of other reference genes in those experiments (Bernardi, 2011).

Significantly higher expression of the *SOD* gene was observed with 48-h exposure periods to both $AgNO_3$ and AgNP in comparison to 24-h exposure time of both toxicants. This indicated that the *SOD* gene was up-regulated to both AgNP and $AgNO_3$ presumably in order to protect the organism against larger amounts of ROS produced in worms exposed to the toxicants for a longer period (Zelko *et al.,* 2002). However, this was not directly proven as neither enzyme activity nor protein quantities were measured. Increased expression of *SOD3,* which is the most recently identified and least characterized of the SOD subfamily, in *C. elegans* was reported following exposure to both AgNP and $AgNO_3$ (Zelko *et al.,* 2002). According to the known partially sequenced *SOD mRNA* from *L. terrestrus* and *L. rubellus* and *E. fetida*, the *A. caliginosa SOD* gene is most likely to be a Cu-Zn/SOD which is a *SOD1* (Chang *et al.,* 1988; Keller *et al.,* 1991; Crapo *et al.,* 1992). In *C. elegans*, there was no significant change in gene expression of *SOD1* by exposure to either AgNP or $AgNO_3$ (Zelko *et al.,* 2002), which might be explained by genomic difference between species. Moreover, this raises the question as to whether the *SOD* in the *A. caliginosa* earthworm is only a single gene such as *SOD1 or SOD3*, or whether it is a member of a gene family. To resolve this question, sequence extension will be followed with a gene expression study. To date, there is no published information on the toxicity of AgNP and $AgNO_3$ to earthworms or any closely related annelid species. The study of the *SOD* gene in the *A. caliginosa* earthworm, which belongs to the Lumbricidae family, may initiate a new area of research on NP toxicity effects on earthworms.

In this experiment, *SOD* gene expression was significant higher in the head region of *A. caliginosa* earthworms exposed to AgNP (1.62 fold-change, $P < 0.05$) in comparison with the tail region. The original idea of using RNA extracted from different earthworm body regions was to facilitate the identification of this *SOD* gene. For example, *SOD3* genes are predicted to be mitochondrial and are observed to be expressed mainly in the head and tail of *C. elegans* (Kirstein-Miles and Morimoto, 2010). In addition, based on gene expression comparison at 24 h and 48 h, the accumulation of *SOD* transcripts in correlation with longer exposure times would also be indicative of *SOD* genes. However, according to the result of this gene expression study based on RNA from different regions, it was not identified as preferentially expressed in either the head or tail in *A. caliginosa*. Dividing the earthworm into smaller and more specific regions for RT-qPCR analysis might be valuable to identify

SOD gene expression regions in future study. A similar approach to that used here could also be applied to other annelid species.

The expression of the *SOD* gene was much higher when exposed to $AgNO_3$, in comparison to AgNP, at 48 h. However, it could not be concluded as to which of the toxicants was more toxic, AgNP or $AgNO_3$. In a study of *C. elegans*, increased *SOD3* gene expression in exposed worms was considered to confirm the involvement of oxidative stress in AgNP-induced toxicity, as the enzymes involved in the breakdown of ROS play an important role in ROS-related toxicity (Zelko *et al.*, 2002). Both AgNP and Ag^+ ions generate ROS, thus based on the same mass concentration in this study due to the unknown AgNP molecular formula, higher Ag^+ concentration could lead to higher *SOD* gene expression levels.

In conclusion, for the first time a *SOD* gene has been identified in *A. caliginosa* and the expression of this gene in response to AgNP has been studied. Increased *SOD* gene expression in exposed worms might be due to the oxidative stress caused by Ag^+ (Roh *et al.*, 2009). The differential expression of the *SOD* gene on exposure to AgNP and $AgNO_3$ is interesting. The factors responsible for this are not known but solubility, particle size, and mobility of AgNP may have affected the bioavailability and hence the gene expression.

Chapter 6
General Discussion and Future Research

6.1 General discussion

With the growing use of AgNP, environmental contamination by AgNP exacerbates concerns about its ecological risks (Geranio *et al.,* 2009; Mueller and Nowack, 2008). However, such predictions cannot be validated due to a lack of experimental data. One of the major issues related to the determination of the environmental concentration of AgNP is the lack of analytical techniques and equipment (Fabrega *et al.,* 2010). Also, the toxicity and biological mechanism of AgNP in biosystems are still poorly known. Therefore, it is valuable to examine the ecotoxic effects of AgNP, thereby to contribute to establishing the ecological risk of AgNP to the environment.

Bacteria are single-celled organisms widespread in the environment (Berg *et al.,* 2002). Bacteria have commonly been used in traditional risk analysis to establish the toxicity of chemical compounds (Hansen and Sørensen, 2001). Many ecological studies of NPs have been based on bacterial studies because it is easier to work with bacterial cells and they play an important role in ecotoxicology (Thiel, 1999). Silver and AgNP are well-known anti-microbial agents (Rai *et al.,* 2009). The toxicity of AgNP was attributed to either free Ag^+ ions (Lok *et al.,* 2007; Su *et al.,* 2007) or particle size (Ahmad *et al.,* 2007). Earthworms are key terrestrial organisms and play a major role in soil fertility. *A. caliginosa* is the most abundant earthworm in grasslands and agricultural ecosystems in New Zealand (Pérez-Losada *et al.,* 2009). The focus of my master's research was on understanding the toxic effects of AgNP to two key environmental organisms, bacteria and earthworms. In all experiments the toxicity of AgNP was compared with exposure to a commonly used conventional aqueous conterpart of Ag, $AgNO_3$.

The SciTox^{TM} rapid DTA Assay is based on using a whole-cell microbial biosensor to measure the impact of toxic chemicals on biological materials resident in the environment (Pasco *et al.,* 2005). The respiratory inhibition index, IC_{50} (median inhibitory concentration), can be determined by using a standard dose–response curve. In this research, the bacterium *E. coli* was evaluated as a bio-component in a whole-cell-based toxicology bioassay in order to study the toxicity of AgNP as compared with $AgNO_3$.

Standard DTA assays were applied to *E. coli* bacteria exposed to a standard toxicant, 2,4-DCP, then AgNP and $AgNO_3$. Since AgNP did not respond even at the highest concentration (2000 ppm) used in this study, a modified method with an additional centrifuge step was used in the DTA Assay. The aim of the modification was to avoid any influence of AgNP particles on the electrodes in the SciTox™ rapid assay. EC_{50} values of 2,4-DCP and $AgNO_3$ from both the original (Method I) and the modified method (Method II) were relatively close, which meant that the modified method was as accurate as the original SciTox™ rapid assay to the toxicants. When compared to the standard toxin 2,4-DCP, $AgNO_3$ was more toxic based on its lower EC_{50} value. In both methods, AgNP did not show a clear dose–response relationship to *E. coli*. In a previous study, it was stated that when compared as a function of the Ag^+ concentration, the toxicity of AgNP appeared to be much higher than that of $AgNO_3$ (Navarro *et al.,* 2008). However, all toxicants in this experiment were calculated by mass concentration. There was no dose-response as AgNP mass concentration was from 0 to 2000 mg L^{-1}, whereas the bacterial cells showed a clear dose-dependent response to $AgNO_3$ at a lower concentration range (Figure 3.4 and 3.5). From previous studies, the toxicity of AgNP was attributed to two main characteristics, free Ag^+ ions (Lok *et al.,* 2007; Su *et al.,* 2007) and the nano size of the particles (Ahmad *et al*, 2007). However, with the molecular formula of AgNP unknown, the comparison of toxicity could only be based on mass concentration. The molecular weight of $AgNO_3$ is 169.9 g mol^{-1}, whereas that of AgNP used in this research was 500 g mol^{-1}. If the molecular formula of AgNP is $[Ag^+]_n[NP^{-n}]$ and $n = 1$, then the Ag^+ concentration in AgNP solution would only be 11.5% of $AgNO_3$ with the same mass weight; if $n > 1$, then the Ag^+ concentration in the AgNP solution would be even less. The behaviour of NPs is different compared to the classical salt. This might explain why there was no dose–response relationship observed for AgNP over the 0–2000 mg L^{-1} interval. In future research, it would be important to use AgNP with known molecular formula, molecular weight and their physical properties in experiments. Then comparison studies with other Ag^+ solutions can be based on Ag^+ ion concentration and not on mass concentration.

Nevertheless, even though there was no observed AgNP toxicity dose-reponse shown with the DTA Assay, a growth inhibition assay showed that AgNP can inhibit the growth of *E. coli* (Figure 3.6) which is in agreement with the anti-microbial activity of AgNP (Choi and Hu, 2008). Even though there was a clear positive inhibition response observed, which confirmed AgNP's antibacterial ability, the bacterial growth inhibition in this assay was only 38% at AgNP concentration of 10 mg L^{-1}, which was significantly lower than the 86% that was reported at 1 mg L^{-1} AgNP concentration in the extant respirometric assay (Choi and Hu, 2008). In the extant respirometric assay, the lowest Ag^+ concentration to make the AgNP

suspensions was 27 mg L^{-1}, whereas at the completion of the reaction, the residual Ag^{+} concentration was 0.6 ± 0.1 mg L^{-1} (Choi and Hu, 2008). The growth inhibition assay in my research involved 16-h incubation at 37°C. It is possible that the final AgNP concentration may have declined during the study and could have been even lower than 0.6 mg L^{-1} because AgNP solutions are not very stable especially during the first 24 h (Choi and Hu, 2008). However, a manuscript on the preparation of AgNP has reported that the stability of a homogeneous colloidal solution of AgNP could be from less than 2 weeks up to over 4 months (Das *et al.,* 2009). Moreover, it was also pointed out that the optical, electronic, magnetic and catalytic properties of the metal NPs depended on the size, shape and chemical surroundings. Therefore, in AgNP synthesis, it is very important to control not only particle size but also particle shape and morphology (Das *et al.,* 2009). In future studies of AgNP, in order to achieve reliable and accurate results, it is always important to prepare a stable solution with correct particle size, shape, and a higher solubility. After I had completed my research, I found an old but an interesting method to synthesize AgNP from $AgNO_3$ (Carey Lea, 1889).

A. caliginosa earthworms are the most abundant earthworms in grasslands and agricultural ecosystems (Pérez-Losada *et al.,* 2009). It is also the most common indigenous earthworm in New Zealand. Because of their abundance on New Zealand farms, *A. caliginosa* was used in all experiments of my master research to study the ecotoxicity of AgNP compared with the effects caused by $AgNO_3$. Only a few toxicity studies have been carried out on exposure of earthworms to AgNP and $AgNO_3$ (Fabrega *et al.,* 2010). It appears that earthworms are highly tolerant of AgNP (Shoults-Wilson *et al.,* 2011), which was also the case in this research as no mortality occurred even at 2000 ppm exposure for 48 h in my soil acute toxicity experiment. It is also possible that the bioavailability of my AgNP was low. Total 48-h earthworm mortality in the control replicates was nil and according to the validity criteria of the OECD Petri-dish test protocols for earthworms it should be less than 10% (OECD 1984), and therefore this study complies with OECD guidelines. Moreover, it appears that even inorganic Ag as in $AgNO_3$ may not be that toxic, which is different to the reports for other heavy metals such as Cd and Pb (Muangphra and Gooneratne, 2011a).

Previous studies have shown the toxic effects of AgNP on human liver carcinoma cells, causing DNA damage (Saddler *et al.,* 2012). The Comet Assay is a sensitive and rapid method for detecting DNA damage (Tice *et al.,* 2000). Moreover, the Micronucleus Test, a well-established assay in genotoxicity testing, also provides information on nuclear anomalies caused by chromosomal damage, such as binucleated, blebbed, notched and lobed nuclei

(Toyoshima *et al.,* 1999). Results of the earthworm coelomocyte Comet Assay carried out in this research showed that by comparison with controls (no toxicant exposure) there was little or no DNA damage (Figure 4.10 – 4.15). Thereby, it can be stated that there was no harmful effects of either toxicant (AgNP and $AgNO_3$) to *A. caliginosa* earthworm coelomocyte DNA. It is possible that a 48-h exposure to AgNP and $AgNO_3$ aqueous solutions may not have been adequate to cause damage to the *A. caliginosa* earthworm coelomocyte DNA. The detection of a significant increase in both MN and BN indicated chromosomal aberrations and cytokinesis failure at higher AgNP and $AgNO_3$ concentrations (Figure 4.8). Because *A. caliginosa* earthworms were able to survive for more than 48 h in aqueous AgNP and $AgNO_3$ solutions, a longer AgNP aqueous solution exposure time could be considered in future acute toxicity studies, although it would not be a standard practice.

In this study, new genetic information was generated for the *A. coliginosa* earthworm. Primers were designed from conserved areas identified by multiple alignment of *SOD* genes from *L. rubellus*, *E. fetida* and the New Zealand blue mussel (*M. edulis*). A partial sequence homologous to the *SOD* gene was detected using standard PCR protocols. This gene sequence showed 90% similarity to the *SOD* gene in both *L. terrestris* and *L. rubellus*, and 88% similarity to the *E. fetida SOD* gene (Figure 5.2 and 5.3). Even after converting the gene sequence to amino acid at protein level, the sequence similarity was still > 93%. According to Hennessy and Spiers (2007), homologies at protein level that achieve ≥ 40% identity compared to known sequences of other species predict the gene family relationships. Therefore, this study reports for the first time a new coding *SOD* gene sequence for *A. caliginosa*. However, by comparing this detected gene size with other partial and complete *SOD* genes from either *Lumbricus* species or *E. fetida*, this *SOD* gene detected in *A. coliginosa* is clearly a partial sequence from the whole gene. In future studies it should be extended to obtain the full-length genomic sequence. In addition, a full-length *SOD* sequence would provide more detailed information on the base sequence and structure of this gene in Lumbricidae family members and may facilitate gene discovery in other earthworm species because of the high sequence similarity of *SOD* genes within earthworm species. The complete *SOD* gene sequence information would be useful for designing primers to discover unknown *SOD* gene sequencing from other Lumbricidae family members. After the *SOD* gene detection and sequencing, a study of *SOD* gene expression in *A. caliginosa* earthworms exposed to AgNP by RT-qPCR was performed. Significantly higher expression of the *SOD* gene was observed with longer exposure periods to both $AgNO_3$ and AgNP, which indicated a potential increase in SOD enzyme activity to protect the organism against the supposedly higher amounts of ROS produced in earthworms exposed to the heavy metal toxicants (Zelko

et al., 2002). Increased *SOD* gene expression in earthworms exposed to AgNP might be due to the oxidative stress caused by Ag (Roh *et al.*, 2009). There was a significantly higher *SOD* gene expression with exposure to $AgNO_3$ at 48 h (30-fold increased as shown in Figure 5.4). The differential expression of the *SOD* gene on exposure to AgNP and $AgNO_3$ is interesting. The factors responsible for this are not known but solubility, particle size, and mobility may have played a role.

6.2 Future research

In my SciTox™ rapid DTA assay, due to the molecular formula of AgNP being unknown and probably due to the lower bioavailability of the AgNP and therefore the non-response in the classical and modified DTA Assay, the EC_{50} on *E. coli* could not be identified unlike with $AgNO_3$. It is important to use a highly soluble AgNP in future research. The actual particle formula would also be highly desirable for any further study on AgNP in terms of calculating the actual Ag concentration the organisms would be exposed to. Exposure to microorganisms, preparation of a stable and uniform distributed homogeneous colloidal solution of AgNP is critical for the SciTox™ rapid DTA Assay. According to my study, it was difficult to determine whether the modified DTA method (Method II) had eliminated any influence of AgNP particles on the electrodes since there was no dose-reponse observed from either method. Further modifications can be considered to the original SciTox™ rapid DTA Assay in toxicity studies of AgNP in future.

A limitation of the acute toxicity assay in this research is the toxicant exposure time on *A. caliginosa* earthworms. It was stated that earthworms are generally tolerant to AgNP (Shoults-Wilson *et al.*, 2010). Moreover, some evidence for avoidance of AgNP by *E. fetida* earthworms have also been described by Shoults-Wilson *et al.* (2011). This explained the reason why no deaths were observed at 48 h in the AgNP soil study on *A. caliginosa*. Therefore, the acute toxicity assay of AgNP on *A. caliginosa* has been eliminated from soil exposure for further studies. Without soil as an intake food, adult *A. caliginosa* were observed to survive in control solution (without any toxicants) for only 4 days. In this case, any harmful effects from AgNP, caused at low concentration but with long-term exposure (e.g. more than 4 days), could not be studied in *A. caliginosa* in aqueous solution. Because exposure to AgNP and Ag^+ ions generates ROS (Roh *et al.*, 2009), the lipid peroxidation assay could be a valuable method for studying oxidative stress. However, if bioavailability of AgNP in

aqueous solution is low, the only tissues most likely to undergo lipid peroxidation would be the epidermal tissues.

The gene sequence detected from standard PCR from my research has been confirmed as only a partial sequence of the putative *A. caliginosa SOD* gene. Therefore, this sequence should be extended to obtain the full-length genomic sequence, which will further confirm the identity of the *SOD* gene within the Lumbricidae family. Some organisms have only one *SOD* gene, whereas others may have more than one isoform with completely different functions. At present, the *SOD* genes in *Lumbricus* species and *E. fetida* have similar SOD enzyme activity to *SOD1* in other species. If the full-length *A. caliginosa* gene sequence could be determined, it might bring us to the new territory of including *A. caliginosa* in the *SOD* gene classification in earthworms. The partial *A. caliginosa SOD* gene could be extended by repeating the 3' RACE method together with the 5' RACE amplification in combination with a cloning step. The full-length *SOD* gene sequence information would be useful for designing new primers to discover unknown *SOD* gene sequencing from other Lumbricidae family members. In this case, the active enzyme of SOD in *A. coliginosa* earthworm and of other Lumbricidae family members could be clarified with more detailed information.

To improve the RT-qPCR assessment, it is necessary to include three or more validated reference genes in sample sequences to minimize or remove the technical variation as much as possible (Piana *et al.*, 2008). The strategy applied in this study to find the novel *SOD* gene sequence may be used for the finding of other reference genes in future studies. A number of common reference genes have been described previously (Stürzenbaum and Kille, 2001), which may provide choice of additional validated reference genes rather than the β-actin that I used here.

References

Ahamed M, Alsalhi MS and Siddiqui MK (2010). Silver nanoparticle applications and human health. Clinica Chimica Acta **411**: 1841–1848.

Benedicte RA, Johanna W and Kathryn MR (2009). Large scale geographic clines of parasite damage to *Populus tremula* L. Ecography **33**: 483-493.

Berg J.M, Tymaczko J.T and Stryer L (2002). Molecular Cell Biology, 5th ed, 2002. WH Freeman. ISBN 0-7167-4955-6.

Bernardi G (2011). *ABCB1* gene in *Aporrectodea caliginosa* – a prospective ecotoxicological tool. A thesis submitted in partial fulfilment of the requirements for the Degree of Master of Applied Science. Lincoln University, Christchurch, New Zealand.

Bhattacharya R and Mukherjee P (2008). Biological properties of "naked" metal nanoparticles. Advanced Drug Delivery Reviews **60**: 1289–1306.

Bohlen PJ (2002). Earthworms. R. Lal (Ed.), Encyclopedia of Soil Science, Marcel Dekker, Inc., New York : 370–373.

Bourdon JA, Saber AT, Jacobsen NR, Jensen KA, Madsen AM, Lamson JS, Wallin H, Moller P, Loft S, Yauk CL and Vogel UB (2012). Carbon black nanoparticle instillation induces sustained inflammation and genotoxicity in mouse lung and liver. Particle and Fibre Toxicology, **9**: 5.

Brousseau P, Dunier M, De Guise S and Fournier M (1997). Marqueurs immunologiques. In: Ramade JF et al. (Ed.), Biomarqueurs en Ecotoxicologie, Aspects Fondamentaux Masson, Paris, 287–315.

Buzea C, Pacheco II and Robbie K (2007) Nanomaterials and nanoparticles: sources and toxicity. Biointerphases **2**: MR17-71.

Calhoun MW and Gebbis RB (1993). Demonstration of separate gebetic loci encoding distinct membrane-bound respiratory NADH Dehydrogenases in *Escherichia coli*. Journal of Bacteriology, **175**: 3013–3019.

Casabé NB, Piola L, Fuchs JS, Oneto ML, Pamparato L and Basack S (2007). Ecotoxicological assessment of the effects of glyphosate and chlorpyrifos in an Argentine soya field. Journal of Soils and Sediments **7**: 232–239.

Cataldo F (2002). A study on the thermal stability to 1000 degrees C of various carbon allotropes and carbonaceous matter both under nitrogen and in air. Fullerenes Nanotubes and Carbon Nanostructures **10**: 293–311.

Cavas T, Garanko NN and Arkhipchuk VV (2005). Induction of micronuclei and binuclei in blood, gill and liver cells of fishes subchronically exposed to cadmium chloride and copper sulphate. Food and Chemical Toxicology **43**: 569–574.

Chaubey A and Malhotra BD (2002). Review of mediated biosensors, transduction principles and applications, Biosensors and Bioelectronics **17**: 441–456.

Carey Lea, M. (1889). On allotrophic forms of silver. American Journal of science, **37**: 476–491.

Chang C, Kokontis J and Liao S (1988). Molecular Cloning of Human and Rat Complementary DNA Encoding Androgen Receptors. Science **240, 324**: 324–326.

Chen X and Schluesener HJ (2008). Nanosilver: a nanoproduct in medical application. Toxicol Lett 2008; **176**: 1–12.

Chen C, Zhou Q, Liu S and Xiu Z (2011). Acute toxicity, biochemical and gene expression responses of the earthworm *Eisenia fetida* exposed to polucyclic musks. Chemosphere, **83**: 1147–1154.

Choi O and Hu Z (2008). Size dependent and reactive oxygen species related nanosilver toxicity to nitrifying bacteria. Environmental Science and Technolgy, **42**: 4583–4588.

Cooper EL and Stein EA (1981). Invertebrate Blood Cells. Academic Press, London San Francisco: 75–140.

Cotelle S and Ferard J (1999). Comet assay in ecotoxicology: a review Environmental and Molecular Mutagenesis. **34**: 246–255.

Crapo JD, Oury T, Rabouille C, Slot JW and Chang LY (1992). Copper, zinc superoxide dismutase is primarily a cytosolic protein in human cells. Proc Natl Acad Sci USA **89**: 10405–10409.

Das R, Nath SS, Chakdar D, Gop G and Bhattacharjee R (2009). Preparation of Silver Nanoparticles and Their Characterization. Journal of Nanotechnology Online DOI: 10.2240/azojono0129.

Derveaux S, Vandesompele J and Hellemans J (2010). How to do successful gene expression analysis using real-time PCR. Methods, **50**: 227–230.

Dibrov P, Dzioba J, Gosin KK and Hase CC (2002). Chemiosmotic Mechanism of Antimicrobial Activity of Ag^{+} in *Vibrio cholera*. Antimicrob Agents Chemother **46**: 2668–2670.

Dionysiou DD (2004). Environmental applications and implications of nanotechnology and nanomaterials. Journal of Environmental Engineering ASCE **130**: 723–724.

Dos Santos P, Kowaltowski AJ, Laclau M, Subramanian S, Paucek P, Boudina S, Thambo JB, Tariosse L and Garlid K (2002). Mechanisms by which opening the mitochondrial ATP-sensitive K^{+} channel protects the ischemic heart. Heart and Circulatory Physiology: American Journalk of Physiology **283**: 284–295.

Doshi R, Braida W, Christodoulators C, Wazne M and O'Connor G (2008). Nano-aluminum: Transport through sand columns and environmental effects on plants and soil communities. Environmental Research **106**: 296–303.

D' Sousa SF (2001). Microbial biosensors. Biosensors and Bioelectronics **16**: 337–353.

Ema M, Kobayashi N, Naya M, Hanai S and Nakanishi J (2010). Reproductive and developmental toxicity studies of manufactured namomaterials. Reproductive Toxicology **30**: 342–352.

Eyambe SG, Goven AJ, Fitzpatrick LC, Venables BJ and Cooper EL (1991). A non-invasive technique for sequential collection of earthworm (*Lumbricus terrestris*) leukocytes during subchronic immuno-toxicity studies. Laboratory Animals **25**: 61–67.

Fabrega J, Luoma SN, Tyler CR, Galloway TS and Lead JR (2010). Silver nanoparticles: behaviour and effects in the aquatic environment. Environmental International **37**: 517–531.

Farah MA, Ateeq B and Ahmad W (2006). Antimutagenic effect of neem leaves extract in freshwater fish, Channa punctatus evaluated by cytogenetic tests. Science of the Total Environment **364**: 200–241.

Fares H and Greenwald I (2001). Genetic analysis of endocytosis in *Caenorhabditis elegans* : coelomocyte uptake defective mutants. *Genetics* **159**: 133–145.

Fenchel T, King GM and Blackburn TH (2006). Bacterial Biogeochemistry: The Ecophysiology of mineral cycling (2nd ed), Elsevier. ISBN 978-0121034559.

Fortner JL, Sayes DYCM, Boyd AM, Falkner J, Hotze E and Alemany L (2005). C60 in water: nanocrystal formation and microbial response. Environ Sci Technol **39**: 4307–4316.

Fourie F, Reinecke SA and Reinecke AJ (2007). The determination of earthworm species sensitivity differences to cadmium genotoxicity using the comet assay. Ecotoxicology and Environmental Safety **67**: 361–368.

Fridovich I (1978). The biology of oxygen radicals. Science **201**: 875.

Gelperina S, Kisich K, Iseman,MD and Heifets L (2005). The potential advantages of nanoparticle drug delivery systems in chemotherapy of tuberculosis. American Journal of Respiratory and Critical Car Medicine **172**: 1487–1490.

Geranio L, Heuberger M and Nowack B (2009). The behavior of silver nanotextiles during washing. Environmental Science Technology **43**: 8113–8118.

Gooneratne SR, Buser A, Lindsay P and Wellby M (2011). Ecotoxicological assessment of acid mine drainage: Electrophysiological changes in an earthworm (*Aporrectodea caliginosa*) and aquatic oligochaete (*Lumbriculus variegatus*). Journal of Environmental Monitoring **13**: 1360–1365.

Gottschalk F, Sonderer T, Scholz RW and Nowack B (2009). Modeled environmental concentrations of engineered nanomaterials (TiO_2), ZnO, Ag, CNT, Fullerenes) for different regions. Environmental Science Technology **43**: 9216–9222.

Grunenwald H (2003). Optimization of Polymerase Chain Reaction. 2nd ed. PCR protocols, Methods in Molecular Biology, ed. JM Walk. Totowa: Human Press Inc. **226**: 89–99.

Hamadeh HK, Bushel P, Paules RS and Afshari CA (2001). Discovery in toxicology: Mediation by gene expression array technology. Journal of Biochemical and Molecular Toxicology **15**: 231–242.

Hamed SS, Kauschke E and Cooper EL (2002). Cytochemical properties of earthworm coelomocytes enriched by Percoll. A new model for analyzing antimicrobial peptides with biomedical applications. IOS Press, Ohmsha: 29–37.

Handy RD, von der Kammer F, Lead JR, Hassellov M, Owen R and Crane M (2008). The ecotoxicology and chemistry of manufactured nanoparticles. Ecotoxicology 17, pp. 287–314.

Hansen LH and Sørensen SJ (2001). The use of whole-cell biosensors to detect and quantify compounds or conditions affecting biological systems. Microbial Ecology **42**: 483–494.

Hayashi K, Adachi T and Ohta H (1992). The site of nonenzymic glycation of human extracellular-superoxide dismutase *in vitro*. Free Radical Biology and Medicine **13**: 205–210.

Hennessy M and Spiers JP (2007). A primer on the mechanics of P-glycoprotein the multidrug transporter. Pharmacological Research, **55**: 1–15. doi:10.1016/j.phrs. 2006.10.007.

Hoet PHM, Brüske-Hohlfeld I and Salata OV (2004). Nanoparticles – knonw and unknown health risks. Journal of Nanobiotechnology **2**:12.

Homa J, Olchawa E, Stürzenbaum SR, Morgan AJ and Plytycz B (2005). Early-phase immunodetection of metallothionein and heat shock proteins in extruded earthworm coelomocytes after dermal exposure to metal ions. Environmental Pollution **135**: 275–280.

Homa J, Klimek M, Kruk J, Cocquerelle C, Vandenbulcke F and Plytycz B (2010). Metal-specific effects on metallothionein gene induction and riboflavin content in coelomocytes of *Allolobophora chlorotica*. Ecotoxicology and Environmental Safety, **73**: 1937–1943.

Hossain Z and Huq F (2002). Studies on the interaction between Ag+ and DNA. Journal of Inorganic Biochemistry **91**: 398–404.

Hu CW, Li M, Cui YB, Li DS, Chen J and Yan LY (2010). Toxicological effects of TiO2 and ZnO nanoparticles in soil on earthworm *Eisenia fetida*. Soil Biology and Biochemistry **42**: 586–591.

Hwang ET, Lee JH, Chae YJ, Kim YS, Kim BC, Sang BI and Gu MB (2008). Analysis of the toxic mode of action of silver nanoparticles using stress-specific bioluminescent bacteria. Small **4**: 746–750.

Hyndman DL and M Mitsuhasi (2003). PCR primer design. 2nd ed. PCR protocols , Methods in Molecular Biology, ed. J.M. Walk. Human Press Inc.: Totowa **226**: 81–88.

Hyung H, Fortner JD, Hughes JB and Kim JH (2007). Natural organic matter stabilizes carbon nanotubes in the aqueous phase. Environmental Science and Technology **41**:179–184.

Judelson H (2002). PCR Standard Protocol (with Taq polymerase).

Ju-Nam Y and Lead JR (2008). Manufactured nanoparticles: An overview of their chemistry, interactions and potential environmental implications. Science of the Total Environment **400**: 396–414.

Jung JY, Lee IK, Seok SJ, Lee HJ, Kim YH and Yun BS (2008). Antioxidant polyphenols from the mycelial culture of the medicinal fungi *Inonotus xeranticus* and *Phellinus linteus*. Journal of Applied Microbiology **104**: 1824–1832.

Kaiser KLE and Palabrica VS (1991). Photobacterium phos-phoreum toxicity data index. Journal of Water Pollution, Canada **26**: 361–431.

Keller JN, Hanni KB and Markesbery WR (1999). Oxidized low-density lipoprotein induces neuronal cell death: impli-cation for calcium, reactive oxygen species and caspases. Journal of Neurochemistry. **72**: 2601–2609.

Kim DW, Hong GH, Lee HH, Choi SH, Chun BG, Won CK, Hwang IK and Won MH (2007). Effect of colloidal silver against the cytotoxicity of hydrogen peroxide and naphthazarin on primary cultured cortical astrocytes. International Journal of Neuroscience **117**: 387–400.

Kirstein-Miles J and Morimoto RI (2010). Caenorhabditis elegans as a model system to study intercompartmental proteostasis: Interrelation of mitochondrial function, longevity, and neurodegenerative diseases. Devlopmental Dynamics **239**: 1529–1538.

Klobučar GIV, Koziol B, Markowicz M, Kruk J and Plytycz B (2006). Riboflavin as a source of autofluorescence in *Eisenia fetida* coelomocytes. Photochemical and Photobiology, **82**: 570–573.

Koch A (2003). Bacterial wall as target for attack: past, present, and future research. Clinic Microbiology Review **16**: 673–687.

Komatsu T, Tabata M, Kubo-Irie M, Shimizu T, Suzuki K, Nihei Y and Takeda K (2008). The effects of nanoparticles on mouse testis Leydig cells in *vitro*. Toxicology in Vitro **22**: 1825–1831.

Lagadic L and Caquet T (1998). Invertebrates in testing of environmental chemicals: are they alternatives? Environ Health Perspect 106 Suppl 2: 593–611.

Lapied E, Moudilou E, Exbrayat JM, Oughton DH and Joner EJ (2010). Silver nanoparticle exposure causes apoptotic response in the earthworm *Lumbricus terrestris* (Oligochaeta). Nanomedicine (Lond) **5**:975–984.

Leacoanet HF, Bottero JY, Wiesner MR (2004). Laboratory assessment of the mobility of nanomaterials in porous media. Environmental Science and Technology **38**: 5164–5169.

Limbach LK, Wick P, Manser P, Grass RN, Bruinink A and Stark WJ (2007). Exposure of engineered nanoparticles to human lung epithelial cells: Influence of chemical composition and catalytic activity on oxidative stress. Environmental Science and Technology **41**: 4158–4163.

Livak KJ and Schmittgen TD (2001). Analysis of Relative Gene Expression Data Using Real-Time Quantitative PCR and the $2^{-\Delta\Delta CT}$ Method. Melthods **25**: 402–408.

Lok CN, Ho CM, Chen R, He QY, Yu WY, Sun H, Tam KHP, Chiu JF and Che CM (2007). Silver nanoparticles: partial oxidation and antibacterial activities. Journal of Biological Inorganic Chemistry **12**: 527–534.

Menzel R, Rodel M, Kulas J and Steinberg CE (2005). CYP35: xenobiotically induced gene expression in the nematode Caenorhabditis elegans. Archives of Biochemistry and Biophusics **438**: 93–102.

Moore MN (2006). Do nanoparticles present ecotoxicological risks for the health of the aquatic environment? Environment International **32**: 967–976.

Morones JR, Elechiguerra JL, Camacho A, Holt K, Kouri JB, Ramírez JT and Yacaman MJ (2005). The bactericidal effect of silver nanoparticles. Nanotechnology **16**: 2346–2353.

Mroz RM, Schins RP, Li H, Jimenez LA, Drost EM, Holownia A, MacNee W and Donaldson K (2008). Nanoparitcle-driven DNA damage mimics irradiation-related carcinogenesis pathways. European Respiratory Journal **31**: 241–25.

Muangphra P and Gooneratne R (2010). Comparative genotoxicity of cadmium and lead for earthworm coelomocytes in a filter paper study. Biology Department, Faculty of Science, Silpakorn University, Thailand. Faculty of Agriculture and Life Science, Lincoln University, New Zealand.

Muangphra P and Gooneratne SR (2011a). Comparative genotoxicity of cadmium and lead in earthworm coelomocytes. Journal of Applied and Environmental Soil Science, Article ID 218929, pp. 1–7, doi:10.1155/2011/218929.

Muangphra P and Gooneratne SR (2011b). Toxicity of commercial neem extract to earthworm (*Pheretima peguana*). Journal of Applied and Environmental Soil Science Article ID 925950, pp. 1–8, doi:10.1155/2011/925950.

Muangphra P, Kwankua W and Gooneratne SR (2012). Genotoxic effects of glyphosate and paraquat on earthworm coelomocytes. Environmental Toxicology (in the press).

Mueller NC, and Nowack B (2008). Exposure modeling of engineered nanoparticles in the environment. Environmental Science Technology **42**: 4447–4453.

Navarro E, Baun A, Behra R, Hartmann NB, Filser J, Miao AJ, Quigg A, Santschi PH and Sigg L (2008). Environmental behavior and ecotoxicity of engineered nanoparticles to algae, plants, and fungi. Ecotoxicology **17**: 372–386.

Nowack B and Bucheli TD (2007). Occurrence, behaviour and effects of nanoparticles in the environment. Environmental Pollution **150**: 5–22.

Oberdörster E, Zhu S, Blickley TM, McClellan-Green P and Haasch LM (2006). Ecotoxicology of carbon-based engineered nanoparticles: Effects of fullerene (C60) on aquatic organisms. Carbon **44**: 1112–1120.

OECD Guideline for Testing of Chemicals 208 (1984). Proposal for updating guideline 208.

Park HJ, Kim YY, Kim J, Lee JH, Hahn JS, Gu MB and Yoon J (2009). Silver-ion-mediated reactive oxygen species generation affecting bacterial activity. Water Research **43**: 1027–1032.

Pasco N, Baronian K, Jeffries C, Webber J and Hay J (2004). MICREDOX®- development of a ferricyanide-mediated rapid biochemical oxygen demand method using an immobilised *Proteus vulgaris* biocomponent, Biosensors and Bioelectronics **20**: 524–532.

Pasco N, Goonerate R, Daniel R, Czollner A and Scott AJ (2008). Toxicity assessment of chlorophenols using a mediated microbial toxicity assay. International Journal of Environmental Analytical Chemistry **88**: 1063–1075.

Pasco N, Hay J and Morris K (2005). Rapid mediated bioassay for the measurement of biochemical oxygen demand (BOD) and direct toxicity assessment (DTA). Devel. Applied Microbiology and Biotechnology **2**: 123–149.

Pasco N, Weld R, Hay J and Gooneratne SR (2011). Invited Review: Development and applications of whole-cell biosensors for ecotoxicity testing for a Special issue on 'Microorganisms for analysis'. Analytical and Bioanalytical Chemistry **400**: 931– 945.

Percival SL, Bowler PG and Russell D (2005). Bacterial resistance to silver in wound care. Journal of Hospital Infection **60**: 1–7.

Perez-Losada M, Ricoy M, Marshall JC and Dominguez J (2009). Phylogenetic assessment of the earthworm Aporrectodea caliginosa species complex (Oligochaeta: Lumbricidae) based on mitochondrial and nuclear DNA sequences. Molecular Phylogenetics and Evolution **52**: 293–302.

Piana C, Wirth M, Gerbes S, Viernstein H, Gabor F and Toegel S (2008). Validation of reference genes for qPCR studies on Caco-2 cell differentiation. European Journal of Pharmaceutics and Biopharmaceutics **69**: 1187–1192.

Ponchel F, Toomes C, Bransfield K, Leong FT, Douglas SH, Field SL, Bell SM, Combaret V, Puisieux A, Mighell AJ, Robinson PA, Inglehearn CF, Isaacs JD and Markham AF (2003). Real-time PCR based on SYBR-Green I fluorescence: An alternative to the TaqMan assay for a relative quantification of gene rearrangements, gene amplifications and micro gene deletions. BMC Biotechnology **3**: 18.

Rael LT, Thomas GW, Craun ML, Gerald Curtis C, Bar-Or R and Bar-Or D (2004). Lipid peroxidation and the thiobarbituric acid acid assay: standardization of the assay when using saturated and unsaturated fatty acids. Journal of Biochemistry and Molecular Biology **37**: 749–752.

Rai M, Yadav A and Gade A (2009). Silver nanoparticles as a new generation of antimicrobials. Biotechnology Advances **27**: 76–83.

Reinecke SA and Reinecke AJ (2004). The comet assay as biomarker of heavy metal genotoxicity in earthworms. Archives of Environmental and Contaminant Toxicology **46**: 208–215.

Risom L, Moller P and Loft S (2005). Oxidative stress-induced DNA damage by particulate air pollution. Mutation Research **592**: 119–137.

Roberts AP, Mount AS, Seda B, Souther J, Qiao R, Lin S, Ke PC, Rao AM and Klaine SJ (2007). In vivo biomodification of lipid-coated carbon nanotubes by Daphnia magna. Environmental Science and Technology **41**: 3025–3029.

Robichaud CO, Tanzil D and Wiesner MR (2007). Assessing life-cycle risks of nanomaterials. In Environmental Nanotechnology, Applications and Impacts of Nanomaterials **2007**: 481–524.

Rogers K R (2006). Recent advances in biosensor techniques for environmental monitoring, Analytica Chimica Acta **568**: 222–231.

Roh JY, Sim SJ, Yi J, Park K, Chung KH, Ryu DY and Choi J (2009). Ecotoxicity of Silver Nanoparticles on the Soil Nematode *Caenorhabditis elegans* Using functional Ecotoxicogenomics. Environmental Science and Technology **43**: 3933–3940.

Saddler KL, Ndebele K, Tchounwou P and Graham B (2012). *In-vitro* cytotoxicity assessment of silver nanaoparticles using human liver carcinoma cells. Ninth International Symposium on Recent Advances in Environmental Health Research. #W912HZ-10-2-0045.

Salata OV (2004). Application of nanoparticles in biology and medicine. Journal of Nanobiotechnology **l 2**: 1–12.

Sanchez-Galan S, Linde AR, Ayllon F and Garcia-Vazquez E (2001). Induction of micronuclei in eel (*Anquilla anquilla L.*) by heavy metals. Ecotoxicology and Environmental Safety **49**: 139–143.

Savigny JC (1826). Anylyse d'un mémoir sur les Lombrics par Cuvier. Member of Academic Science Institute France. **5**: 176–184.

Sayes CM, Fortner JD, Guo W, Lyon D, Boyd AM and Ausman KD (2004). The differential cytotoxicity of water soluble fullerenes. Nanoletters **4**: 1881–1887.

SCENIHR (2006). Modified opinion (after public consultation) on the appropriateness of existing methodologies to assess the potential risks associated with engineered and adventitious products of nanotechnologies. European, Scientific Committee on Emerging and Newly Identified Health Risks.

Schlegel R and MacGregor JT (1982). The persistence of micronuclei in peripheral blood erythrocytes: detection of chronic chromosome breakage in mice. Mutation Research, **104**: 367–369.

Schmittgen TD and Livak KJ (2008). Analyzing real-time PCR data by the comparative C_T method. Nature Protocols **3**:1101–1108.

Semeykina AL and Skulachev VP (1990). Submicromolar Ag^+ increases passive Na^+ permeability and inhibits the respiration-supported formation of Na^+ gradient in bacillus ftu vesicles. FEBS Letters, **1**: 69–72.

Shampo MA and Kyle RA (2002). "Kary B. Mullis - Nobel Laureate for procedure to replicate DNA". Mayo Clinic proceedings. Mayo Clinic **77**: 606.

Shaw LJ, Beaton Y, Glover LA, Killham K and Meharg AA (1999). Reinoculation of autoclaved soil as a non-sterile treatment for xenobiotic sorption and biodegradation studies. Applied Soil Ecology **11**: 217–226.

Shoults-Wilson WA, Reinsch BC, Tsyusko OV, Bertsch PM, Lowry GV and Unrine JM (2011). Role of particle size and soil type in toxicity of silver nanoparticles to earthworms. Soil Science Society of America Journal **75**: 33–45.

Singh NP, McCoy MT, Tice RR and Schneider EL (1988). A simple technique for quantitation of low levels of DNA damage in individual cells. Experimental Cell Research, **175**: 184–191.

Slawson RM, Van Dyke MI, Lee H and Trevors JT (1992). Germanium and silver resistance, accumulation, and toxicity in microorganisms. Plasmid, **27**: 72–79.

Smith CJ, Shaw BJ and Handy RD (2007). Toxicity of single walled carbon nanotubes to rainbow trout, (*Oncorhynchus mykiss*): respiratory toxicity, organ pathologies, and other physiological effects. Aquatic Toxicology. **82**: 94–109.

Snape J R, Maund SJ, Pickford DB and Hutchinson TH (2004). Ecotoxicogenomics: the challenge of integrating genomics into aquatic and terrestrial ecotoxicology. Aquatic Toxicology. **67**: 143–154.

Spurgeon DJ, Svendsen C, Hankard PK, Weeks JM, Kille P, Fishwick SK (2002). Review of Sublethal Ecotoxicological Tests for Measuring Harm in Terrestrial Ecosystems P5-063/TR1, Environment Agency, Bristol, UK.

Stürzenbaum SR and Kille P (2001). Control genes in quantitative molecular biological techniques: the cariability of invariance. Comparative Biochemistry and Physiology Part B: Biochemistry and Molecular Biology, **130**: 281–289.

Su JF, Wang LX and Ren L (2007). Synthesis of polyurethane microPCMs containing n-octadecane by interfacial polycondensation: Influence of styrene-maleic anhydride as a surfactant. Colloids Surfaces A: Physicochemical and Engineering Aspects, **299**: pp. 268–275.

Templeton RC, Ferguson PL, Washburn KM, Scrivens WA and Chandler GT (2006). Life-cycle effects of single-walled carbon nanotubes (SWNTs) on an estuarine meiobenthic copepod. Environmental and Science Technology **40**: 7387–7393.

Thiel T (1999). Department of Biology, University of Missouri. Introduction to bacteria. Science in the Real World: Microbes in Action.

Tice RR, Agurell E, Anderson D, Burlinson B, Hartmann A, Kobayashi H, Miyamae Y, Rojas E, Ryu, JC and Sasaki YF (2000). The single cell gel/comet assay: Guidelines for *in vitro* and *in vivo* genetic toxicology testing. Environmental Molecular Mutagenesis **35**: 206–221.

Tizzard A, Webber J, Gooneratne R, John R, Hay J and Pasco N (2004). MICREDOX®: application for rapid biotoxicity assessment, Analytica Chimica Acta **522**: 197–205.

Toyoshima M, Ohno K, Katsumoto T, Maki H and Takeshita K (1999). Cellular senescence of angiofibroma stroma cells from patients with tuberous sclerosis. Brain and Development, **21**: 184–191.

Trouiller B, Reliene R, Westbrook A, Solaimani P and Schiestl RH (2009). Titanium dioxide nanoparticles induce DNA damage and genetic instability in vivo in mice. Cancer Research, **69**: 8784–8789.

Udroin I (2006). The micronucleus test in piscine erythrocytes. Aquatic Toxicology, **79**: 201–204.

Van Heijenoort. J (2001). Formation of the glycan chains in the synthesis of bacterial Peptidoglycan. Glycobiology **11**: 25R–36R.

Voet D, Voet JG and Pratt CW (2006). Fundamentals of Biochemistry: Life at the molecular level (2nd ed), pp. 99; 546–547; 570.

Wang X, Chang L and Sun Z (2011). Differential expression of genes in the earthworm *Eisenia fetida* following exposure to *Escherichia coli* O157:H7. Developmental & amp; Cpmparatoe Immunology, **35**: 525–529.

Weisiger RA and Fridovich I (1973). Superoxide Dismutase: Organelle Specificity. The Journal of Biology Chemistry **248**: 3582–3592.

Wiesner MR, Lowery GV, Alvarez P, Dionysiou D and Biswas P (2006). Assessing the risks of manufactured nanomaterials. Environmental Science and Technology **40**: 4336–4345.

Yang W, Peters JI and Williams III RO (2008). Inhaled nanoparticles – A current review. International journak of Pharmaceutics **356**: 239–247.

Yang L and Watts DJ (2005). Particle surface characteristics may play an important role in phytotoxicity of alumina nanoparticles. Toxicology Letters. **158**: 122–132.

Yoshida S, Ono N, Tsukue N, Oshio S, Umeda T, Takano H and Takeda K (2006). In utero exposure to diesel exhaust increased accessory reproductive gland weight and serum testosterone concentration in male mice. Environmental Sciences **13**: 139–147.

Yperman J, DeVisscher G, Holvoet P and Flameng W (2004). Beta-Actin cannot be used as a control for gene expression in ovine interstitial cells derived from heart valves. Journal of Heart Valve Disease **13**: 848–853. September 2004.

Zelko IN, Mariani TJ and Folz RJ (2002). Superoxide dismutase multigene family: A comparison of the CuZn-SOD (SOD1), Mn-SOD (SOD2), and EC-SOD (SOD3) gene structures, evolution, and expression. Free Radical Biology and Medicine **33**: 337–349.

Zhu S, Oberdörster E and Haasch M (2005). Toxicity of an engineered nanoparticle (fullerene, C60) in two aquatic species, Daphnia and fathead minnow. Marine Environmental Research, in press.

Zhu Y, Zhao Q, Li Y, Cai X and Li W (2006). The interaction and toxicity of multi-walled carbon nanotubes with Stylonychia mytilus. Journal of Nanoscience and Nanotechnology. **6**: 1357–1364.

Appendix A

Statistical Analysis of Micronucleus Test Results

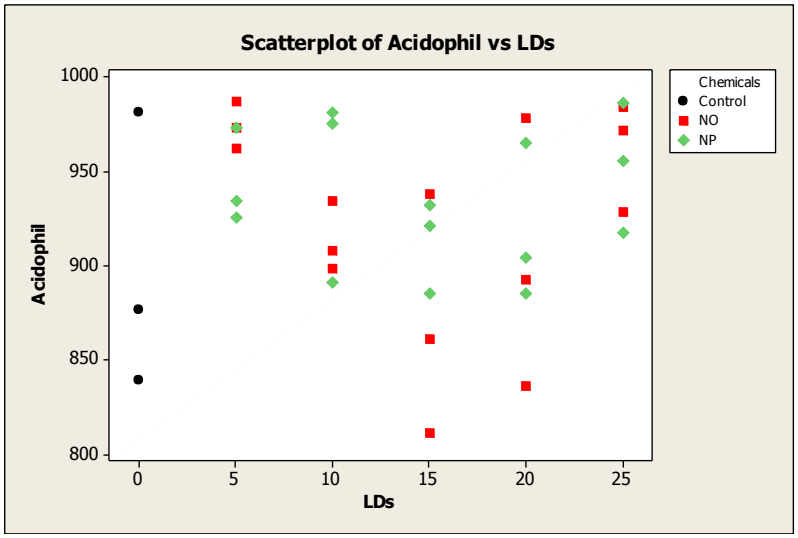

Variate: Acidophil

Source of variation	d.f.	s.s.	m.s.	v.r.	*F* pr.
Treated	1	2621.	2621	1.27	0.272
Treated.chemicals	1	941.	941	0.46	0.507
Treated.LDs	4	20742.	5185	2.51	0.071
Treated.chemicals.LDs	4	5536.	1384	0.67	0.620
Residual	22	45451.	2066		
Total	32	75290.			

Tables of means (Variate: Acidophil)

Grand mean 926.8

Treated	0	1
	898.7	929.7
rep.	3	30

Treated	Chemicals	Control	NO	NP
0		898.7		
	rep.	3		
1			924.1	935.3
	rep.		15	15

Treated	LDs	0	5	10	15	20	25
0		898.7					
	rep.	3					
1			959.0	931.2	891.3	910.0	956.8
	rep.		6	6	6	6	6

Treated	Chemicals	LDs	0	5	10	15	20
0	Control		898.7				
1	NO			974.0	913.3	870.0	902.0
	NP			944.0	949.0	912.7	918.0

Treated	Chemicals	LDs	25
1	NO		961.0
	NP	952.7	

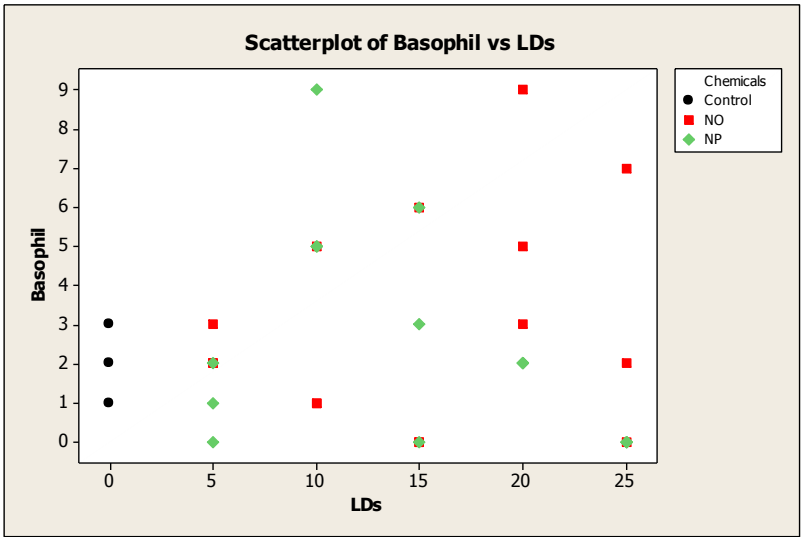

Variate: Basophil

Source of variation	d.f.	s.s.	m.s.	v.r.	*F* pr.
Treated	1	1.603	1.603	0.31	0.581
Treated.chemicals	1	2.700	2.700	0.53	0.475
Treated.LDs	4	38.867	9.717	1.90	0.147
Treated.chemicals.LDs	4	59.133	14.783	2.89	0.046
Residual	22	112.667	5.121		
Total	32	214.970			

Tables of means (Variate: Basophil)

Grand mean 2.70

Treated	0	1
	2.00	2.77
rep.	3	30

Treated	Chemicals	Control	NO	NP
0		2.00		

	rep.	3					
1			3.07	2.47			
	rep.		15	15			
Treated	LDs	0	5	10	15	20	25
0		2.00					
	rep.	3					
1			1.67	4.33	2.50	3.83	1.50
	rep.		6	6	6	6	6
Treated	Chemicals	LDs	0	5	10	15	20
0	Control		2.00				
1	NO			2.33	2.33	2.00	5.67
	NP			1.00	6.33	3.00	2.00
Treated	Chemicals	LDs	25				
1	NO		3.00				
	NP	0.00					

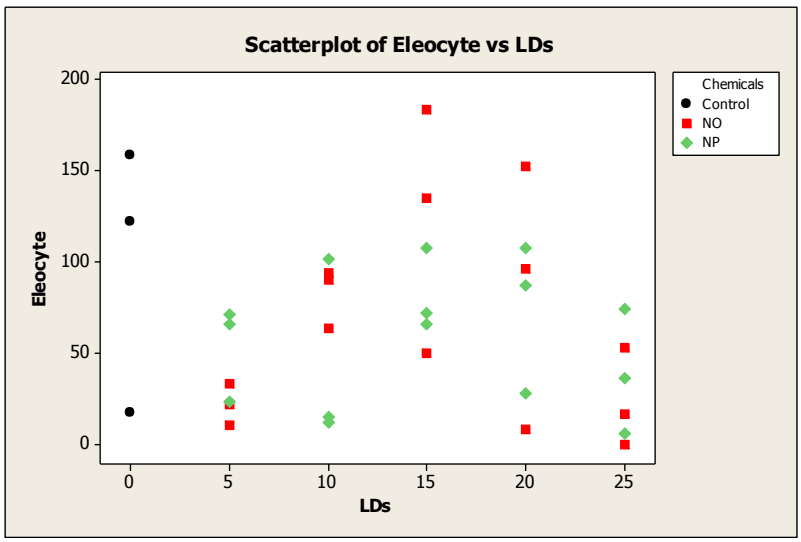

Variate: Eleocyte

Source of variation	d.f.	s.s.	m.s.	v.r.	*F* pr.
Treated	1	3627.	3627.	1.74	0.201
Treated.chemicals	1	599.	599.	0.29	0.597
Treated.LDs	4	20975.	5244.	2.52	0.071
Treated.chemicals.LDs	4	6348.	1587.	0.76	0.561
Residual	22	45835.	2083.		
Total	32	77384.			

Tables of means (Variate: Eleocyte)

Grand mean 65.8

Treated	0	1
	99.0	62.5
rep.	3	30

Treated	Chemicals	Control	NO	NP
0		99.0		
	rep.	3		

1			67.0	58.1			
	rep.		15	15			
Treated	LDs	0	5	10	15	20	25
0		99.0					
	rep.	3					
1			37.5	62.5	102.2	79.7	30.8
	rep.		6	6	6	6	6
Treated	Chemicals	LDs	0	5	10	15	20
0	Control		99.0				
1	NO			21.7	82.3	122.7	85.3
	NP			53.3	42.7	81.7	74.0
Treated	Chemicals	LDs	25				
1	NO		23.0				
	NP		38.7				

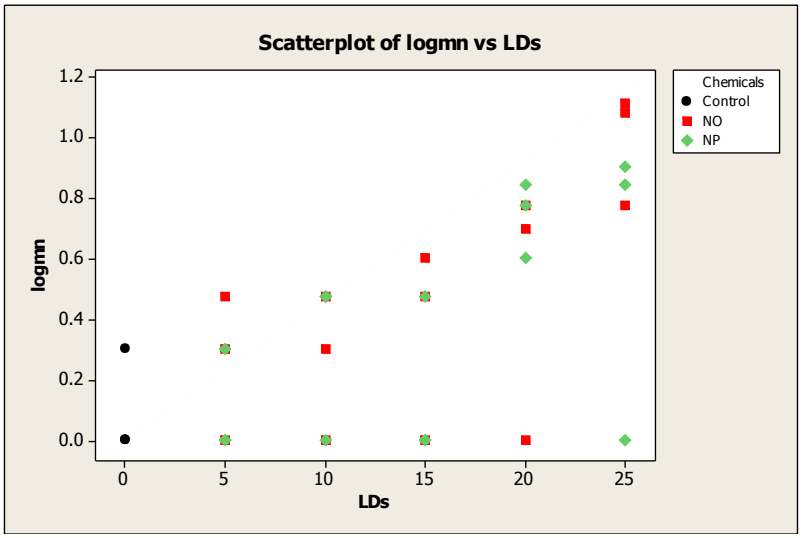

Variate: logmn

Source of variation	d.f.	s.s.	m.s.	v.r.	*F* pr.
Treated	1	0.28981	0.28981	3.47	0.076
Treated.chemicals	1	0.06330	0.06330	0.76	0.393
Treated.LDs	4	1.64226	0.41057	4.92	0.005
Treated.chemicals.LDs	4	0.38285	0.09571	1.15	0.361
Residual	22	1.83665	0.08348		
Total	32	4.21487			

Tables of means (Variate: logmn)

Grand mean 0.397

Treated	0	1
	0.100	0.426
rep.	3	30

Treated	Chemicals	Control	NO	NP
0		0.100		
	rep.	3		
1			0.472	0.380

	rep.		15	15			
Treated	LDs	0	5	10	15	20	25
0		0.100					
	rep.	3					
1			0.180	0.289	0.259	0.617	0.787
	rep.		6	6	6	6	6
Treated	Chemicals	LDs	0	5	10	15	20
0	Control		0.100				
1	NO			0.259	0.259	0.360	0.492
	NP			0.100	0.318	0.159	0.742
Treated	Chemicals	LDs	25				
1	NO		0.990				
	NP	0.583					

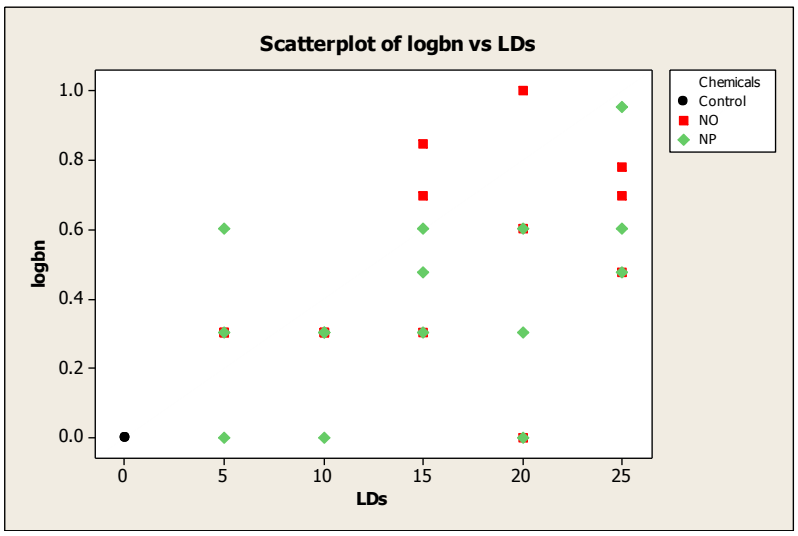

Variate: logbn

Source of variation	d.f.	s.s.	m.s.	v.r.	**F** pr.
Treated	1	0.51444	0.51444	8.67	0.007
Treated.chemicals	1	0.06401	0.06401	1.08	0.310
Treated.LDs	4	0.69238	0.17310	2.92	0.045
Treated.chemicals.LDs	4	0.06959	0.01740	0.29	0.879
Residual	22	1.30528	0.05933		
Total	32	2.64571			

Tables of means (Variate: logbn)

Grand mean 0.395

Treated	0	1
	0.000	0.434
rep.	3	30

Treated	Chemicals	Control	NO	NP
0		0.000		
	rep.	3		

1			0.481	0.388			
	rep.		15	15			
Treated	LDs	0	5	10	15	20	25
0		0.000					
	rep.	3					
1			0.301	0.251	0.538	0.418	0.665
	rep.		6	6	6	6	6
Treated	Chemicals	LDs	0	5	10	15	20
0	Control		0.000				
1	NO			0.301	0.301	0.615	0.534
	NP			0.301	0.201	0.460	0.301
Treated	Chemicals	LDs	25				
1	NO		0.651				
	NP		0.678				

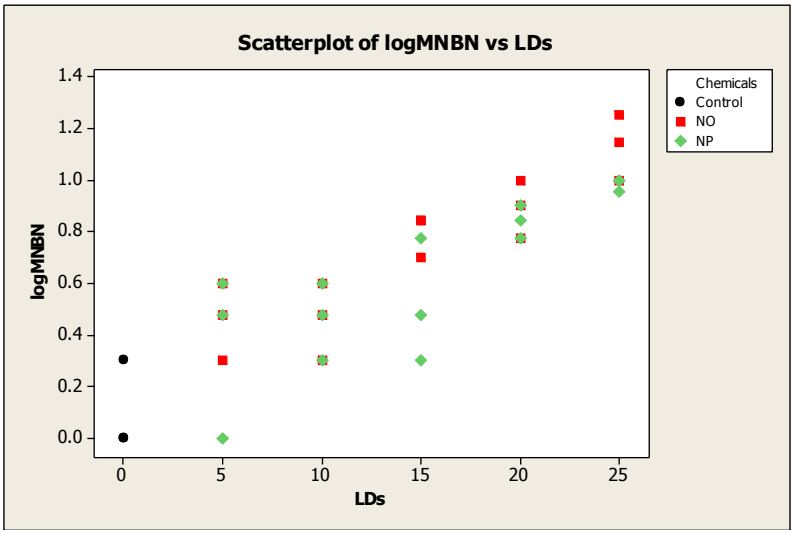

Variate: logMN+BN

Source of variation	d.f.	s.s.	m.s.	v.r.	*F* pr.
Treated	1	0.95132	0.95132	35.06	<.001
Treated.Chemicals	1	0.10045	0.10045	3.70	0.067
Treated.LDs	4	1.80236	0.45059	16.61	<.001
Treated.Chemicals.LDs	4	0.06759	0.01690	0.62	0.651
Residual	22	0.59698	0.02714		
Total	32	3.51870			

Tables of means (Variate: logMNBN)

Grand mean 0.637

Treated	0	1
	0.100	0.691
rep.	3	30

Treated	Chemicals	Control	NO	NP
0		0.100		
	rep.	3		

1			0.749	0.633			
	rep.		15	15			
Treated	LDs	0	5	10	15	20	25
0		0.100					
	rep.	3					
1			0.410	0.460	0.658	0.868	1.059
	rep.		6	6	6	6	6
Treated	Chemicals	LDs	0	5	10	15	20
0	Control		0.100				
1	NO			0.460	0.460	0.796	0.894
	NP			0.360	0.460	0.519	0.842
Treated	Chemicals	LDs	25				
1	NO		1.134				
	NP		0.985				

A.1 Regression analysis

Response variate: logMN+BN

Fitted terms: Constant, LDs

A.2 Summary of analysis

Source	d.f.	s.s.	m.s.	v.r.	F pr.
Regression	1	2.6869	2.68686	100.13	<.001
Residual	31	0.8318	0.02683		
Total	32	3.5187	0.10996		

Percentage variance accounted for 75.6

Standard error of observations is estimated to be 0.164.

A.3 Estimates of parameters

Parameter	estimate	s.e.	t(31)	t pr.
Constant	0.1511	0.0563	2.68	0.012
LDs	0.03565	0.00356	10.01	<.001

Log (MN+BN) = (0.03565) x dose + 0.1511

Appendix B
Sequencing and Alignment

B.1 PCR product forward sequence

5′- AGTTTATCTG TCAGTTCAAA CTTGGCAACA CCAGATTCA TCAGCTACCA

CATTGCCGAG ATCCCCCAAC ATGCCTCTCC TGATCTTCT GGAGCTCCAT

GAGTCTTTCC AAATGGGTTG AAGTGAGCAC C -3′

The similarity of alignment with *E. fetida SOD* mRNA was 93–94% (Figure 6.1), which was a high percentage of identical gene sequence.

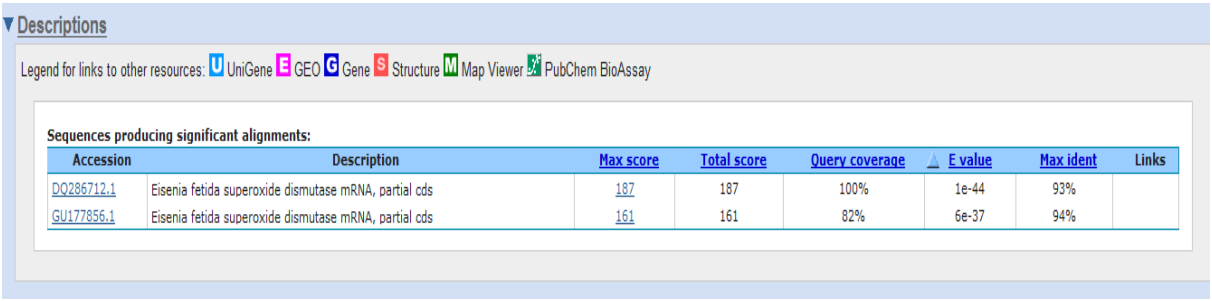

Figure 6.1 Alignment result: *SOD* gene (PCR product) forward sequence with sequence identity percentage to *E. fetida SOD* mRNA**.**

B.2 PCR product reverse sequence

5′- ATCAGGAGAG GCATGTTGGG GGATCTCGGC AATGTGGTAG CTGATGAATC

TGGTGTTGCC AAGTTTGAAT GACAGATAAA CTCCTCAATT TGACTGGACC

AAACTCAATC ATTGGACGTA CAATGGTGGT ACATGAGCTG GTGGATGATC

TG -3′

The similarity of alignment with *L. terrestrus* and *L. rubellus SOD* mRNA was 91% and 92% respectively (Figure 6.2), which were high percentages of identical gene sequence.

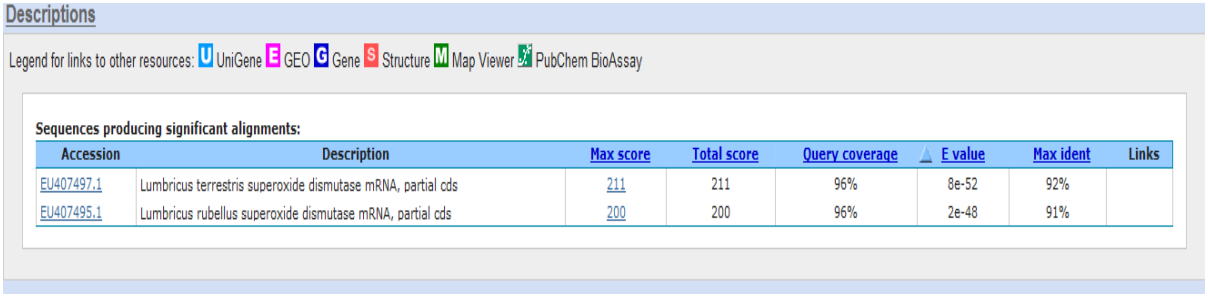

Descriptions

Legend for links to other resources: UniGene GEO Gene Structure Map Viewer PubChem BioAssay

Sequences producing significant alignments:

Accession	Description	Max score	Total score	Query coverage	E value	Max ident	Links
EU407497.1	Lumbricus terrestris superoxide dismutase mRNA, partial cds	211	211	96%	8e-52	92%	
EU407495.1	Lumbricus rubellus superoxide dismutase mRNA, partial cds	200	200	96%	2e-48	91%	

Figure 6.2 Alignment result of *SOD* gene (PCR product) reverse sequence with sequence identity percentage to *L. terrestrus* and *L. rubellus SOD* mRNA**.**

B.3 PCR product concensus sequence (*SOD* gene)

```
5′- CAGATCATCC ACCAGCTCAT GTACCACCAT TGTACGTCCA ATGATTGAGT

    TTGGTCCAGT CAAATTGAGG AGTTTATCTG TCAGTTCAAA CTTGGCAACA

    CCAGATTCAT CAGCTACCAC ATTGCCGAGT CCCCCAACAT GCCTCTCCTG

    ATCTTCTGGA GCTCCATGAG TCTTTCCAAA TGGGTTGAAG TGAGCACC -3′
```

The similarity of alignment with *L. terrestrus*, *L. rubellus* and *E. fetida SOD* mRNA was 89% to 94% (Figure 6.3), which were high percentages of identical gene sequence.

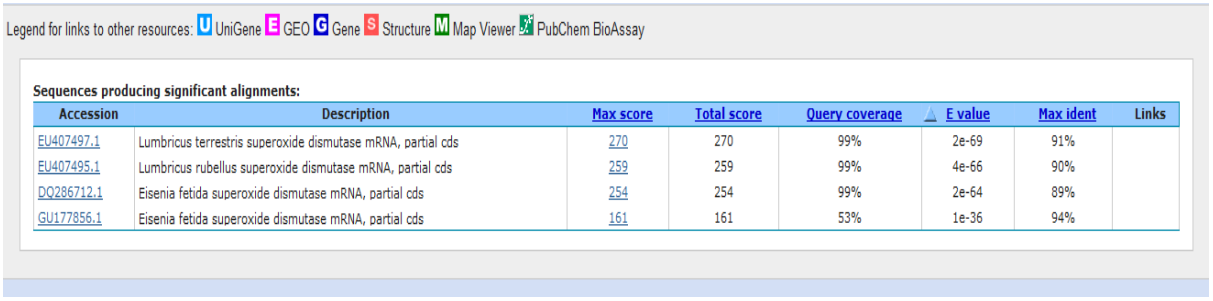

Legend for links to other resources: UniGene GEO Gene Structure Map Viewer PubChem BioAssay

Sequences producing significant alignments:

Accession	Description	Max score	Total score	Query coverage	E value	Max ident	Links
EU407497.1	Lumbricus terrestris superoxide dismutase mRNA, partial cds	270	270	99%	2e-69	91%	
EU407495.1	Lumbricus rubellus superoxide dismutase mRNA, partial cds	259	259	99%	4e-66	90%	
DQ286712.1	Eisenia fetida superoxide dismutase mRNA, partial cds	254	254	99%	2e-64	89%	
GU177856.1	Eisenia fetida superoxide dismutase mRNA, partial cds	161	161	53%	1e-36	94%	

Figure 6.3 Alignment result for the *SOD* gene (PCR product) concensus sequence (confirmed as *A. caliginosa SOD* gene) with sequence identity percentage to *L. terrestrus*, *L. rubellus* and *E. fetida SOD* mRNA**.**

Appendix C

SOD Protein Alignment

C.1 *A. caliginosa* SOD protein alignment with *Lumbricus*

```
FILE: Multiple_Sequence_Alignment

PROJECT:

NUMBER: 2

MAXLENGTH: 106

NAMES: AC frame 1 reverse Lumbricus protein

MAXNAMELEN: 19

ORIGIN

AC frame 1 reverse .....................................IR 2

Lumbricus protein ltpgkhgfhvhefgdntngctsagahfnpfglthgapedR 40

Consensus                                                r


AC frame 1 reverse   RGMLGDLGNVVADESGVAKFELTDKLLNLTGPNSIIGRTM 42

Lumbricus protein    erhvGDLGNVVADESGVAKFELTDKLiNLTGPNSIIGRTv 80

Consensus                gdlgnvvadesgvakfeltdkl nltgpnsiigrt


AC frame 1 reverse    VVHELVDDL 51

Lumbricus protein     VVHELVDDLgkgghefskttgntgar 106

Consensus             vvhelvddl
```

Yellow – active site residues as highly-conserved sequence,

copper binding site also = reside 83 (histidine)

Green = dimer interface

C.2 *A. caliginosa* SOD protein alignment with *E. fetida*

```
FILE: Multiple_Sequence_Alignment

PROJECT:

NUMBER: 2

MAXLENGTH: 106

NAMES: A caliginosa protein Eisenia fetida

MAXNAMELEN: 19

ORIGIN

A caliginosa protein .....................GAHFNPFGKTHGAPEDQ 17

Eisenia fetida       ltpgkhgfhvhefgdntngctsaGAHFNPFGKTHGAPEDQ 40

Consensus                                   gahfnpfgkthgapedq


A caliginosa protein  ERHVGGLGNVVADESGVAKFELTDKLLNLTGPNSIIGRTM 57

Eisenia fetida        ERHVGdLGNViADESGVAKFEvTDKLLNLTGPNSIIGRTv 80

Consensus             erhvg lgnv adesgvakfe tdkllnltgpnsiigrt


A caliginosa protein     VVHELVDDL 66

Eisenia fetida           VVHELVDDLgkgghefskttgntgar 106

Consensus                vvhelvddl
```

Yellow – active site residues as highly conserved sequence,

copper binding site also = reside 34 (histidine)

Blue = zinc binding site reside 26 and 43 (histidines)

Green = dimer interface